NATIONAL TECHNICAL UNIVERSITY OF ATHENS

School of Rural, Surveying and Geoinformatics Engineering (SRSE)

Department of Infrastructure and Rural Development

Integration of Unmanned Aerial Vehicles (UAVs) in multimodal transportation systems. Parameters and decision-making methodology.

For the Degree of

Doctor of Philosophy

by

Konstantinos Kouretas

Civil / Transportation Engineer NTUA, MSc UVA

Supervisor:

Konstantinos Kepaptsoglou

Associate Professor, NTUA

October 2023

Athens, Greece

ΕΘΝΙΚΟ ΜΕΤΣΟΒΙΟ ΠΟΛΥΤΕΧΝΕΙΟ

Σχολή Αγρονόμων Τοπογράφων Μηχανικών - Μηχανικών Γεωπληροφορικής

Τομέας Έργων Υποδομής και Αγροτικής Ανάπτυξης

Ενσωμάτωση μη Επανδρωμένων Αεροσκαφών σε συστήματα συνδυασμένων μεταφορών. Παράμετροι και μεθοδολογία λήψης αποφάσεων.

Για την απόκτηση

Διδακτορικού Διπλώματος

Κωνσταντίνος Κουρέτας

Πολιτικός Μηχανικός ΕΜΠ, Συγκοινωνιολόγος, MSc UVA

Επιβλέπων:

Κωνσταντίνος Κεπαπτσόγλου

Αναπληρωτής Καθηγητής ΕΜΠ

Οκτώβριος 2023

Αθήνα

Συμβουλευτική Επιτροπή

Κωνσταντίνος Κεπαπτσόγλου, Αν. Καθηγητής ΣΑΤΜ-ΜΓ ΕΜΠ

Κωνσταντίνος Καράντζαλος, Καθηγητής ΣΑΤΜ-ΜΓ ΕΜΠ

Αθανάσιος Μπαλλής, Καθηγητής ΠΜ ΕΜΠ

Εξεταστική Επιτροπή

Κωνσταντίνος Κεπαπτσόγλου, Αν. Καθηγητής ΣΑΤΜ-ΜΓ ΕΜΠ

Κωνσταντίνος Καράντζαλος, Καθηγητής ΣΑΤΜ-ΜΓ ΕΜΠ

Αθανάσιος Μπαλλής, Καθηγητής ΠΜ ΕΜΠ

Χαράλαμπος Ιωαννίδης, Καθηγητής ΣΑΤΜ-ΜΓ ΕΜΠ

Ελένη Βλαχογιάννη, Καθηγήτρια ΣΠΜ ΕΜΠ

Σωκράτης Μπάσμπας, Καθηγητής ΤΑΤΜ ΑΠΘ

Κωνσταντίνος Γκιοτσαλίτης, Επίκ. Καθηγητής ΣΠΜ ΕΜΠ

Preface

This dissertation is a result of continuous efforts in understanding and decoding specific challenges in transportation today and the foreseeable future. Despite its sometimes-complex scientific background, it is intended to be of practical value and make an actual difference out in the field, especially for underprivileged and remote communities. This motivation was vivid throughout the entire process.

It is fair to say that this would not be possible if not for some special people. It was Assoc. Prof. Konstantinos Kepaptsoglou who first suggested I should take on this challenge and now, some years later, we should both agree he was right. I thank him for showing me this path and being there with and for me all the time, as a supervisor and as a friend.

Also, my colleagues in the lab for the good times. Orfeas, we shared visions, ideas and concerns and always had each other's back. Christina, thank you for your guidance and unwavering support in science and in life and for being funny when nothing else would work.

To my family and closest ones, this one meant we could enjoy less time together, but I never felt you were away.

Acknowledgments

Funding: The implementation of the article was co-financed by Greece and the European Union (European Social Fund-ESF) through the Operational Programme «Human Resources Development, Education and Lifelong Learning» in the context of the Act "Enhancing Human Resources Research Potential by undertaking a Doctoral Research" Sub-action 2: IKY Scholarship Programme for PhD candidates in the Greek Universities.

Abstract

Synergetic transport schemes are extensively used in parcel delivery operations, exploiting the best features of each mode, and achieving better performance. Last mile deliveries and the approach of remote areas with limited transport connections form a particular challenge. This research is based on a new flexible, modular framework for integrated Conventional Vehicle – Unmanned Aerial Vehicle (CV-UAV) parcel delivery operations. Several items must be delivered to certain Delivery Locations (DL), from a Central Depot (CD). A CV is equipped onboard with multiple UAVs. Several types of locations facilitate UAV deployment, collectively namely Launch Sites (LS): Remote Depots (RD), which are facilities with in-house available UAVs (also available in the CD), and Virtual Hubs (VH), which are pre-determined locations for convenient UAV deployment by the CV operator, such as parking lots. Based on site characteristics, some of the DLs may also serve as locations for CV-based UAV deployment. For UAV flights, we are considering the presence of Restricted Zones (RZ), e.g., because of airports and a probabilistic Weather Forecast, which also affects flights. No-fly areas result from the presence of RZs and accepted risk in weather forecast and thus flight paths are not always straight. The solution methodology includes a specifically developed Assignment and Routing Optimization nested GA (AROnGA) scheme for obtaining the best mode assignment and routing solution under given/fixed conditions. The algorithm is additionally modified to perform scenario-based robust optimization, yielding a solution which performs well under most anticipated conditions. The methodology is gradually adapted in GIS environment, streamlining with common practice in terms of input file types in network design, airspace control and weather forecasting but also taking advantage of ever evolving sophisticated and powerful tools. The framework and the solution methodology are useful for strategic decisions on infrastructure and for operations planning with satisfactory performance and less risk.

Keywords: *stochastic optimization, vehicle routing, electromobility, sustainable transportation, multimodal transport, UAV, drones*

Περίληψη

Συνεργατικά σχήματα μεταφορών χρησιμοποιούνται ευρέως σε επιχειρήσεις διανομής πακέτων, αξιοποιώντας τα καλύτερα χαρακτηριστικά κάθε μέσου και πετυχαίνοντας καλύτερη απόδοση. Παραδόσεις τελευταίου μιλίου και η προσέγγιση δυσπρόσιτων περιοχών με περιορισμένες συνδέσεις αποτελούν ιδιαίτερες προκλήσεις. Αυτή η έρευνα βασίζεται σε ένα νέο, ευέλικτο και αρθρωτό πλαίσιο για επιχειρήσεις διανομής πακέτων με συνδυασμό Συμβατικού Οχήματων (ΣΟ) και Συστημάτων μη Επανδρωμένων Αεροσκαφών (ΣμηΕΑ). Ορισμένα πακέτα πρέπει να παραδοθούν σε Θέσεις Παράδοσης (ΘΠ), από μια Κεντρική Αποθήκη (ΚΑ). Ένα ΣΟ είναι εξοπλισμένο με πολλαπλά ΣμηΕΑ. Διάφοροι τύποι τοποθεσιών μπορούν να υποστηρίξουν την εκτόξευση και συλλογή (ανάπτυξη) ΣμηΕΑ, όλες επονομαζόμενες και Σημεία Εκτόξευσης (ΣΕ): Απομακρυσμένες Αποθήκες (ΑΑ), δηλαδή εγκαταστάσεις με διαθέσιμα ΣμηΕΑ εντός τους (όπως και εντός της ΚΑ) και Εικονικοί Κόμβοι (ΕΚ), που είναι προκαθορισμένες τοποθεσίες για ευχερή ανάπτυξη ΣμηΕΑ από τον χειριστή του ΣΟ, όπως π.χ. ανοιχτοί χώροι στάθμευσης. Βάσει χαρακτηριστικών τοποθεσίας, ορισμένες ΘΠ μπορούν επίσης να εξυπηρετήσουν ως θέσεις για ανάπτυξη ΣμηΕΑ από το ΣΟ. Για τις πτήσεις ΣμηΕΑ, λαμβάνουμε υπόψη την παρουσία Απαγορευμένων Ζωνών (ΑΖ), π.χ. λόγω αεροδρομίων και μια Πιθανοτική Πρόβλεψη Καιρού, που επίσης επηρεάζει τις πτήσεις. Οι περιοχές απαγόρευσης πτήσεων προκύπτουν από την παρουσία ΑΖ και ένα αποδεκτό ρίσκο ως προς την καιρική πρόβλεψη, συνεπώς οι διαδρομές πτήσης δεν είναι πάντα ευθείες γραμμές. Η μεθοδολογία επίλυσης περιλαμβάνει έναν ειδικά ανεπτυγμένο εμφωλευμένο γενετικό αλγόριθμο βελτιστοποίησης ανάθεσης και δρομολόγησης (Assignment and Routing Optimization nested-GA: AROnGA), για την εύρεση της βέλτιστης λύσης ανάθεσης μέσου για κάθε πακέτο και δρομολόγηση του ΣΟ κάτω από δεδομένες συνθήκες. Ο αλγόριθμος τροποποιείται επιπλέον για να εκτελέσει μια εύρωστη βελτιστοποίηση με βάση σενάρια, προσφέροντας μια λύση που αποδίδει καλά κάτω από τις περισσότερες αναμενόμενες

συνθήκες. Η μεθοδολογία προσαρμόζεται σταδιακά σε περιβάλλον Γεωγραφικών Συστημάτων Πληροφοριών (Geographic Information Systems – GIS), ευθυγραμμιζόμενη με την κοινή πρακτική όσον αφορά στους τύπους αρχείων εισόδου για ανάλυση δικτύων, έλεγχο εναερίου χώρου και καιρικές προβλέψεις, αξιοποιώντας τα σχετικά συνεχώς εξελισσόμενα, πολύπλοκα και ισχυρά εργαλεία ανάλυσης. Το πλαίσιο και η μεθοδολογία επίλυσης είναι χρήσιμα για στρατηγικές αποφάσεις ως προς την υποδομή και για σχεδιασμό επιχειρήσεων με ικανοποιητική απόδοση και λιγότερο ρίσκο.

Λέξεις κλειδιά: *στοχαστική βελτιστοποίηση, δρομολόγηση οχημάτων, ηλεκτροκίνηση, βιώσιμες μεταφορές, συνδυασμένες μεταφορές, ΣμηΕΑ, επιχειρησιακή έρευνα*

Εκτεταμένη Περίληψη

Αντικείμενο έρευνας

Η εκτέλεση του μεταφορικού έργου αντιμετωπίζει συνεχώς διαφορετικές προκλήσεις. Με την πάροδο των χρόνων μεταβάλλονται οι ανάγκες και οι τρόποι εκτέλεσης, ανάλογα με το αντικείμενο των μεταφορών, τα υπάρχοντα δίκτυα, τις τεχνολογικές εξελίξεις, την οικονομία, το περιβάλλον, τον τρόπο ζωής και πλήθος άλλων παραμέτρων, που αλληλοεπιδρούν μέσω μιας συχνά αμφίδρομης σχέσης. Ο συνδυασμός διαφορετικών μέσων μεταφοράς επιχειρεί να συνθέσει τις πρακτικές και δυνατότητες κάθε μέσου, ώστε να προκύψουν κατά το δυνατόν βέλτιστες λύσεις από άποψη ταχύτητας, αξιοπιστίας και οικονομικής απόδοσης. Η ταχύτατη εξέλιξη στον τομέα των μη επανδρωμένων αεροσκαφών δημιουργεί μια νέα πραγματικότητα και θέτει το ερώτημα της δυνατότητας αξιοποίησής τους, ως ενταγμένων σε ένα σύστημα συνδυασμένων μεταφορών. Η χρήση μη επανδρωμένων αεροσκαφών παρουσιάζει ένα σύνολο πλεονεκτημάτων, αλλά και περιορισμών, σημαντικά διαφορετικών από τα αντίστοιχα των συμβατικών έως τώρα μέσων μεταφορών.

Η επιλογή του κατάλληλου συνδυασμού μεταφορικών μέσων εξαρτάται σε μεγάλο βαθμό από τη συνδεσιμότητα μεταξύ προέλευσης, προορισμού και ενδιάμεσων σταθμών και την αποτελεσματικότητα με την οποία αξιοποιείται το δίκτυο από το κάθε μέσο. Η εκτέλεση του μεταφορικού έργου δυσχεραίνεται ή και ακυρώνεται σαν επιλογή όταν το δίκτυο είναι κατά τόπους ανεπαρκές ή και ανύπαρκτο. Στις περιπτώσεις που παρατηρούνται ελλιπείς ή προβληματικές συνδέσεις από άποψη χωρητικότητας, ασφάλειας, επιπέδου εξυπηρέτησης και άλλων παραμέτρων, προκύπτει η ανάγκη για εναλλακτική δρομολόγηση, με μεγάλο οικονομικό, χρονικό και περιβαλλοντικό κόστος. Ταυτόχρονα, η εκτέλεση του τελευταίου τμήματος ενός δρομολογίου παρουσιάζει επίσης ιδιαιτερότητες και προκλήσεις βελτιστοποίησης, καθώς η μεταφορά ενός αγαθού ξεφεύγει από τον κοινό άξονα μεταξύ κόμβων διαμετακόμισης. Συνοπτικά, παραδόσεις

τελευταίου μιλίου και η προσέγγιση δυσπρόσιτων περιοχών με περιορισμένες συνδέσεις αποτελούν ιδιαίτερες προκλήσεις και αποτελούν βασικό αντικείμενο αυτής της έρευνας.

Επιπρόσθετα, πέρα από την εκτέλεση φυσικού μεταφορικού έργου, η ίδια πρόκληση υπάρχει για απομακρυσμένες υπηρεσίες συλλογής και ανάλυσης δεδομένων. Αυτό πραγματοποιείται με χρήση αισθητήρων και καμερών λήψης δεδομένων που μπορεί να είναι είτε οπτικές είτε φασματικές (πολυφασματικές, υπερφασματικές, θερμικές, κοκ) και να λαμβάνουν είτε εικόνες είτε βίντεο. Είναι πλέον δυνατόν να διακρίνονται περισσότερα χαρακτηριστικά ή να αξιοποιούνται αυτόματοι αλγόριθμοι επεξεργασίας, που αναγνωρίζουν πιο αποτελεσματικά οχήματα ή αντικείμενα ή καλούν συναγερμό εκτάκτων αναγκών. Υπάρχει η δυνατότητα για επεξεργασία πραγματικού χρόνου πάνω στο αεροσκάφος και να μεταδίδονται ζωντανά αποτελέσματα της ανάλυσης.

Με κίνητρο την ανταπόκριση στις παραπάνω προκλήσεις, η προτεινόμενη έρευνα εξετάζει τις δυνατότητες αξιοποίησης μη επανδρωμένων αεροσκαφών. Η διατριβή ασχολείται ειδικότερα με το αντικείμενο της ανάπτυξης συνδυασμένων συστημάτων μεταφορών πακέτων, όπου μη επανδρωμένα αεροσκάφη και συμβατικά οχήματα αξιοποιούνται συνδυαστικά. Συνεργατικά σχήματα μεταφορών χρησιμοποιούνται ευρέως σε επιχειρήσεις διανομής πακέτων, αξιοποιώντας τα καλύτερα χαρακτηριστικά κάθε μέσου και πετυχαίνοντας καλύτερη απόδοση.

Μεθοδολογικό πλαίσιο

Η διδακτορική διατριβή αναπτύσσεται σε στάδια. Αρχικά θεωρούνται οι βασικές παράμετροι του προβλήματος και ο προσδιορισμός των στόχων με βάση την υφιστάμενη βιβλιογραφία και τις περιοχές με ανοιχτό αντικείμενο έρευνας. Διαμορφώνεται το θεμελιώδες πλαίσιο του συστήματος, το οποίο θα πρέπει να είναι αρθρωτό, ευέλικτο και προσαρμοστικό σε διαθεσιμότητα υποδομών, χαρακτηριστικά οχημάτων και ευρύτερων συνθηκών λειτουργίας των μεταφορικών μέσων. Χρησιμοποιούνται συνήθεις μαθηματικές συμβάσεις στον σχεδιασμό δικτύων και την επιχειρησιακή έρευνα ως βάση

για τη μοντελοποίηση και τη μεθοδολογία επίλυσης. Προτείνεται, έτσι, ένα αποδοτικό και έτοιμο προς χρήση εργαλείο λήψης στρατηγικών αποφάσεων και υπηρεσίες μεταφορών πακέτων, μαζί με μια ειδικά ανεπτυγμένη μεθοδολογία βελτιστοποίησης. Πιο συγκεκριμένα, προτείνεται ένα νέο, ευέλικτο και αρθρωτό πλαίσιο για επιχειρήσεις διανομής πακέτων με συνδυασμό Συμβατικού Οχήματος (ΣΟ) και Συστημάτων μη Επανδρωμένων Αεροσκαφών (ΣμηΕΑ). Ορισμένα πακέτα πρέπει να παραδοθούν σε Θέσεις Παράδοσης (ΘΠ), από μια Κεντρική Αποθήκη (ΚΑ). Ένα ΣΟ είναι εξοπλισμένο με πολλαπλά ΣμηΕΑ. Διάφοροι τύποι τοποθεσιών μπορούν να υποστηρίξουν την εκτόξευση και συλλογή (ανάπτυξη) ΣμηΕΑ, όλες επονομαζόμενες και Σημεία Εκτόξευσης (ΣΕ): Απομακρυσμένες Αποθήκες (ΑΑ), δηλαδή εγκαταστάσεις με διαθέσιμα ΣμηΕΑ εντός τους (όπως και εντός της ΚΑ) και Εικονικοί Κόμβοι (ΕΚ), που είναι προκαθορισμένες τοποθεσίες για ευχερή ανάπτυξη ΣμηΕΑ από τον χειριστή του ΣΟ, όπως π.χ. ανοιχτοί χώροι στάθμευσης. Βάσει χαρακτηριστικών τοποθεσίας, ορισμένες ΘΠ μπορούν επίσης να εξυπηρετήσουν ως θέσεις για ανάπτυξη ΣμηΕΑ από το ΣΟ. Η μεθοδολογία επίλυσης περιλαμβάνει έναν ειδικά ανεπτυγμένο εμφωλευμένο γενετικό αλγόριθμο βελτιστοποίησης ανάθεσης και δρομολόγησης (Assignment and Routing Optimization nested-GA: AROnGA), για την εύρεση της βέλτιστης λύσης ανάθεσης μέσου για κάθε πακέτο και δρομολόγηση του ΣΟ κάτω από δεδομένες συνθήκες.

Στη συνέχεια, αναγνωρίζοντας τις πραγματικές συνθήκες πτήσεων ΣμηΕΑ, εντάσσεται στο μοντέλο η παρουσία εναέριων Απαγορευμένων Ζωνών (ΑΖ). Τα ΣμηΕΑ ακολουθούν βέλτιστες διαδρομές με αποφυγή των απαγορευμένων ζωνών και μέρος της μεθοδολογίας πλέον ενσωματώνει εργαλεία Γεωγραφικών Συστημάτων Πληροφοριών (Geographic Information Systems – GIS), ακολουθώντας τις σύγχρονες τάσεις σε βάσεις δεδομένων και σχεδιασμό δικτύων και αξιοποιώντας τα σχετικά συνεχώς εξελισσόμενα, πολύπλοκα και ισχυρά εργαλεία ανάλυσης.

Στην τελική φάση η έρευνα επεκτείνεται στον στοχαστικό σχεδιασμό υπό αβέβαιες συνθήκες τόσο για το συμβατικό όχημα, όσο και τα ΣμηΕΑ. Η αβεβαιότητα αφορά π.χ. κυκλοφοριακές συνθήκες επί του δικτύου κίνησης του συμβατικού οχήματος, ή καιρικές συνθήκες που επηρεάζουν την ασφάλεια των πτήσεων ΣμηΕΑ, οι οποίες παρέχοντες ως πιθανοτικές προβλέψεις. Για τις πτήσεις ΣμηΕΑ, λαμβάνουμε υπόψη την παρουσία Απαγορευμένων Ζωνών (AZ), π.χ. λόγω αεροδρομίων και μια Πιθανοτική Πρόβλεψη Καιρού, που επίσης επηρεάζει τις πτήσεις. Οι περιοχές απαγόρευσης πτήσεων προκύπτουν από την παρουσία AZ και ένα αποδεκτό ρίσκο ως προς την καιρική πρόβλεψη. Στο τέλος παρουσιάζεται μια μεθοδολογία επίλυσης που προτείνει εύρωστες λύσεις με καλή απόδοση σε ένα εύρος πιθανών συνθηκών, ώστε να είναι δυνατός ο πρότερος σχεδιασμός των επιχειρήσεων με μικρότερο ρίσκο και καλή απόδοση. Ο αλγόριθμος AROnGA τροποποιείται επιπλέον για να εκτελέσει μια εύρωστη βελτιστοποίηση με βάση σενάρια, προσφέροντας μια λύση που αποδίδει καλά κάτω από τις περισσότερες αναμενόμενες συνθήκες. Κάθε υποψήφια γενική λύση συγκρίνεται με βάση τη βέλτιστη κάθε σεναρίου και επιλέγεται αυτή που αποδίδει κατά μέσο όρο καλύτερα. Το πλαίσιο και η μεθοδολογία επίλυσης είναι χρήσιμα για στρατηγικές αποφάσεις ως προς την υποδομή και για σχεδιασμό επιχειρήσεων με ικανοποιητική απόδοση και λιγότερο ρίσκο.

Συμπεράσματα και συνεισφορά έρευνας

Η διατριβή αναδεικνύει τις δυνατότητες χρήσης συνδυασμένων συστημάτων μεταφορών πακέτων μέσω συμβατικών οχημάτων και ΣμηΕΑ και την ανάγκη συμπερίληψης παραμέτρων όπως περιορισμοί στην εναέρια κυκλοφορία και αβεβαιότητα συνθηκών. Προτείνεται μια μοντελοποίηση του προβλήματος και μια μεθοδολογία παραγωγής βέλτιστων λύσεων που ανταποκρίνεται σε μεγάλο εύρος πραγματικών πιθανών συνθηκών ως προς την υποδομή, τον εξοπλισμό και τις συνθήκες λειτουργίας των οχημάτων και επιτρέπει την εύκολη προσαρμογή για πιο σύνθετα

προβλήματα ή περαιτέρω βελτιστοποίηση της διαδικασίας. Ταυτόχρονα, ανοίγει τον δρόμο για πρακτική εφαρμογή στην βιομηχανία των μεταφορών.

Κοινές πρακτικές προκλήσεις σε τέτοιες επιχειρήσεις, όπως δυσμενείς γεωμετρίες δικτύων, θέσεις παράδοσης εκτός δικτύου, εναέριοι περιορισμοί, κακές καιρικές συνθήκες και αβεβαιότητες στον δρόμο αντιμετωπίζονται μέσω της ευέλικτης δομής του μοντέλου και τη μεθοδολογία επίλυσης. Η αγνόηση περιορισμών όπως Απαγορευμένες Ζώνες και οι κακές καιρικές συνθήκες αποτελεί σημαντική απλούστευση ως προς το πώς πραγματικά μπορούν να λειτουργούν συνεργατικά σχήματα Συμβατικών Οχημάτων με ΣμηΕΑ. Η βάση της πλατφόρμας μπορεί να χρησιμοποιηθεί και για διαφορετικούς τύπου Συμβατικών Οχημάτων, δηλαδή φορτηγά, τραίνα, ή ακόμα και πλοία, ενώ η παράδοση πακέτων μπορεί εναλλακτικά να είναι κάποια άλλη υπηρεσία, όπως έλεγχος, έρευνα και διάσωση κτλ. Η ίδια η μετατροπή του αρχικού μοντέλου, ώστε να συμπεριλάβει την παρουσία Απαγορευμένων Ζωνών και μετέπειτα τον στοχαστικό σχεδιασμό κάτω από αβέβαιες συνθήκες αποδεικνύει την ευελιξία και προσαρμοστικότητα της πλατφόρμας.

Η πρακτική εφαρμογή και χρήση του μοντέλου γίνεται εύκολη μέσω μιας απλοποιημένης ροής εργασιών εισόδου/εξόδου, που είναι διαχωρισμένη από την υπόλοιπη αναλυτική διαδικασία υπολογισμών. Παρ' όλ' αυτά, όλο το μοντέλο και η μεθοδολογία επίλυσης υποστηρίζεται από ένα ισχυρό μαθηματικό υπόβαθρο. Επιτρέπει προσαρμοσμένες παρεμβάσεις σε παραμέτρους που αφορούν τις υποδομές και τα οχήματα και την εξέταση λύσεων με προκαθορισμένες προτεραιότητες (π.χ. χρήση μόνο συμβατικού οχήματος ή μόνο ΣμηΕΑ, παράδοση με συγκεκριμένο τύπο οχήματος λόγω προτίμησης πελάτη κτλ), αξιοποιώντας μέρος των εργαλείων βελτιστοποίησης. Η χρήση της πλατφόρμας με πειραματική λογική (εξέταση σεναρίων) βοηθάει στην ανάπτυξη στρατηγικών και στον τομέα των επενδύσεων που αφορά σε εγκαταστάσεις και εξοπλισμό (π.χ. ανεύρεση καλύτερων τοποθεσιών για αποθήκες, αλλαγή χαρακτηριστικών ΣμηΕΑ κτλ).

Κατά τη διάρκεια της έρευνας αντιμετωπίστηκαν πολλές προκλήσεις, αναμενόμενες και μη. Η δημιουργία ενός εξωτερικά απλού, κατανοητού μοντέλου που καλύπτει όμως πολλές διαφορετικές περιπτώσεις προϋποθέτει βαθιά γνώση του προβλήματος και αρκετές αρχικές ιδέες χρειάστηκε να τροποποιηθούν αφού αναδείχθηκαν αδυναμίες κατά την εκτέλεση πειραμάτων. Η εξέταση του μοντέλου σε ειδικά δίκτυα με ακραία χαρακτηριστικά βοήθησε στην επιβεβαίωση της λειτουργίας του με βάση τις προδιαγραφές τις εκτιμώμενες δυνατότητές του.

Καθώς οι εναέριοι περιορισμοί σε αστικό περιβάλλον είναι συχνά πολύ αυστηροί, η χρήση των ΣμηΕΑ ενδέχεται να είναι περιορισμένη. Ως προς την πρακτική εφαρμογή, προτείνεται η χρήση του μοντέλου περισσότερο για αγροτικές περιοχές, περιοχές προαστίων, για παραδόσεις μεταξύ πόλεων π.χ. περιφερειακά ενός μεγάλου αστικού κέντρου. Επίσης, μπορεί να γίνει χρήση του δικτύου κεντρικών αυτοκινητοδρόμων, των σταθμών εξυπηρέτησης αυτοκινήτων και των χώρων στάθμευσης για ανάπτυξη ΣμηΕΑ. Μια άλλη ενδιαφέρουσα περίπτωση θα ήταν η χρήση του σιδηροδρομικού δικτύου, με αξιοποίηση των σταθμών για χρήση ως Απομακρυσμένες Αποθήκες.

Η διατριβή συνεισφέρει στην επιστήμη και την πρακτική εφαρμογή, συνοπτικά, ως εξής:

- Αναγνωρίστηκαν οι σύγχρονες τάσεις στη βιβλιογραφία των συνδυασμένων μεταφορών με χρήση ΣμηΕΑ, οι περιορισμοί των υφιστάμενων προτάσεων, όπως και οι επιστημονικές περιοχές που χρήζουν επιπλέον έρευνας.
- Υπηρετήθηκε καθ' όλη τη διάρκεια της ανάπτυξης των μοντέλων και μεθοδολογιών ο στόχος της σύνδεσης με τις ανάγκες της κοινωνίας και η ευκολία αξιοποίησης της πλατφόρμας από εξωτερικούς χρήστες.
- Αναπτύχθηκε ένας πρότυπος, εξειδικευμένος εμφωλευμένος γενετικός αλγόριθμος βελτιστοποίησης που αφορά στην ανάθεση προϊόντων σε μέσα μεταφοράς και δρομολόγησης του συμβατικού οχήματος, ο οποίος μπορεί να αξιοποιηθεί τόσο υπό δεδομένες συνθήκες, όσο και στοχαστικές.

- Πραγματοποιήθηκε εντός του πλαισίου της ίδιας της διατριβής σειρά τροποποιήσεων τμημάτων της αρθρωτής μεθοδολογίας, αποδεικνύοντας την ευελιξία της.
- Χρησιμοποιήθηκαν και εντάχθηκαν στη μεθοδολογία σύγχρονα εργαλεία ανάλυσης (Γεωγραφικά Συστήματα Πληροφοριών – GIS, αυτοματοποίηση και βελτιστοποίηση μέσω προγραμματισμού), συνδέοντας την έρευνα με τις αναδυόμενες τάσεις ως προς την οργάνωση, συλλογή και ανάλυση δεδομένων.

Πιο συγκεκριμένα, η εν λόγω έρευνα παρουσιάζει μεθοδολογικά χαρακτηριστικά που καλύπτουν κενά ή αναπτύσσουν περαιτέρω τομείς με λίγη εμβάθυνση ως τώρα στη διεθνή βιβλιογραφία, στα εξής σημεία:

- Προτείνεται ένα μικτό σύστημα Σημείων Εκτόξευσης, με διαφορετικά χαρακτηριστικά μεταξύ τους. Οι Θέσεις Παράδοσης μπορούν να χρησιμοποιηθούν για ανάπτυξη ΣμηΕΑ από το Συμβατικό Όχημα, αν το επιτρέπουν οι τοπικές συνθήκες (χώρος, ασφάλεια, εναέριοι περιορισμοί, έγκριση πελάτη κτλ). Οι Εικονικοί Κόμβοι, για παράδειγμα (ανοιχτοί χώροι, χώροι στάθμευσης κτλ) μπορούν να χρησιμοποιηθούν για ανάπτυξη ΣμηΕΑ. Και στις δύο περιπτώσεις το ΣΟ πρέπει να περιμένει τα ΣμηΕΑ να επιστρέψουν. Αυτή η υποχρέωση αναμονής δεν υπάρχει στην Κεντρική Αποθήκη ή στις Απομακρυσμένες Αποθήκες, καθώς η ανάπτυξη ΣμηΕΑ γίνεται από το προσωπικό τους. Η χρήση όλων των σχετικών Σημείων Εκτόξευσης δεν είναι υποχρεωτική.
- Γίνονται παραδόσεις τόσο από Συμβατικό Όχημα όσο και από ΣμηΕΑ.
- Το δίκτυο του Συμβατικού Οχήματος είναι διαθέσιμο για χρήση, αλλά δεν χρησιμοποιούνται απαραίτητα όλοι οι κόμβοι και οι σύνδεσμοί του. Διαχωρίζονται οι υποχρεωτικοί κόμβοι βάσει των δράσεων (παράδοση πακέτου, ανάπτυξη ΣμηΕΑ, αρχή και τέλος διαδρομής), δημιουργώντας ένα δίκτυο-κέλυφος. Αυτό προσθέτει στην ευελιξία του μοντέλου και τη χρήση του υπό οποιεσδήποτε συνθήκες ζήτησης ή λειτουργίας εγκαταστάσεων.

- Ο ειδικός αλγόριθμος Ανάθεσης και Δρομολόγησης αναπτύχθηκε ειδικά για το εν λόγω πρόβλημα και τα δύο του βήματα λειτουργίας είναι διασυνδεμένα, ενώ χρησιμοποιείται διαφορετική μεθοδολογία για το εσωτερικό και εξωτερικό του τμήμα. Ο Αλγόριθμος, ταυτόχρονα, είναι ευέλικτος στη χρήση τόσο σε προκαθορισμένες όσο και αβέβαιες συνθήκες.
- Έχουν ληφθεί υπόψη Απαγορευμένες Ζώνες κάθε σχήματος ή μεγέθους και το μοντέλο έχει προσαρμοστεί ώστε να εξαλείφονται οι μη προσεγγίσιμες θέσεις για ΣμηΕΑ, είτε λόγω ένταξής τους σε τέτοιες ζώνες, είτε λόγω υπέρβασης της μέγιστης απόστασης πτήσης ΣμηΕΑ, μετά την αλλαγή της διαδρομής του.
- Τμήμα της ανάλυσης πραγματοποιείται σε περιβάλλον GIS, με χρήση σύγχρονων εργαλείων.
- Η μοντελοποίηση του συστήματος και της μεθοδολογίας επίλυσης γίνεται με απλοποιημένο αλλά μοναδικό τρόπο, επιτρέποντας τροποποιήσεις σε κάθε βήμα, χωρίς να επηρεάζεται το τελικό αποτέλεσμα, λόγω ανελαστικών διασυνδέσεων των επιμέρους διεργασιών. Είναι εύκολη η χρήση του για εξέταση εναλλακτικών σεναρίων (π.χ. απόφαση για εγκατάσταση Απομακρυσμένων Αποθηκών ή Εικονικών Κόμβων σε ένα δίκτυο), τροποποιώντας απλώς τον χαρακτήρα κόμβων.
- Εντάσσουμε στη μεθοδολογία στοιχεία αβεβαιότητας τόσο για το Συμβατικό Όχημα (συνθήκες κίνησης επί του δικτύου), όσο και για τα ΣμηΕΑ (καιρικές συνθήκες). Αναπτύσσεται μια ειδική μεθοδολογία για προγραμματισμό επιχειρήσεων επόμενης μέρας υπό αβεβαιότητα, επιτρέποντας σχεδιασμό με ικανοποιητική απόδοση και λιγότερο ρίσκο.
- Κυριότερο ίσως όλων, η συμπερίληψη όλων των παραπάνω στοιχείων σε μια ολοκληρωμένη μέθοδο.

Προτάσεις για μελλοντική έρευνα

Βασικός στόχος της έρευνας ήταν να αναπτυχθεί η πλατφόρμα με τέτοιο τρόπο, ώστε να είναι ανοιχτή σε τροποποιήσεις, βελτιώσεις και επεκτάσεις. Αξιοποιώντας

αυτές τις ιδιότητες, μπορούν να προταθούν ορισμένες κατευθύνσεις για μελλοντική έρευνα.

Στο κομμάτι της βελτιστοποίησης των λύσεων αναπτύχθηκε ένας ειδικός εμφωλευμένος γενετικός αλγόριθμος, όμως μπορεί να εξεταστεί η χρήση άλλων μεθόδων βελτιστοποίησης ή η ανάπτυξη νέας.

Η χρήση ενός Συμβατικού Οχήματος και πολλαπλών ΣμηΕΑ ήταν η βάση για το μοντέλο της εν λόγω έρευνας. Η πραγματικότητα των επιχειρήσεων μεταφορών πακέτων δείχνει ότι αξιοποιούνται πολλαπλά Συμβατικά Οχήματα για διαφορετικές περιοχές. Μια επέκταση του μοντέλου για συμπερίληψη πολλών Συμβατικών Οχημάτων και κάλυψης ακόμα μεγαλύτερων περιοχών διανομής θα ήταν ενδιαφέρουσα προοπτική.

Τέλος, ειδικά σε περιοχές εκτός αστικών κέντρων, απομακρυσμένες τοποθεσίες και για διανομές σε μεγάλη απόσταση η παρουσία έντονου εδαφικού αναγλύφου αναμένεται να παίζει σημαντικό ρόλο στη διαμόρφωση της τελικής διαδρομής των ΣμηΕΑ, λαμβάνοντας υπόψη και τον περιορισμό σε ύψος πτήσης. Μια τρισδιάστατη προσέγγιση των πορειών πτήσης των ΣμηΕΑ μπορεί να αποτελέσει ένα επιπλέον βήμα ανάλυσης.

Contents

Tables

Figures

Photographs

Abbreviations

AROnGA	Assignment and Routing Optimization nested Genetic Algorithm
AWZ	Adverse Weather Zone
CD	Central Depot
CD′	Central Depot (Duplicate)
CV	Conventional Vehicle
CVN	Conventional Vehicle Network
CVT	Conventional Vehicle (total travel) Time
DL	Delivery Location
LS	Launch Site
RD	Remote Depot
RZ	Restricted Zone
SN	Service Nodes
TOT	Total Operations Time
UAV	Unmanned Aerial Vehicle (aka drone)
UL	UAV visitable Location
VH	Virtual Hub
VTOL	Vertical Take-Off and Landing (type of UAV)

1 Introduction

This section discusses the scientific background and motivation behind this Thesis and then the general problem is defined.

1.1 Background and Motivation

General

This research has been inspired by experience and challenges met out in the field, and emerging trends in transportation research. After many years of involvement in transportation engineering projects, best practices and constraints were identified. Problems were often addressed with smart planning and workarounds; however certain limitations still exist and require another step forward.

Commonly used conventional vehicles (CV) for logistics services are a significant source of pollution and energy mismanagement. A more efficient and environmentally friendly scheme would benefit all parts involved. Network discontinuities, or unfavorable sprawl patterns make it more difficult to efficiently integrate transport or any type of assistance services with urban or suburban operations and make the latter fast and profitable for companies. In this context, conceptualizing and finally setting up an efficient multimodal transport system consisting of conventional vehicles and Unmanned Aerial Vehicles (UAVs) may prove useful in many ways.

UAVs in transport

The idea of using UAVs, commonly referred to as "drones", for transport purposes is not new; however, it was seriously considered only when significant advances in technology were made, and their commercial use skyrocketed during the last two decades. The use of UAVs is expected to have significant effects on various sectors, with their impact on transport economy, the environment, employment, and infrastructure being a matter of developing research (ITF, 2021). Several applications are identified, such as automation of intralogistics,

first/last mile parcel delivery, supply of medical goods or even transportation of air freight when UAV specs allow (Roland Berger Gmbh, 2020). DHL launched its "Parcelcopter 4.0" pilot project for medical supplies delivery in Tanzania back in 2018, (UAV speed 130 km/h, max flight time 40 min, payload 4kg, over 65km distances), while Zipline has been offering similar services - primarily blood samples and blood products- in Rwanda since 2014 (Roland Berger Gmbh, 2020). Matternet (Matternet, 2023) is another company offering parcel delivery services, producing their own aircraft, and establishing take-off/landing bases. Their integration in the transport system still faces great challenges in terms of the existing regulatory framework, societal acceptance, and ground infrastructure ("droneports"). Surveys have shown a cautious acceptance by the public, appreciating the potential benefits in speed of delivery and environmental impact, but citing concerns primarily about safety (more than 40% of respondents in various regions worldwide), privacy (13-29%) and noise (9-21%) (McKinsey & Company, 2021).

The EU has set ambitious targets for 2020-2030, aiming for reduction of 40% of GHGs relative to 1990 levels and a share of 35% of zero or low-emission new cars and vans by 2030 (European Commission, 2017). A 100% zero-emission fleet is envisioned in cities by 2050 and several countries are set to ban internal combustion engines in urban areas by 2032 (Witkamp, van Gijlswijk, Bolech, Coosemans, & Hooftman, 2017). Rapid consumer behavioral changes have led to a significant increase in online shopping and at-home/at-work deliveries. This transport work relies heavily on conventional vehicles, running on fossil fuels, such as delivery trucks or vans; and this is especially true for last-mile deliveries, which could account to up to 20%-30% of a city's CO2 emissions (Davies, 2020). The result is a deterioration in terms of traffic congestion, air, and noise pollution. Moreover, poor road connections, missing links, combined with urban sprawl and the isolation of traditionally segregated areas are additional sources of inequality.

Witnessing the problem in real life

A special case - representing much of this research's motivation- is serving remote and underprivileged areas with downgraded or non-existent transport connections. This may refer to providing everyday basics or humanitarian help. Such locations are often not very far from large urban areas or may even form remote clusters themselves. Thus, service of these areas remains insufficient, adding to their unattractiveness and worsening life quality.

A vivid example that fueled our motivation was met during a series of visits to the mountains north of Kigali, Rwanda for a big road improvement project, back in 2015. It was impressive to see the amount of distance covered on foot or bicycle just to get everyday basics. Truck deliveries were scarce, because of the downgraded road network and the relative position of villages. At the same time, it was more than obvious that certain locations were not actually too far off between them, assuming an as-the-crow-flies path.

Photograph 1: Pushing loaded bicycles on dirt road (section: Nyacyonga – Mukoto, Rwanda)

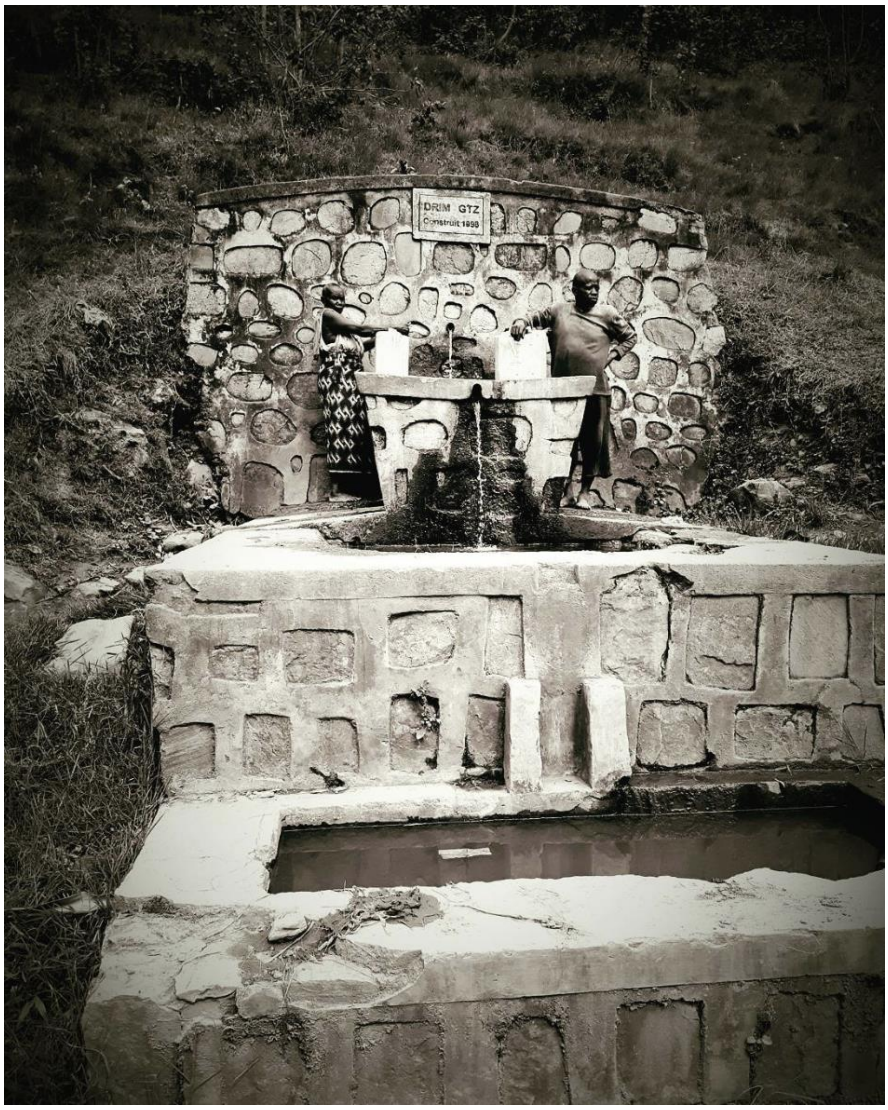

Photograph 2: Filling water barrels at water source (section: Nyacyonga – Mukoto, Rwanda)

Research in designing cooperative transport systems with UAVs.

Each transport mode has its own advantages and limitations. Conventional vehicles rely on a fixed network, which does not guarantee access to any given point of demand. UAVs are more flexible and can fly as straight as free airspace allows. However, they are often limited in range because of battery capacity and are also affected by the weather. Thus, a growing research interest has emerged on the specific problem of UAV – ground transport cooperation. After all, multimodal transport systems of various combinations have been

devised throughout history; trucks, trains, airplanes, and ships have been working together in the supply chain. Each mode comes to complement each other, to exploit the best of both (or more) modes.

In literature, the problem is commonly categorized in the wider Vehicle Routing Problem (VRP) family. It is essentially a concurrent mode assignment and vehicle routing problem where ground vehicles (usually trucks) are combined with drones to serve last mile goods transport. The problem is more specifically named Vehicle Routing Problem with Drone (VRP-D), Truck and Drone Routing Problem (TDRP), or Two-Echelon Vehicle Routing Problem with Drone (2E VRP-D). The special actions concerning drone deployment are also commonly referred to as Launch and Recovery Operations (LARO).

A widely cited research work on this field is the one of Murray & Chu (Murray & Chu, 2015), introducing the "Flying Sidekick Traveling Salesman Problem" (FSTSP), where customers can be served either by a truck or a UAV (working in tandem), the latter being able launch from the truck or the depot to customers and return to the same or a different location. There is no restriction to the feasibility of paths for the truck, while the UAV is limited by its operational range; all locations in the said formulation are customer locations. A separate case is identified, where some customers are relatively close to the depot (within UAV range) and others significantly farther. This is defined as parallel drone scheduling traveling salesman problem (PDTSP), where the truck and a fleet of UAVs start from the depot together. Additional work on the originally introduced FSTSP was done by Murray & Raj (Murray & Raj, 2020), where multiple UAVs are available, the truck can launch or retrieve one UAV at a time and the UAV cannot return to its launch location. Multiple UAVs and a truck are also used by Ferrandez et al (Ferrandez, Harbison, Weber, Sturges, & Rich, 2016), where no path constraints for the truck or the UAVs are assumed, and the truck moves along a TSP route. Similar work by Moshref-Javadi et al (Moshref-Javadi, Hemmati, & Winkenbach, 2020), allows a different take-off and landing location for UAVs but still consider delivery locations as potential stop points. Agatz et al (Agatz, Bouman, & Schmidt, 2018) assume

launch sites only at delivery locations, a different take-off and landing point for the UAVs. Moshref-Javadi et al (Moshref-Javadi, Lee, & Winkenbach, 2020) assume a single truck and multiple UAVs, considering routes only involving the depot and customer locations with identical take-off and landing points for each UAV route; the objective is minimizing customer waiting times and thus there is no demand for a final return to the depot. Salama and Srinivas (Salama & Srinivas, 2022) propose a system where not all delivery locations can be used as launch/recovery sites, but non-customer locations can also serve as ones. All items lying on the truck's route must be served by the truck. Assignment of items to a vehicle, truck routing and operations scheduling are key decisions.

A distinct concept, allowing also en-route launch/recovery of UAVs rather than only at specific nodes was introduced by Marinelli et al (Marinelli, Caggiani, Ottomanelli, & Dell'Orco, 2017). Chand & Lee (Chang & Lee, 2018) use a single truck – multiple UAVs system with identical take-off and landing locations for each UAV route. Moving launch and recovery locations (LRLs) along the truck arcs (TDRP-SA) were studied by Li et al (Li, Chen, Wang, & Zhao, 2022). Different altitudes for package deliveries and the drones' energy consumption are included in the calculations by Momeni et al. (Momeni, Mirzapour Al-e-Hashem, & Heidari, 2023), who considered a drone-only delivery system. Boysen et al. (Boysen, Briskorn, Fedtke, & Schwerdfeger, 2018) use fixed routes and stops for the truck and then attempt to synchronize the drones at said locations for LARO. Customer locations as LARO points were assumed by Li & Wang (Li & Wang, 2022), structuring a truck-drone routing problem with time windows (TDRP-TW). Jeonga et al. (Jeonga, Song, & Lee, 2019) considered the parcel weight effect on drone energy consumption and assumed circular restricted flying areas. Re-chargeable drones meeting with the truck for battery changes at customer locations are studied by González-Rodríguez et al. (González-Rodríguez, Canca, Andrade-Pineda, Calle, & Leon-Blanco, 2020).

Mathematical background and solution methodologies

Apart from setting up the cooperative scheme, various techniques have been applied to obtain optimal solutions. Despite the specificity of such newly introduced problems, a common base reference for this family is the well-studied Traveling Salesman Problem (TSP) and its variants. Various solution methods have been developed and TSP itself is a known NP-hard problem (Dantzig, Fulkerson, & Johnson, 1954), (Bellman, 1962), (Little, Murty, Sweeney, & Karel, 1963), (Garey & Johnson, 1979), (Applegate, Bixby, Chvátal, & Cook, 1995), (Applegate, Bixby, Chvátal, & Cook, 2008). A comprehensive guide on the TSP, real applications and solution methodologies is presented by Rardin (Rardin, 2015). A family of sequencing problems such as the TSP, scheduling and assembly-line balancing are treated through dynamic programming by Held & Karp (Held & Karp, 1962). Genetic algorithms (Holland, 1975), tabu search (Glover, 1986), (Glover, 1989), (Glover, 1990) simulated annealing (Kirkpatrick, Gelatt, & Vecchi, 1983), k-means clustering (MacQueen, 1967) are among the most used solution methods met in literature concerning this family of problems.

Extending from the TSP to real-world applications, the Vehicle Routing Problem (VRP) appears also in various forms and similar solution methods are used. Iliopoulou et al (Iliopoulou, Kepaptsoglou, & Karlaftis, 2015) used a genetic algorithm to solve a capacitated VRP for the design of passenger seaplane routes. A multi-objective VRP model, was also studied by Iliopoulou et al (Iliopoulou, Kepaptsoglou, & Schinas, 2018), this time considering environmental risks for the development of an oil maritime transportation service. Another similar formulation for our problem is the hub-and-spoke setup, which is met in sea or air transport, because of the geographical location of ports and their extensive use as transshipment nodes.

Part of exploring optimal solutions in routing depends on finding shortest paths between locations. Numerous exact algorithms and heuristics have been developed for this purpose, such as the original Dijkstra algorithm for source-to-all paths calculations (Dijkstra, 1959), the A* algorithm for finding the shortest path between any pair of nodes (Hart, Nilsson,

& Raphael, 1968) and its future variants, such as the Iterative Deepening Algorithm (or IDA*) (Korf, 1985) and the Lifelong Planning A* (or LPA*) (Koenig, Likhachev, & Furcy, 2004).

In the specific area of cooperative schemes involving UAVs, similar methods have been used. Simulated annealing and Tabu-search were used by Moshref-Javadi et al (Moshref-Javadi, Lee, & Winkenbach, 2020). Salama (Salama & Srinivas, 2022) solved the problem in a route first – cluster second approach, using simulated annealing and variable neighborhood search for optimization. Chand & Lee (Chang & Lee, 2018) develop a solving methodology using initially formed k-means clusters and then testing shifts-weights to move their centers, which will ultimately define the truck route. Optimal stop/launch locations are found also using k-means clustering by Ferrandez et al (Ferrandez, Harbison, Weber, Sturges, & Rich, 2016). Agatz et al (Agatz, Bouman, & Schmidt, 2018) set up a route-first, cluster-second optimization approach, using local search and dynamic programming heuristics. González-Rodríguez et al. (González-Rodríguez, Canca, Andrade-Pineda, Calle, & Leon-Blanco, 2020) used an iterated greedy heuristic based on the iterative process of destruction and reconstruction of solutions, assisted by a global optimization scheme through a simulated annealing (SA) algorithm. An exact algorithm for the solution of the two-echelon truck and drone problem was developed by Zhou et al. (Zhou, Qin, Cheng, & Rousseau, 2023), this time considering multiple vehicles and drones and employing an exact branch-and-price algorithm, after an initial tabu search application. An agent-based method to solve the Truck-Multi-Drone Team Logistics Problem (TmDTL) was proposed by Leon-Blanco et al. (Leon-Blanco, Gonzalez-R, Andrade-Pineda, Canca, & Calle, 2022).

Macrina et al. (Macrina, Pugliese, Guerriero, & Laporte, 2020) presented a review of relevant research and practices, highlighting gaps and future research topics and pointed at the inclusion of more realistic parameters, considering dynamic conditions and uncertainty.

How does this research make things go forward?

In our understanding, research focus has been laid mostly into exploring theoretical schemes and optimization methods for best performance. However, we wanted to create

something which is backed scientifically but can also be of real value in the industry; an ergonomic front-end, with a complex but solid background. Through thorough understanding of any modelling, optimization, and practical application challenges, we elaborate a transport system setup which is scalable, flexible, and adaptive to infrastructure and equipment. The framework is almost entirely modular, extending from the moment any initial input is given to the last steps of the solution optimization. It is intentionally developed in such a way that various types of network and demand patterns can be tackled: dead-ends, missing links, deliveries along corridors or scattered at remote locations, railway, or sea transport networks. This very nature of the original concept is exploited even within the scope of this research, as it is further expanded in two more stages: planning under regulatory airspace restrictions and risk-based planning, acknowledging uncertainties in conventional vehicle network conditions and weather forecast. A detailed mathematical representation of each concept is developed, and relevant performance calculation workflows are described. We develop an efficient solution optimization process, through a dedicated assignment and routing optimization nested genetic algorithm scheme. The same algorithm can be used as a basis to obtain solutions both under known and uncertain conditions. Through a series of experiments on specifically designed case studies, we have demonstrated the model's capabilities, verifying its flexibility, reliability, and robustness under various circumstances. The initial design can indeed adapt to a spectrum of networks, infrastructure, and equipment specifications, using a simplified input-output structure. The presence of restricted zones greatly affects the results of the assignment and routing optimization process and should be considered in strategic planning of such operations. Additionally, uncertainty of conditions over the fixed network or the airspace (weather) are a major hindrance for obtaining optimal solutions, but our robust optimization method offers a way to minimize risk and lost time with prior planning.

Because of the need for safe UAV deployment sites and the high presence of restricted airspace zones in urban environments, the intended field of application is assumed to be the delivery of small packages in rural and under-connected areas, the execution of inter-city

deliveries, and the expansion of a city's original service range. Putting together years of research and work experience, this research aspires to create a platform destined for future evolution, while offering tools for optimizing parcel delivery services.

Summing up our contribution, several aspects of our method can be seen as novel individually, but mostly when regarded as a holistic approach that includes all of them:

- We are proposing a mix of variable launch sites for LARO, featuring different characteristics among them. Customer locations can be used for CV-based UAV deployment, if local conditions allow (space, safety, airspace restrictions, customer approval, etc.). Virtual Hubs, for example, open spaces, parking lots, etc., can also be used for CV-based LARO. In both of those cases, the CV must wait for all its UAVs to return. UAVs can also be deployed from the Central Depot at the start, without any CV involvement, but also at the end, receiving items from the CV. Remote Depots are another facility type where the CV can leave items for UAV delivery, and LARO is performed by the Depot personnel. Not all LARO locations are necessarily used.
- Deliveries can be made both by CV and UAV.
- The CV network is available for routing and LARO, but not all nodes and links are necessarily used. We distinguish the mandatory nodes for actions and routing after the assignment process, creating the so-called "shell network". This allows for our model to be practically implemented with different demands and infrastructure each time.
- The Assignment and Routing Optimization nested GA is developed specifically for our problem, with its two steps being interconnected and using different methods for the inner and outer GA (discrete values resulting from the service nodes for the assignment process and random keys-based ordering of nodes for routing). The core of the algorithm is used both for obtaining solutions under fixed/given conditions and under uncertainty.

- We have considered the presence of Restricted Zones of any shape and size and adjusted our model to filter out non-reachable locations, either because they are in such zones or because the resulting UAV paths are longer than the UAV range allows.
- We are adjusting the model, incorporating spatial and optimal path analysis with GIS as part of the methodology, and opening to modern methods and input norms.
- The formulation is conveniently simplified but unique to its kind since it must address the specific setup. It creates a modular and open platform that is open to modifications, and we present all the analytical calculations involved. This also helps with strategic planning, e.g., deciding where to establish Remote Depots or Virtual Hubs, by conveniently testing alternative locations.
- We are considering uncertainty both on the ground and in the air, acknowledging the stochasticity in travel times over the CV network and the Weather. A special methodology for producing next-day assignment and routing plans has been elaborated, allowing for operations with satisfactory performance and less risk.
- The consideration of all the above in a single proposed method, in a comprehensive and holistic approach.

1.2 General Problem Statement

Multiple items need to be transported from a Central Depot (CD) to customers located at Delivery Locations (DL). The items can be delivered to the DLs either by a Conventional Vehicle (CV) or an Unmanned Aerial Vehicle (UAV). The CV follows a fixed network for transportation, while UAVs offer more flexibility but have limitations in terms of range. The CV is not limited by its operational range and is expected to be able to complete the entire journey without refueling or charging. The UAVs are assumed to be electric, and a battery swap is executed at the start of operations or during the UAV preparation at each site when

the same UAV is used again. Potential no-fly zones and adverse weather conditions can affect the UAVs, while conditions over the CV network have an impact on its speed and routing options. Each item is assigned a specific mode of transportation for either the final segment or the entire journey. Based on certain characteristics, UAVs can only be launched or recovered at designated locations throughout the network. A decision is required, dictating the final mode assignment for each item, the nodes used for UAV deployment and the CV route.

Expanding a bit on the basic notion, the terms “conventional vehicle”, “item”, “delivery” and “customer” mostly carry a symbolic meaning. For instance, instead of parcel deliveries, one could assume any form of service needed at a specific location, e.g., reconnaissance, inspection, search & rescue, aid drop-off. Additionally, a conventional vehicle could be a truck, train or sea vessel and the equivalent network can be used.

2 Research Evolution and Structure

The research is developed through a layered process, resulting from different levels of ongoing understanding and complexity.

First, the core aspects of the general problem are addressed. In this sense, a fundamental transportation system setup is developed, suggesting types of facilities and the way the CV and the UAVs can be utilized. The framework should be modular, scalable, and adaptive to infrastructure and demand, offering options over each of its components for optimization or preference-based solutions. Common mathematical conventions in network design and operations research are used as the basis for modeling the problem and its solution methodology; however, throughout the entire process, it is essential to keep focus on real-life challenges and direct implementation capabilities. As such, a more practical-oriented approach is being followed. The goal is to present an efficient and ready-to-use decision-making tool for transport services at a strategic level, which also includes a custom optimization methodology. This is the most integral part of this research, where all further expansions within its scope will be based, but it also unleashes the potential for future research by any interested party. The framework and solution methodology produce an optimized suggestion for the execution of transport services, assigning each item to a final mode of transport, highlighting the locations where UAVs are deployed from and what route the CV should follow to complete the operations in the minimum amount of time possible.

Next, acknowledging the reality in UAV flight operations, the presence of Restricted (or no-fly) Zones is considered. An updated workflow is developed, taking advantage of the fundamental design's modular nature. The same workflow can be used for any type of airspace restriction, including the weather or other threats, i.e., habitats of birds, magnetic, navigation, or telecommunications interference etc., which would ultimately lead to zones of compromised UAV safety and reliability. For this Stage, the framework encoding, analysis, and optimization is additionally carried out in Geographical Information Systems (GIS)

format, to align with common database practices in the business and exploit modern tools in spatial and network analysis. This rationale is followed also through the next stage.

Finally, an expansion towards stochastic planning and designing under uncertainty is pursued. Uncertainty may refer to conditions on the fixed network (e.g., traffic delays), or the weather, which comes as a probabilistic forecast on critical metrics (e.g., wind, precipitation). A new methodology is developed to care for a robust solution which would work satisfactorily under a range of expected conditions. It is possible to define the level of risk one is willing to take and obtain a suggestion for the planning of next-day services.

The general phases of the research are hereby presented as:

i. Fundamental Conceptual Design
ii. Design under Restricted Airspace
iii. Stochastic Planning

Each phase is explained with more case-specific background, its methodology and application on a case study [a]. Results and discussion follow. Figure 1, below, illustrates the general plan of this research and the structure followed along its evolution.

[a] *Networks for case studies were originally design in a CAD environment (AutoCAD Civil 3D) and then geometry data was transformed into simple .csv format. Coding of the entire core workflow and solution methodology algorithms was executed in Python 3.9 (Spyder IDE), on Windows 8.1 and Windows 11. Part of the nested-GA algorithm was coded using the PyGAD open-source Python library. QGIS and ArcGIS were used for network re-encoding, spatial and optimal path analysis, and illustration purposes.*

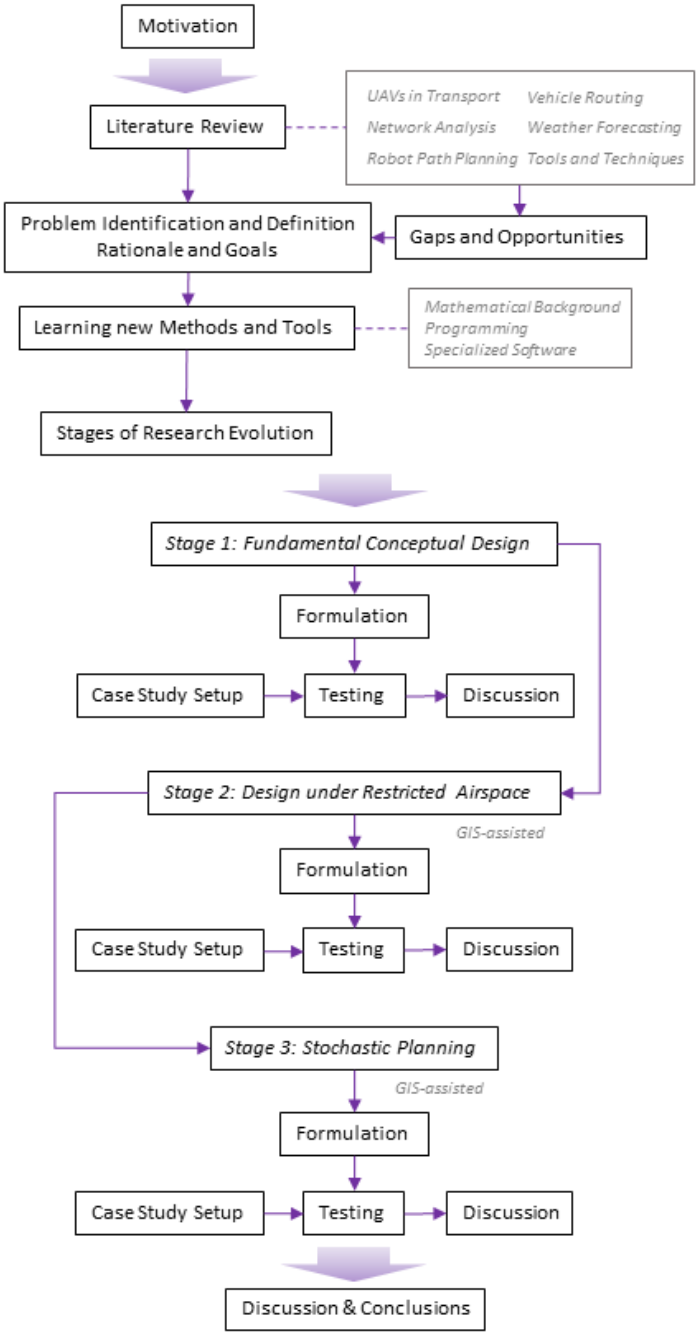

Figure 1: General Research Plan and Evolution

3 Stage 1 - Fundamental Conceptual Design

This chapter explains the fundamental conceptual design of our framework and the developed solution optimization methodology in detail. A case study is used to test for the entire model's efficiency and its practical value in operations planning.

3.1 Transport System Setup

The CV can travel through a specific, fixed network, hereby known as Conventional Vehicle Network (CVN). For the case of trucks, this is essentially the traversable road network within the intended area of operations.

UAVs can be deployed from four different types of locations, collectively named Launch Sites, (LS):

- The Central Depot (CD). UAV deployment can be executed by the Depot personnel and the CV does not get involved.
- Remote Depots (RD). These are organized facilities with available UAVs. UAV deployment can be executed by the Depot personnel and the CV only delivers the items for transshipment.
- Virtual Hubs (VH). Designated locations, such as parking lots, where UAV deployment is conveniently executed by the CV operator. The CV must wait for all deployed UAVs to return.
- Delivery Locations (DL). Some of the DLs can also be used for UAV deployment, provided the site is safe. The CV must wait for all deployed UAVs to return.

It is important to keep in mind that launching and collecting a UAV is possible in other locations than just the CD and DLs. Additionally, not all DL are potential LSs. This is different from the assumption commonly met in literature of cooperative truck-drone systems, where drones can only fly from/to customer locations or the central depot. It is also self-evident that

a LS must belong to the original CVN. Figure 2 illustrates the potential relationships between the sets of nodes.

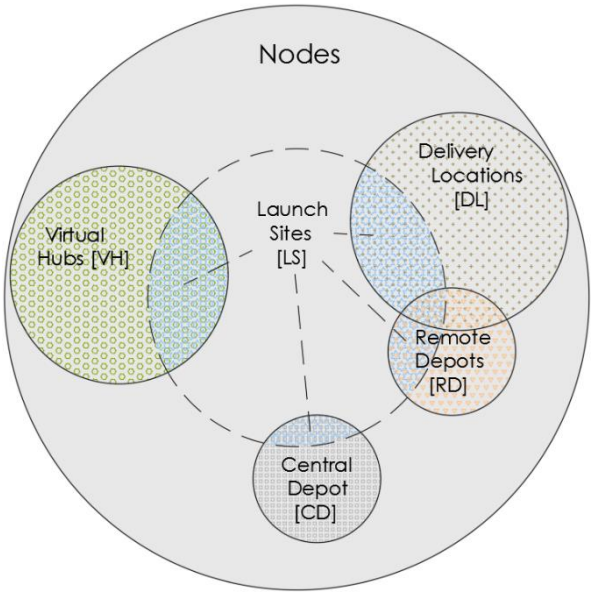

Figure 2: Venn diagram; schematic representation of Node sets

3.2 Assumptions and Constraints

A set of general assumptions can be summarized as follows:

- A single CV is assumed to be available, departing from the CD and attempting to deliver the items to their destinations.
- The vehicle is assumed to be of adequate capacity for the items and any UAVs may be needed onboard.
- Vertical Take-off and Landing (VTOL) UAVs are selected.
- Each destination can be visited once for delivery or UAV deployment (or both, during the same stop) but can be accessed more than once for routing purposes.
- There is no predefined mode assignment for the items, but there is an option of forcing one if needed.
- There is no predefined order of visit for the destinations, but there is an option of forcing one if needed.

- The CD is the start and end node for the conventional vehicle tour.

The initial given input for the problem is the fixed network which is available for the CV. CVs can travel over this fixed, known network. UAVs have no fixed network to fly through, and their ultimate course is determined by take-off and landing location, following a direct straight path, if the route is feasible based on the UAV's range.

We also assume that:

- Each item is assigned to one Vehicle for the final step of delivery.
- The CV can be assigned to multiple destinations.
- Each UAV has capacity for one item.
- Each UAV can travel to and return from one destination per tour (the same UAV can be later re-deployed, but we have assumed enough UAVs for all operations anyway).
- UAVs can be deployed as a fleet from a single station.
- Launching of all UAVs from a launch site is simultaneous, but each one returns at a different time depending on the length of its tour.
- A UAV is recovered at the same location from where it was launched.
- RDs can deploy UAVs without the CV having to wait for their return. Certain transshipment time is still required.
- The CD, used at the start of operations, can deploy UAVs without the CV having the wait and no transshipment time is required.
- Only one transfer between vehicles is allowed per item.

We have drafted a series of examples and drawings to explain the general concept in simple terms at first. The legend in Figure 3 below explains the basic symbols and notations used.

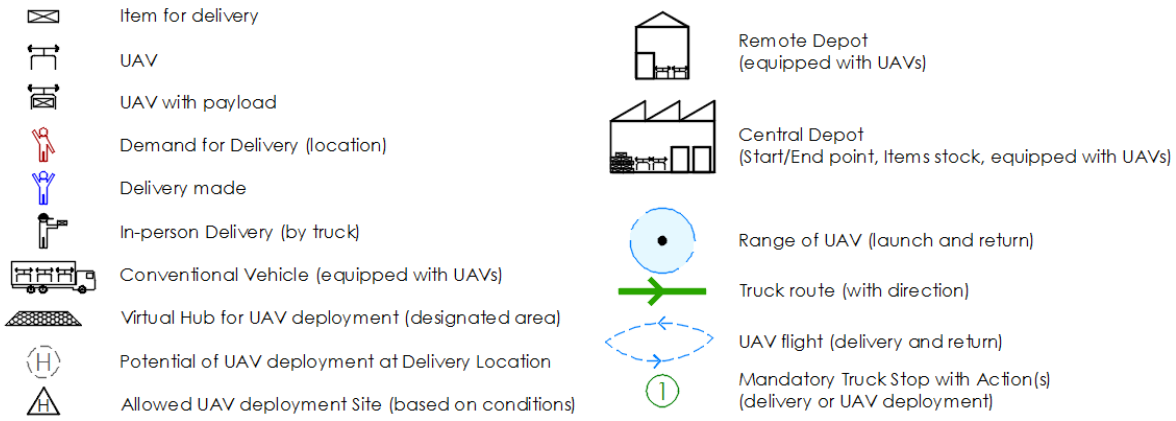

Figure 3: Symbols and notations for general concept

In this hypothetical network, there is a supposed demand for service at certain locations. We form three cases of demand and available infrastructure and then some of the potential assignment and routing solutions are presented. Our framework supports many more combinations, but the most important for the general understanding are included here.

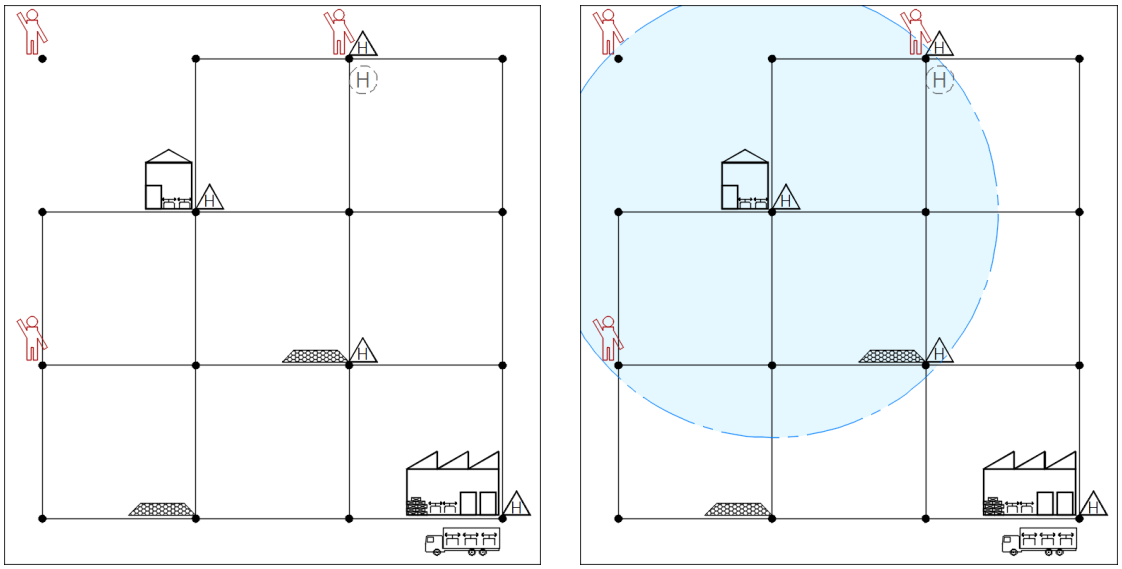

Figure 4: Example 1 - Infrastructure, Demand and UAV Range (indicative, from one of the launch sites)

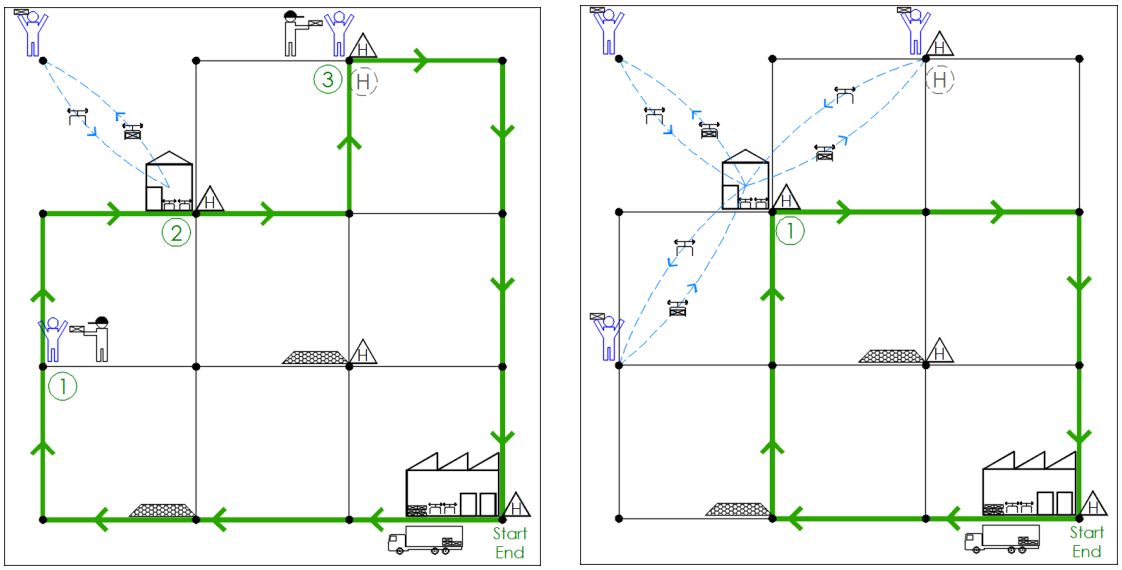

Figure 5: Example 1 – Possible assignment and routing solutions (solution 1 - left, solution 2 - right)

In solution 1 (left), the truck departs from the CD. It reaches a customer for in-person delivery (Stop 1). Then it visits a RD (Stop 2), where it leaves an item for UAV delivery to be executed by the Depot personnel. It leaves without waiting for the deployed UAV to return and goes on to Stop 3, where another in-person delivery is made. It then returns to the Central Depot.

In solution 2 (right), the truck departs from the CD. It reaches a RD (Stop 1), where it leaves all items for UAV delivery to be executed by the Depot personnel. It leaves without waiting for the deployed UAVs to return and it then returns to the CD.

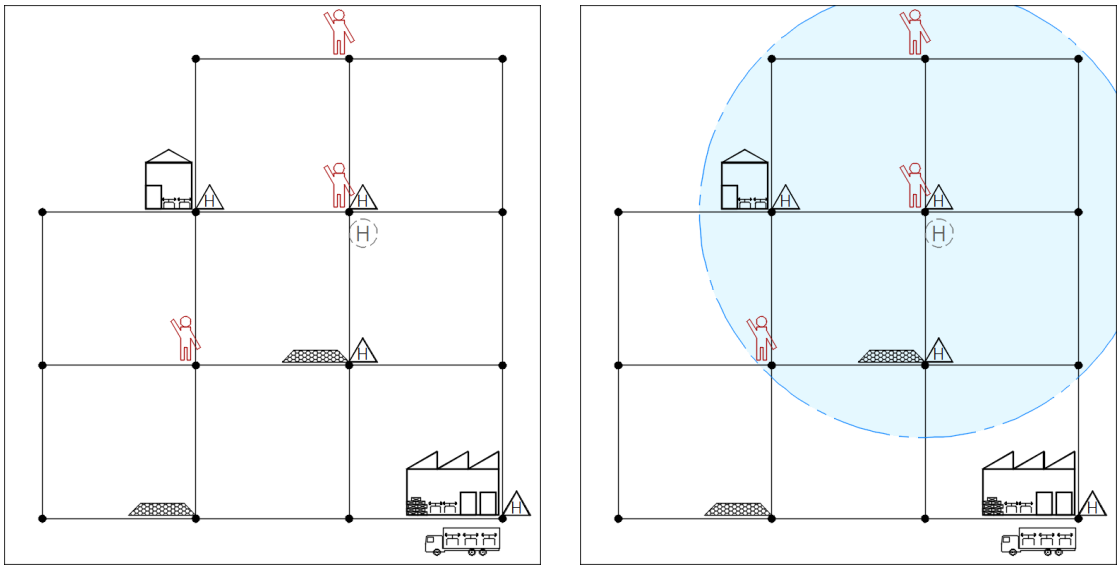

Figure 6: Example 2 - Infrastructure, Demand and UAV Range (indicative, from one of the launch sites)

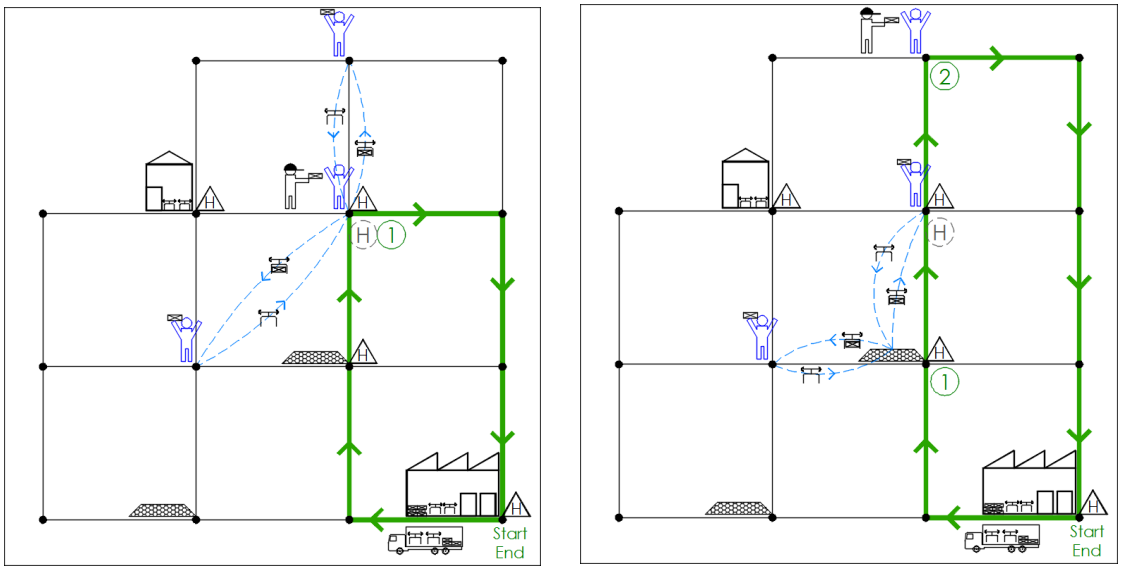

Figure 7: Example 2 – Possible assignment and routing solutions (solution 1 - left, solution 2 - right)

In solution 1 (left), the truck departs from the Central Depot. It reaches a customer for in-person delivery (Stop 1). It stays there after the delivery and deploys the onboard available UAVs to serve two other customers. The truck waits for the deployed UAVs to return and then returns to the Central Depot.

In solution 2 (right), the truck departs from the Central Depot. It reaches a Virtual Hub (Stop 1), namely a designated area for UAV deployment (e.g., parking lot or another reserved platform), where it deploys onboard available UAVs to serve two customers. The truck waits for the deployed UAVs to return and then reaches Stop 2, where an in-person delivery is made. It then returns to the Central Depot.

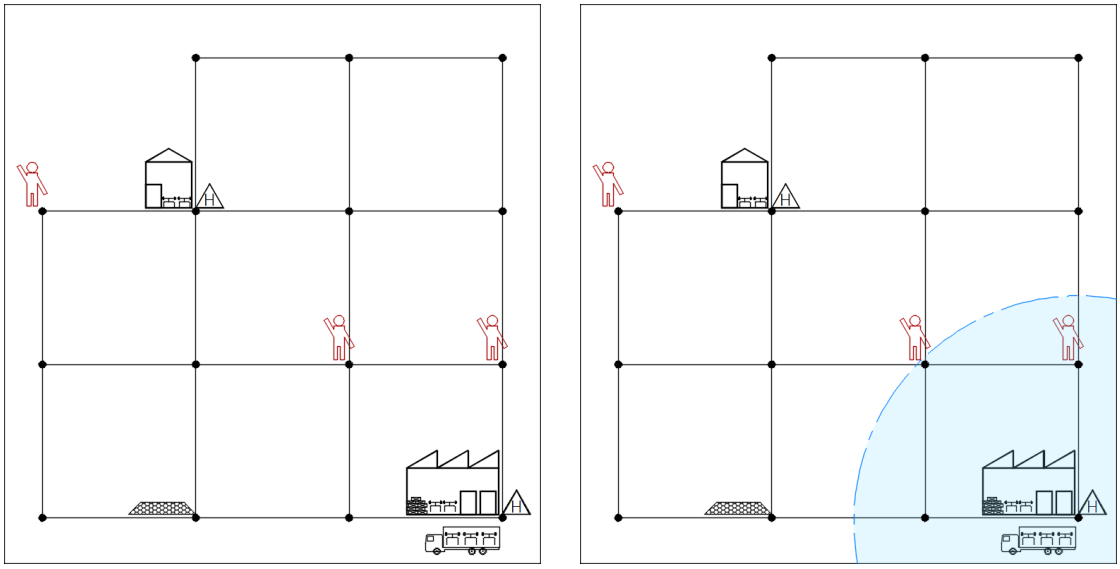

Figure 8: Example 3 - Infrastructure, Demand and UAV Range (indicative, from one of the launch sites)

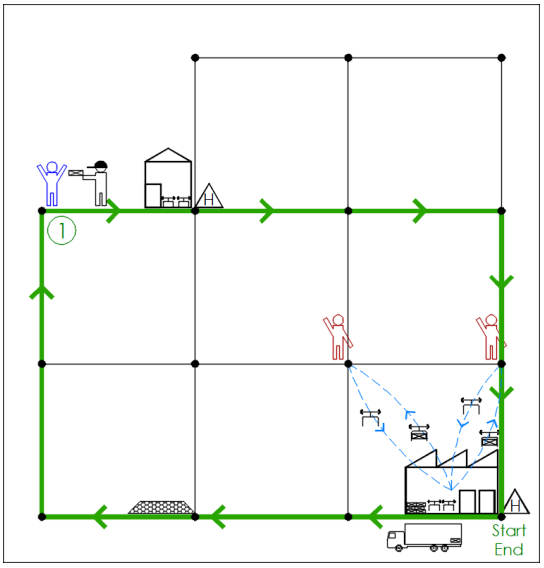

Figure 9: Example 3 – Possible assignment and routing solution

Here, the CD is used for UAV deployment for two customers. The UAVs are launched from the CD, and the truck departs from the CD at the same time, without having to wait for the said UAVs to return. It heads to the farthest customer for in-person delivery (Stop 1). It then returns to the CD.

3.3 Methodology

After establishing the basics of the transport system, a mathematical representation, an analysis workflow, and a solution methodology are developed.

3.3.1 Core Analysis and Solution Workflow

A summarized description of the proposed analysis and solution workflow for the problem at hand is illustrated in Figure 10, below. Detailed analysis follows throughout the next sections.

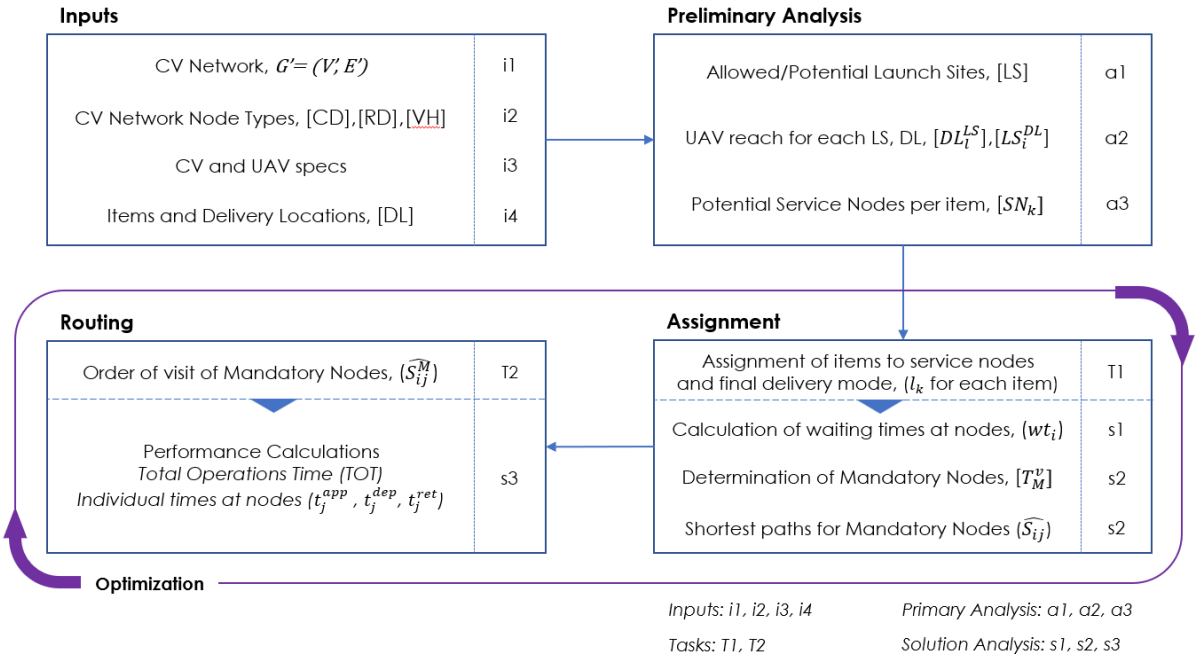

Figure 10: General methodology workflow

In our proposed workflow, Inputs, Tasks, and Analysis are organized in a modular scheme so that a different approach can be followed for some of them.

The initial Inputs include basic information on the physical network (Conventional Vehicle Network - CVN), the infrastructure (Central Depot (CD), Remote Depots (RD), Virtual Hubs (VH)) and equipment specifications (CV and UAV operational characteristics). Demand information follows; a set of Delivery Locations (DL) represents items to be delivered.

Next, Preliminary Analysis defines which sites are finally allowed for UAV deployment (Launch Sites -LS, selected from CD, RDs, VHs and some of the DLs)) and which pairs of DLs and LSs are within UAV range to each other (DL_i^{LS}, LS_i^{DL}). Each item is associated with potential service nodes (Service Nodes Pool - SN_k). A service node for an item may be its own DL node (if within the CVN) or any allowed LS which is reachable by UAV. Analysis "a2" offers an alternative way to perform the assignment later (task T1). Instead of assigning items based on their Service Nodes Pool, we could inversely use the DL_l^{LS} sets of the launch sites. This would be helpful if we were to base our assignment on clustering strategies. If the SN_k of a DL is empty, this means that there is no feasible UAV connection with an LS and that the DL is off the CVN too. In that case, the workflow algorithm excludes this DL from demand and the location is deemed non-serviceable.

The Solution is found through a nested two-level optimization process, seeking optimal assignment of items to a service node (l_k) and optimal CV routing. If the service node coincides with the DL itself, the delivery is executed in-person, by the CV. If not, a UAV is deployed at the service node, executes the delivery, and returns to the same spot. Each time an assignment iteration is produced, a set of mandatory nodes (T^{v_M}) for visit emerges. At each of these nodes, waiting times (wt_i) for the CV are calculated based on the actions required (e.g., in-person delivery, UAV launch and recover, items delivered to an RD for UAV deployment by the personnel).

Shortest paths ($\widehat{S_{ij}}$) between mandatory nodes are calculated, using the given CVN and a new "shell" network is created. The shell network is constructed by the subset of mandatory nodes and travel cost between them. The travel cost results from the pair's shortest path total

cost previously found. Routing for the CV is then a matter of selecting the best order of visit ($\widehat{S_{IJ}^{M}}$) across mandatory nodes. We have opted to use a GA of certain form for tasks T1, T2 and an A* algorithm for analysis s2; however, it is possible to explore other methods.

The target is to minimize the Total Operations Time (TOT), namely the time needed for all vehicles (CV and deployed UAVs) to complete their tasks and return to their intended base. Under this goal, as soon as the best routing is found for the running assignment, the TOT is inherited by the assignment iteration and compared to others.

3.3.2 Model Formulation

We introduce a series of notations and variables, which will be explained later in more detail.

Table 1: Notations and Terminology

Abbreviations			
CV	: Conventional Vehicle (truck, train, vessel, here: truck)	VH	: Virtual Hubs, forming subset T_{VH}^{v}
UAV	: Unmanned Aerial Vehicle (aka drone)	DL	: Delivery Locations, forming subset T_{DL}^{v}
VTOL	: Vertical Take-Off and Landing (UAV type)	LS	: Launch Sites, forming subset T_{LS}^{v}
CVN	: Physical (fixed) network of CV operation	SN	: Service Nodes for item
CD	: Central Depot, forming subset $\boldsymbol{T_{CD}^{v}}$	CVT	: Total time of travel for the CV (since start)
CD'	: Central Depot Duplicate, forming subset $\boldsymbol{T_{CD'}^{v}}$,	TOT	: Global Operations Time, when all vehicles have completed their tasks and have returned to their intended base (since start)
RD	: Remote Depots, forming subset $\boldsymbol{T_{RD}^{v}}$		

Sets and Graphs	
$V' = [0, 1, 2, \ldots, n]$: Set of nodes in CVN	l_k : Assigned service nodes per item k
$E' = \{(i,j) : i, j \in V', i \neq j\}$: Set of edges in CVN	$T_{DLCV}^{v} = [DLCV \subseteq V \mid xd_i = 1,\ i \in DL]$: set of nodes where delivery with CV is executed
$G' = (V', E')$: Graph representing the CVN	$T_{aLS}^{v} = [aLS \subseteq V \mid xl_i = 1,\ i \in LS]$: set of assigned launch sites
$V = [0, 1, 2, \ldots, m]$: Set of nodes combining V' and any DLs not in V'	$T_{M\alpha}^{v} = T_{DLCV}^{v} \cup T_{aLS}^{v}$: set of Mandatory nodes with action (delivery of launch)
$K = [1, 2, \ldots, m]$: *Set of items ("k") for delivery*	$T_{M}^{v} = T_{CD}^{v} \cup T_{M\alpha}^{v} \cup T_{CD'}^{v}$: set of mandatory nodes for CV routing
$\boldsymbol{C_k} = [\boldsymbol{d_1}, \boldsymbol{d_2}, \ldots, \boldsymbol{d_m}] = [\boldsymbol{DL}]$: Set of nodes at Delivery Locations, $\boldsymbol{k \in K}$, $\boldsymbol{C_k \subseteq V}$	
C : attribute matrix for items	
$A = \{(i,j) : i, j \in V, i \neq j\}$: Set of UAV (aerial) edges	

$E = \{(i,j) : i, j \in V, i \neq j\}$: Set of CV edges between nodes in V

$F = (V, A)$: Graph representing UAV network

$G = (V, E)$: Graph, as an expansion of G' including any Delivery Locations not in V'

$\boldsymbol{T^v_{CD}}, \boldsymbol{T^v_{CD'}}, \boldsymbol{T^v_{RD}}, \boldsymbol{T^v_{VH}}, \boldsymbol{T^v_{DL}}, \boldsymbol{T^v_{LS}}$: Subsets of V, including nodes for each respective type, i.e., CD, CD', RD, VH, DL, LS

$\boldsymbol{DL^{LS}_l = \left[A \subseteq V \mid x^{UAV}_{li} = 1,\ i \in DL, l \in LS\right]}$: Delivery Locations within UAV range of Launch Sites

$\boldsymbol{LS^{DL}_i = \left[B \subseteq V \mid x^{UAV}_{il} = 1,\ i \in DL, l \in LS\right]}$: Launch sites within UAV range of Delivery Locations

$\boldsymbol{SN_k = LS^{DL}_{d_k} \cup d_k}$: Pool of service nodes for item; $\boldsymbol{k \in K, d_k \in V'}$

$T^v_{Mc} = T^v_M - (T^v_{CD} + T^v_{CD'})$: set of mandatory nodes without Central Depot and its duplicate

$L_l \subseteq K \mid l_k = l, l \in T^v_{aLS}, k \in K$: set of assigned items per launch site

$G_M = (T^v_M, E_M)$: subgraph for mandatory nodes

$\widehat{S_{ij}}$: specific path of nodes from i to j, $i, j \in V'$,

$\widehat{S_{(i,j)}}$: sequence of edges for specific path from i to j, $i, j \in V'$

$\widehat{S^M_v}$: specific path consisting of mandatory nodes, $i, j \in V',\ e \in E,\ i, j \in T^v_M$

$\widehat{S^M_{(e)}}$: sequence of shell edges for specific path of mandatory nodes, $i, j \in V',\ e \in E$

T^v_{ACCV} : set of accessed nodes

Parameters

S^{CV}	: CV mean speed	R^{UAV}	: UAV range of operation (time)
S^{UAV}	: mean UAV speed at cruising altitude	H^{UAV}	: UAV cruising altitude
$S^{UAV}{}_{asc}$	: mean UAV speed of ascend	tc_i	: transshipment cost (time to deploy/recover UAV)
$S^{UAV}{}_{des}$	: mean UAV speed of descend		

Variables

$\boldsymbol{x^{CD}_i}$	: Binary variable (0,1) indicating node type "Central Depot"	$\lvert L_l \rvert$	: number of items assigned to launch site
		dth_{ij}	: time for UAV deployment-to-home
$\boldsymbol{x^{RD}_i}$	: Binary variable (0,1) indicating node type "Remote Depot"	wt_i	: waiting time of CV on node
		x^{CRD}_i	: binary variable (0,1) indicating whether a node is either type of depots
$\boldsymbol{x^{VH}_i}$	: Binary variable (0,1) indicating node type "Virtual Hub"	ct^M_{ij}	: cost (time) for shortest path between two mandatory nodes
$\boldsymbol{x^{DL}_i}$	: Binary variable (0,1) indicating node type "Delivery Location"	xa_i	: binary variable for access of node by CV
$\boldsymbol{x^{LS}_i}$	: Binary variable (0,1) indicating node type "Launch Site"	uf_{ij}	: binary variable for edge travelled by UAV
		uv_{ij}	: binary variable for edge travelled by CV
$\boldsymbol{L^{CV}_{ij}}$	: Length of CVN edge	pa_{ij}	: cumulative passes over edge by CV
$\boldsymbol{ft_{ij}}$	: UAV flight time at cruising altitude	t^{app}_j	: time of CV approach to node
$\boldsymbol{L^{UAV}_{ij}}$	: Length of UAV edge, at cruising altitude	t^{dep}_j	: time of CV departure from node
$\boldsymbol{tta}$	: Time to ascend (take-off to cruising altitude)		
$\boldsymbol{ttd}$	: Time to descend (cruising altitude to landing)		

$\boldsymbol{tft_{ij}}$	: Total UAV airtime from take-off to landing	t_l^{ret}	: time of return of last UAV, when the launch site is a depot (since start)
$\boldsymbol{x_{ij}^{UAV}}$	: binary variable (0,1) for the existence of direct UAV connection (in range), $\boldsymbol{j \in V, i \neq j}$	dt_k	: time of delivery of item (since start)
$\boldsymbol{xd_i^{CV}}$	: binary variable (0,1) indicating final delivery with CV		

The necessary input data includes the fixed network which is traversable by the CV (Conventional Vehicle Network, or "CVN"). The CVN can be described by an undirected graph, namely *G'= (V', E')*, where each vertex ("node") belongs to the set:

$$V' = [0, 1, 2, ..., n] \quad \text{(Eq. 1)}$$

Edges of the *E' [G']* space result from the connection between two nodes *i* and *j*, as *e(i,j)*, belonging to the respective set:

$$E' = \{(i,j) : i, j \in V', i \neq j\} \quad \text{(Eq. 2)}$$

For each couple of nodes, there may or may not be a direct connection. The existence of a direct CV connection between two nodes is determined by the physical network structure and/or extraordinary conditions (e.g., road closures). This condition is represented by a binary variable, namely "x_{ij}", taking values of 1 or 0, depending on whether such a connection exists. A variable is defined, for the case of the CV:

$$x_{ij}^{CV} = \begin{cases} 0, & no\ direct\ connection\ with\ CV \\ 1, & direct\ connection\ available\ with\ CV \end{cases} \qquad i, j \in V' \quad \text{(Eq. 3)}$$

An edge can be associated with a certain cost; in the present case we will be using time since it is of primary concern in logistics operations and is also a common parameter between edges (travel times) and nodes (service and waiting times). The value for a conventional vehicle trip between neighboring nodes "*i*" and "*j*", provided there is a connection, would be "ct_{ij}" (conventional vehicle travel time).

ct_{ij}, for travel time with Conventional Vehicle $\qquad i, j \in V'$

Naturally, travel time over an edge would result from the edge's length and mean vehicle speed:

$$ct_{ij} = {L_{ij}^{CV}}/{S^{CV}} \quad \text{'}L^{CV}_{ij}\text{'}: \text{length of road link between points } i \text{ and } j,\ i,j \in V,\ \text{'}S^{CV}\text{'}: \text{CV mean speed} \qquad \text{(Eq. 4)}$$

The vehicle can travel an edge in both directions (undirected graph). At this stage, we assume a symmetric problem with $ct_{ij} = ct_{ji}$.

Next input is information on the type of the CVN nodes. Several types are identified and can be passed on the nodes: a Central Depot [CD], which is the starting point for the operations, Remote Depots [RD], which can provide additional UAVs for delivery and Virtual Hubs [VH], which are designated safe areas for UAV deployment (e.g., parking lots, open spaces, organized launch/land bases.) All others are considered generic nodes. Also, there is demand for deliveries; there are locations with a demand for an item (delivery or collection) or service (Delivery Locations [DL]). For simplicity, we will only be using the terms "delivery" and "item".

A list, "K", of "m" items (each element: "k"), is given, along with their geographic position:

$$K = [1, 2, \ldots, m] \qquad \textit{(set of items)} \qquad \text{(Eq. 5)}$$

The DLs may or may not coincide with nodes of the CVN. The latter means that a DL may not be reachable by CV at all. A vertex set, "V", is created, combining CVN and DL nodes ($V = V' \cup [DL]$). The Delivery Location of each item is matched with a vertex of the *"V"* space and is then represented by it. The set of the respective nodes is defined as:

$$C_k = [d_1, d_2, \ldots, d_m] = [DL] \qquad k \in K,\ C_k \subseteq V \quad \text{(Eq. 6)}$$

An attribute matrix is formed, keeping track of relevant information for all items:

$$C = \begin{bmatrix} \overbrace{\overbrace{(k)}^{item\ ID} \quad , \overbrace{(d_k)}^{node} , \overbrace{(x_k, y_k, z_k)}^{location}}^{INPUT} \\ \\ \end{bmatrix} \qquad \text{for all k} = 1 \ldots \text{m}, \ k \in K \qquad \text{(Eq. 7)}$$

For computational convenience, we introduce an expansion of the initial CVN graph including any DLs outside the CVN, namely: $G = (V, E)$, with $E = \{(i,j) : i, j \in V, i \neq j\}$. Nodes outside the initial set V' (resulting from DLs) would naturally have no connection with any other node in V.

UAVs may launch and land at certain locations, based on prevailing restrictions. Apart from the Central Depot, the Remote Depots and the Virtual Hubs, some Delivery Locations may also serve this purpose, but their existence can only be considered after the Delivery Locations are revealed. Such locations are called Launch Sites [LS] and they are potential points for launching and collecting UAVs.

Based on the above, available node types in the vertex set [V], may be:

- Central Depots [CD], forming a sub-set of vertices, T_{CD}^{v}, where $x_i^{CD} = 1$. This subset here only contains one vertex, always named "0".
- Remote Depots [RD], forming a sub-set of vertices, T_{RD}^{v}, $x_i^{RD} = 1$.
- Virtual Hubs [VH], forming a sub-set of vertices, T_{VH}^{v}, $x_i^{VH} = 1$.
- Delivery Locations [DL], forming a sub-set of vertices T_{DL}^{v} ($T_{DL}^{v} = C_k$), $x_i^{DL} = 1$.
- Launch Sites [LS], forming a sub-set of vertices T_{LS}^{v}, $x_i^{LS} = 1$.

For computational reasons, a duplicate node of the Central Depot (CD', forming a set $T_{CD'}^{v}$, is created, along with its associated edges is created, only characterized as a remote depot.

For UAV operations, we define an undirected graph, $F = (V, A)$. Edges of the *A[F]* space result from the connection between two nodes *i* and *j*, as *a(i,j)*, belonging to the set:

$$A = \{(i,j) : i, j \in V, i \neq j\} \quad \text{(Eq. 8)}$$

The typical UAV VTOL behavior implies an initial vertical ascent to the cruising altitude and finally a vertical descent to the landing position.

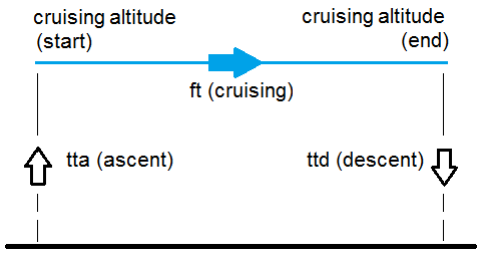

Figure 11: Simplified illustration of VTOL – type flight and associated variables

Also, the UAV can operate within certain range, which is usually expressed in time. As such, another input would be the following UAV specifications: mean cruise speed *(S^{UAV})*, mean speed of ascend *($S^{UAV}{}_{asc}$)*, mean speed of descend *($S^{UAV}{}_{des}$)*, range of operation (time) *(R^{UAV})*, cruising altitude *(H^{UAV})*.

Flight time "*ft_{ij}*" is the time needed for a UAV to fly from location "*i*" to location "*j*", at cruising altitude. This is essentially the weight (in time) of an edge if travelled by UAV. Again, we assume a symmetric problem for the UAV operations, namely *$ft_{ij} = ft_{ji}$*.

$$ft_{ij} = {L_{ij}^{UAV}}/{S^{UAV}}$$

'$L^{UAV}{}_{ij}$': distance between points i and j, $i, j \in V$, 'S^{UAV}': UAV mean flight speed (Eq. 9)

'Time to ascend' ('*tta*') and 'time to descend' ('*ttd*') values are considered. Considering only direct flights between nodes (no stop at other nodes), the total flight time '*tft_{ij}*' between two points is calculated as:

$$tta_i = {H^{UAV}}/{S_{asc}^{UAV}} \qquad ttd_i = {H^{UAV}}/{S_{des}^{UAV}} \qquad \text{(Eq. 10)}$$

$$tft_{ij} = tta_i + ft_{ij} + ttd_j \qquad \text{(Eq. 11)}$$

3.3.2.1 *Preliminary Analysis*

To reduce computational burden, pre-processing for feasible UAV connections may be performed only for nodes of interest, that is the Launch Sites [T_{LS}^{v}] and the Delivery Locations

$[T_{DL}^{v}]$ .As with the CV, we define a variable representing a direct connection between two nodes, for the case of UAV.

$$x_{ij}^{UAV} = \begin{cases} 0, & no\ direct\ connection\ with\ UAV \\ 1, & direct\ connection\ available\ with\ UAV \end{cases} \qquad i,j \in V \text{ (Eq. 12)}$$

The way our framework is set, no other nodes can be part of a UAV tour anyway. The existence of a direct UAV connection between two nodes is determined by the range, 'R^{UAV}', of the UAV and/or extraordinary conditions (e.g., take off/landing restrictions, air traffic rules, the weather). The criterion for setting x_{ij}^{UAV} value is:

$$x_{ij}^{UAV} = \begin{cases} 0, & tft_{ij+}tft_{ji} > R^{UAV} \\ 1, & 0 < tft_{ij+}tft_{ji} \leq R^{UAV} \end{cases} \qquad i,j \in V, i \neq j \quad \text{(Eq. 13)}$$

Based on the above analysis, for each Launch Site and Delivery Location a set of reachable nodes is formed:

$$DL_l^{LS} = \left[A \subseteq V \mid x_{li}^{UAV} = 1,\ i \in DL, l \in LS\right], \quad \textit{(Delivery locations within range of launch site)} \text{ (Eq. 14)}$$

$$LS_i^{DL} = \left[B \subseteq V \mid x_{il}^{UAV} = 1,\ i \in DL, l \in LS\right], \textit{(Launch sites within range of delivery location)} \text{ (Eq. 15)}$$

Each time a package is delivered at a location, a certain service time on the spot is considered. We assume a similar service time for both the case of delivery via conventional vehicle and UAV, namely "st".

A delivery request can be served by CV (at the node of said request) or by UAV (launching from another node, among eligible launch sites). A pool of eligible service nodes can be defined for each item, containing the launch sites within range of the delivery location and the node of the delivery location itself. If the DL is not part of the original CVN, its own node cannot be part of this pool, SN_k.

$$SN_k = LS_{d_k}^{DL} \cup d_k,\ k \in K, d_k \in V' \qquad \text{(Eq. 16)}$$

As briefly explained in section 3.3.1, a DL may be non-serviceable. This happens when it is located outside the CVN, namely no CV can reach this destination, and at the same time no allowed LS is located within UAV range. In our algorithm, this state is plainly described by an empty SN_k pool. In this case, the DL is removed from demand.

3.3.2.2 Assignment and Routing

Having determined the potential launch sites for all delivery locations, assignment of each item to UAV or CV follows. If the item is assigned to a node (let it be "l_k") other than its own (d_k) the request is executed via UAV. If an item is assigned to its own node ($l_k = d_k$) it is self-evident that the delivery is made by the CV.

The original attribute matrix is enriched as follows:

$$C = \left[\overbrace{\underbrace{item\ ID}_{(k)}\ \underbrace{node}_{(d_k)}, \underbrace{location}_{(x_k, y_k, z_k)}}^{INPUT}, \overbrace{\underbrace{mode}_{(CV\ or\ UAV)}, \underbrace{service\ node}_{(l_k)}}^{ASSIGNMENT} \right],\ d_k \in T_{DL}^{v},\ l_k \in SN_k,\ k \in K \quad \text{(Eq. 17)}$$

We use a binary variable "xd_i^{CV}" to define whether a delivery is made by a conventional vehicle at a node or not.

$$xd_i^{CV} = \begin{cases} 0, no\ delivery\ by\ conventional\ vehicle \\ 1, delivery\ by\ conventional\ vehicle \end{cases} \quad \text{(Eq. 18)}$$

These nodes form a subset "delivery with CV": $T_{DLCV}^{v} = [DLCV \subseteq V \mid xd_i = 1,\ i \in DL]$. (Eq. 19)

We also introduce another binary variable "xl_i" to define whether a node is ultimately used for UAV launch or not. These nodes must belong to the CVN.

$$xl_i = \begin{cases} 0, not\ used\ for\ launch \\ 1, used\ for\ launch \end{cases} \quad \text{(Eq. 20)}$$

Nodes form a subset "assigned launch sites": $T_{aLS}^{v} = [aLS \subseteq V \mid xl_i = 1,\ i \in LS]$. (Eq. 21)

Nodes finally assigned as service nodes for either action (UAV launch or CV delivery) are Mandatory Nodes with action(s) (item delivery or UAV launch), named "*TMa*". The CV must visit them at some point of the route and perform an action other than just passing by.

$$T^v_{M\alpha} = T^v_{DLCV} \cup T^v_{aLS} \qquad \text{(Eq. 22)}$$

In our method, this distinction between generic and mandatory nodes is crucial. This is because the full network is given, but not all nodes must be visited and the problem changes depending on infrastructure/conditions/equipment constraints and demand. The full set of mandatory nodes results from the union of the two sets: T^v_{DLCV} (delivery locations served by conventional vehicle) and T^v_{aLS} (assigned launch sites), and the Central Depot (which must be the first and last node to be visited, hence the inclusion of its duplicate):

$$T^v_M = T^v_{CD} \cup T^v_{M\alpha} \cup T^v_{CD'} \quad \text{(Eq. 23)}$$

There is a possibility of the Central Depot or its duplicate themselves being nodes with action (belonging to the $T^v_{M\alpha}$). For computational reasons occurring later in our methodology, we define a "clean" set T^v_{Mc}, excluding the CD and CD', as:

$$T^v_{Mc} = T^v_M - (T^v_{CD} + T^v_{CD'}) \qquad \text{(Eq. 24)}$$

We keep track of the items assigned to the same launch site for UAV delivery. As such, each node belonging to the T^v_{aLS} will feature a list of the assigned items. A respective list is formed for each of the assigned launch sites:

$$L_l \subseteq K \mid l_k = l, l \in T^v_{aLS}, k \in K \quad \text{(Eq. 25)}$$

The number of assigned items per launch site is the length of the list: $|L_l|$

The use of a node as a launch site implies a certain time cost (transshipment cost). This is because of necessary preparations, launching and collecting UAVs back to the vehicle. We include this transshipment cost in a variable, "tc_i". UAVs are assumed to launch simultaneously, but they naturally return at a different time. Transshipment cost is further

analyzed into launch (tl_i) and repackaging (tr_i) times, to distinguish between the time spent to prepare the fleet and the time spent to get it back to the vehicle.

$$tc_i = tl_i + tr_i \qquad \text{(Eq. 26)}$$

When a UAV is deployed, a certain amount of time is required for it to return to its base. This travel time, from deployment at node "i", delivery at node "j" and back to home "i", "dth_{ij}" is calculated as:

$$dth_{ij} = tft_{ij} + st_j + tft_{ji} \qquad \text{(Eq. 27)}$$

At every node, a certain waiting time "wt_i" for the Conventional Vehicle is considered. Each node "i" inherits the "burden" of assigned delivery locations. In case item delivery is its only duty at the node, this time is essentially the service time. If the spot is used for UAV deployment, the waiting time is also a result of transshipment time for each item and time from deployment to home of the last UAV to return. If the launch site is a Remote Depot, the node is only weighted with the delivery of an item via CV (if any) and the time to unload the rest of the items for UAV transport. The typical service time st_i is used for unloading, as if it were a case of normal deliveries. However, we assume that service time here is affected by the number of unloaded items, as it would be for multiple deliveries on the spot. At Depots, the transshipment cost does not affect the CV.

$$wt_i = xd_i^{CV} \cdot st_i + \left(1 - x_i^{CRD}\right) \cdot xl_i \cdot \left[|L_i| \cdot tc_i + \max\left(dth_{ij}\right)\right] + x_i^{RD} \cdot xl_i \cdot |L_i| \cdot st_i \,,\; i \in V',\; j \in L_i \qquad \text{(Eq. 28)}$$

$$x_i^{CRD} = x_i^{RD} + x_i^{CD} \,, \quad i \in V' \qquad \text{(Eq. 29)}$$

For the special case of the Central Depot, since there is no CV delivery and there is no unloading time for any UAV-assigned item, the CV does not have to wait, and everything is processed independently. Any UAV deployment from the Central Depot would normally happen at the start of the operations, but we will be also allowing the Central Depot to host actions as the last node of the tour. The CD duplicate (used as the last node of the tour) carries

the characteristics of a Remote Depot, to emulate the expected procedure of item unloading and UAV deployment.

In our case, where most network types should be addressed, typical TSP constraints concerning multiple node/edge passes and the forced use of all nodes do not apply, since not all nodes are mandatory and both butterfly routes and multiple node/edge passes are allowed (e.g., because of network dead ends or reaching a node for delivery or launch and immediately returning from the same road). We structure our method in a way that it's not hampered by infeasible solutions: All mandatory nodes are always included in the solution (at least once for completing an action) and path continuity is ensured.

For assessing the performance of each solution, a certain route must be constructed, passing through the mandatory nodes and any other nodes necessary to form a continuous path. We will base this two-step method on the principle of optimality, stating that *"in a graph with no negative dicycles, optimal paths must have optimal subpaths"* (Rardin, 2015). We define a subgraph of the original G graph, namely $G_M = (T_M^v, E_M)$. Mandatory nodes (resulting from the assignment process) form the node set T_M^v. Each edge, e_M, is a "shell" edge, representing the shortest path between two nodes through the original network. For each $i, j \in T_M^v, i, j \in V'$ there is a path of nodes $\widehat{S_{ij}} = [i, \dots, j]$ and edges $\widehat{S_{(i,j)}} = [(i, i+1), \dots, (j-1, j)]$, and the cost of the shell edge is:

$$ct_{ij}^M = \sum_{u=i}^{j-1} \sum_{v=u+1}^{j} ct_{uv}$$

(Eq. 30)

The shortest path can be calculated via an appropriate algorithm each time (e.g., Dijkstra (Dijkstra, 1959), A* (Hart, Nilsson, & Raphael, 1968), IDA* (Korf, 1985), LPA* (Koenig, Likhachev, & Furcy, 2004), depending on complexity and size of network.

Now, a certain sequence of visit must be defined through the mandatory nodes. The path always features the Central Depot as the first and last node of visit. As explained before,

the Central Depot's duplicate visited at the end is considered a Remote Depot. A routing solution would be a sequence like:

$$\widehat{S_v^M} = [i, \dots, j] \text{ and } \widehat{S_{(e)}^M} = [(i, i+1), \dots, (j-1, j)] \text{ (mandatory nodes, shell edges), } i, j \in V',\ e \in E,\ i, j \in T_M^v \quad \text{(Eq. 31)}$$

$$\widehat{S_v} = [i, \dots, j] \text{ and } \widehat{S_{(e)}} = [(i, i+1), \dots, (j-1, j)] \text{ (total path, all nodes, and edges), } i, j \in V',\ e \in E \quad \text{(Eq. 32)}$$

After decomposing the solution route to the nodes forming its shell edges, we have the order of visit of all nodes. The selected nodes constitute a subset, namely: T_{ACCV}^v.

$$xa_i = \begin{cases} 0, not\ accessed\ by\ conventional\ vehicle \\ 1, accessed\ by\ conventional\ vehicle \end{cases} \quad \text{(Eq. 33)}$$

The nodes are appended in order of visit within the subset. This subset ultimately describes the problem possible solution each time. A node may be traversed more than once and may be repeated in the sequential order of visit. However, actions of delivery and/or launching only happen once.

If an edge is ultimately used by the conventional vehicle or the UAV, there is a binary variable to keep record.

$$uf_{ij} = \begin{cases} 0, not\ travelled\ in\ UAV \\ 1, travelled\ in\ UAV \end{cases} \quad \text{(Eq. 34)}$$

$$uv_{ij} = \begin{cases} 0,\ not\ travelled\ in\ conventional\ vehicle \\ 1,\ travelled\ in\ conventional\ vehicle \end{cases} \quad \text{(Eq. 35)}$$

Since in our accepted spectrum of network types and based on our problem definition it is possible that a CV edge is traversed more than once, we keep record of the cumulative passes over each edge along the tour, under the variable $pa_{ij} \in \mathbb{Z}$.

For each node there is a time of approach "t_i^{app}" since the start of delivery. Travel times along the selected edges of the conventional vehicle network are added, as well as waiting times of preceding nodes.

Additionally, depending on which actions are taken (delivery at the node, deployment of UAVs), there is the time of departure, "t_j^{dep}" at each node visited by the CV. In this case, the nodes of visit are ordered.

$$t_j^{app} = \sum_{i=0}^{j} \sum_{j=0}^{j} ct_{ij}^{M} + \sum_{i=0}^{j-1} wt_i$$

(Eq. 36)

$$t_j^{dep} = t_j^{app} + wt_j \text{ , or } t_j^{app} = t_{j-1}^{dep} + ct_{j-1,j}^{M} \text{ , } i,j \in T_M^v \quad \text{(Eq. 37)}$$

For the case of a Depot, the UAVs will be returning to their base independently from the CV operations. We still need to know when the last one returns to the Depot. The time of return should be:

$$t_l^{ret} = t_l^{dep} + \left|L_i^k\right| \cdot tc_{i} + \max\left(dth_{ij}\right), \; l \in T_{CD}^v \cup T_{RD}^v \cup T_{CD}^v, \; j \in L_l \qquad \text{(Eq. 38)}$$

Two values regarding the entire operation are of importance: the amount of time spent out for the CV and the entire time spent until any operation (CV and UAV) has finished. CV total time (CVT) is:

$$CVT = \sum_{i=0}^{n} \sum_{j=0}^{n} pa_{ij} \cdot ct_{ij} + \sum_{i=0}^{n} wt_i$$

(Eq. 39)

This value should be identical with the time of approach, t_j^{app}, at the last node. ($i,j \in V'$)

All operations are finished when the CV has returned to the depot and the last remaining UAV has been retrieved at the intended location. This is defined as Total Operations Time (TOT):

$$TOT = \max(\max(t_l^{ret}), CVT), \; l \in [CD] \cup [RD] \quad \text{(Eq. 40)}$$

We use the TOT as the objective function and the goal is to find a solution which minimizes its value.

$$\text{Minimize } \max(\max(t_l^{ret}), CVT)$$

$$\text{Minimize } \max\left(\max(t_l^{ret}), \sum_{i=0}^{n}\sum_{j=0}^{n} pa_{ij} \cdot ct_{ij} + \sum_{i=0}^{n} wt_i\right) \qquad \text{(Eq. 41)}$$

If we were to optimize based on the CVT only the routing of each assignment iteration would essentially be a form of TSP problem among mandatory nodes with weights. In the latter case, however, it is possible that UAVs are still operating even after the CV has completed its own route.

The description of the solution output includes the following minimum information:

- The assignment of items to their respective service node (l_k for each k)
- The order of visit of mandatory nodes (ordered set of T_M^v)

Additional calculations can be made for each item and its delivery process. Let "dt_k" be the delivery time for a package being transported from node "0" (Central Depot) to node "j". Delivery time depends on the modes of transport used for each edge and the waiting times at preceding nodes in the tour. Node "l" is the one used as a hub for launch, should a UAV be used. Again, we assume that UAV launch is executed after a potential delivery by CV at the launch site itself.

$$dt_k = \begin{cases} toa_j + st_j, \;\; if\; xd_j^{CV} = 1\; (delivery\; by\; CV) \\ toa_l + (xd_l^{CV} \times st_l) + |L_l| \cdot tc_l + tft_{lj} + st_j, \;\; if\; xd_j^{UAV} = 1\; (delivery\; by\; UAV) \end{cases} \qquad \text{(Eq. 42)}$$

$$k \in K, \qquad j = d_k, \qquad l = l_k, \qquad j \in T_{DL}^v, \qquad l \in T_{LS}^v$$

If we would like to know the total number of possible assignment solutions ('N'), we would calculate as follows:

$$N = \prod_{k=1}^{m}(|SN_k|) = (|SN_1| \cdot \ldots \cdot |SN_k| \cdot \ldots \cdot |SN_m|)$$

(Eq. 43)

where $|SN_k|$ is the Service Nodes Pool size (number of available nodes) for each item.

The possible solutions in terms of routing (permutations) will have to be calculated for each assignment candidate solution independently. Since the Central Depot and its duplicate are always first and last respectively, we are only looking at the possible order among the rest of the mandatory nodes, namely set T_{Mc}^{v}, which features $n = |T_{Mc}^{v}|$ nodes. We expect $r = n!$ permutations within each assignment iteration.

3.3.3 Assignment and Routing Optimization nested Genetic Algorithm (AROnGA)

We propose a nested Genetic Algorithm (GA) scheme, where a routing optimization algorithm (inner-GA) is executed for each assignment suggestion and the resulting TOT value is used to select the best assignment (shell-GA). It is essentially a cluster-first, routing-second approach, where each clustering iteration is tied with its own optimal routing. GA – based methods are commonly used in this family of problems (Iliopoulou, Kepaptsoglou, & Karlaftis, 2015), mainly because of NP-hardness and complexity (Lenstra & Kan, 1981). In our case, preliminary processing produces discrete alternatives (service nodes pool) for the assignment of items and a sub-set of nodes which need to be ordered. Both are conveniently translated to genes and chromosomes. Additionally, one process essentially depends on the other (routing is applied on mandatory nodes which result from assignment); thus, a nested scheme makes sense.

3.3.3.1 Outer – GA (Mode and Service Node Assignment of Items)

For the outer-GA, the chromosome consists of genes, whose total number equals the number of items, $m = |K|$, (delivery locations). Each gene can take the discrete values of the available service nodes (SN_k) for the respective DL. Random mutation and single point crossover are employed to produce new offsprings and a ranking parent selection is used to qualify best parents for mating.

Table 2: Example of Assignment GA chromosomes and offsprings through single point crossover

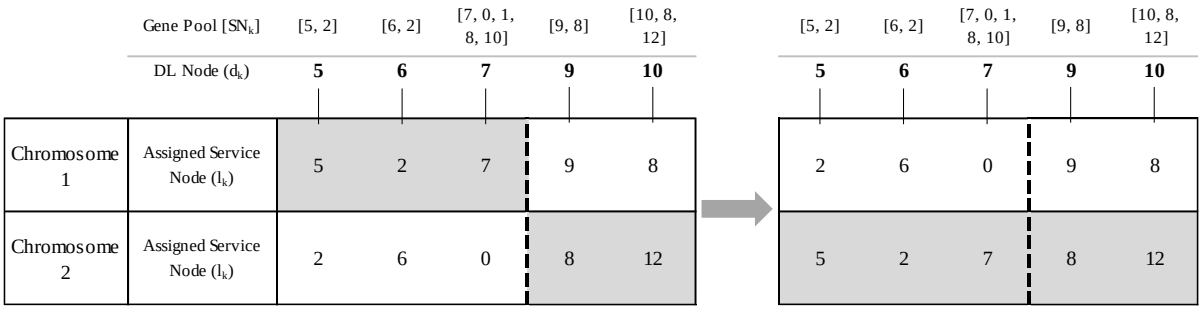

Random mutations are introduced to genes to keep diversity in the population and escape local optima.

3.3.3.2 Inner – GA (Conventional Vehicle Routing)

For the inner-GA, we need to find the optimal order of visit of the mandatory nodes. Since the Central Depot and its duplicate will always be the first and last nodes respectively, the chromosome features genes, one for each of the mandatory nodes, without the start and end node, T_{Mc}^{v}. We employ a random-keys GA (Rardin, 2015), where each node is ordered by ascending order based on its respective gene value. The gene values are randomly produced within a set range (e.g., 0 – 100). Single point crossover and ranking parent selection are used. The final path begins and ends with the Central Depot (its duplicate at the end) and in-between there are the ordered nodes resulting from the previous process. The TOT value resulting from routing is passed to the respective outer GA iteration and used for its own optimization process.

Table 3: Example of Routing GA chromosomes and offsprings

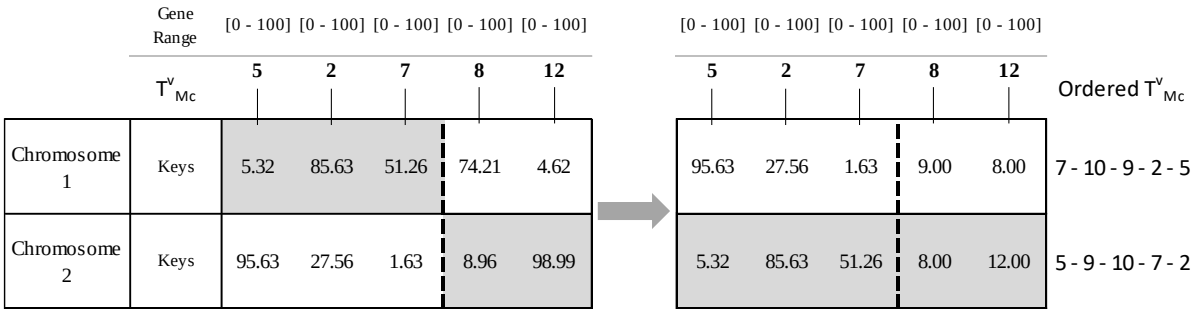

Again, random mutations are introduced to genes to keep diversity in the population and escape local optima.

3.3.3.3 *Shortest paths between mandatory nodes*

For obtaining the complete path, consisting of mandatory but possibly generic nodes as well, we need the actual paths between the mandatory nodes. As previously explained (see section 3.3.1), shortest paths between mandatory nodes are calculated in a separate procedure. We opted to employ the A* algorithm (Hart, Nilsson, & Raphael, 1968) for this purpose. In case of a relatively small network shortest paths can be calculated beforehand for all possible mandatory node couples (among CD, RD, DL and LS) and a reference matrix would be readily available. This would require an initially increased computational effort but offer faster computation within the optimization loops. If the network is of considerable size, the strictly necessary shortest paths can be estimated after each assignment iteration (where each time a different set of mandatory nodes may come up).

Partial intervention based on operational preferences is possible by manually restricting the gene space for assignment and routing or even by bypassing the optimization process altogether and directly passing assignment and routing choices.

3.4 Case Study

3.4.1 Network and Input Data

We devise a CV network to perform the tests. The said network should offer certain features:

- The geographical size of the network should resemble a large city or distances between neighboring cities.

- There must be dead-end edges i.e., edges which are connected to a single node at one end (to resemble last-mile cases with limited connections).

- A node is not necessarily connected to all its closest ones (to emulate missing links).

- At some point there must be a series of consecutive edges with a single node connection in-between (to resemble possible stops along a single corridor).

As far as node types and delivery locations:

- There must be a Central Depot and at least one Remote Depot (apart from the Central Depot duplicate) away from it.

- There must be a few Virtual Hubs, distributed evenly throughout the network (not all Virtual Hubs will necessarily serve as allowed Launch Sites).

- There must be at least one Delivery Location outside the given CV network, where only a UAV can be of service.

Since the CV and UAV will be "competing" based on their specs, we created a more realistic version of the CV network, namely connecting the nodes with non-straight links (length: L^{CV}_{ij}). In our case, both directions are of equal length. The resulting -undirected, symmetric- graph G' (illustrated with straight edges) will be a graph with weighted edges; each edge carries the cost ct_{ij}, resulting from the expected CV travel time over the original link. Next, available CV node types are introduced (Central Depot, Remote Depots, Virtual Hubs).

Table 4: Input CV Network Nodes

v_i	x	y	v_i	x	y
0	0.000	0.000	11	-35652.764	15493.993
1	0.000	0.000	12	-26081.454	-6588.331
2	22200.500	-2246.434	13	-30736.252	-2595.080
3	21339.640	11254.890	14	-37656.441	-6082.275
4	15305.796	19590.346	15	-32594.951	-15883.915
5	26209.829	10341.626	16	-23794.972	-18816.222
6	32795.242	3940.702	17	-9184.639	-14708.946
7	-6200.316	7871.878	18	-814.285	-10979.538
8	-11565.366	18473.235	19	-7208.515	-2587.391
9	-10318.214	30943.160	20	29121.346	-8156.159
10	-19235.476	5729.837			

Central Depot [CD]: ‘0’, Remote Depots [RD]: ‘1’ (duplicate of CD), ‘16’, Virtual Hubs [VH]: ‘3’, ‘8’, ‘18’

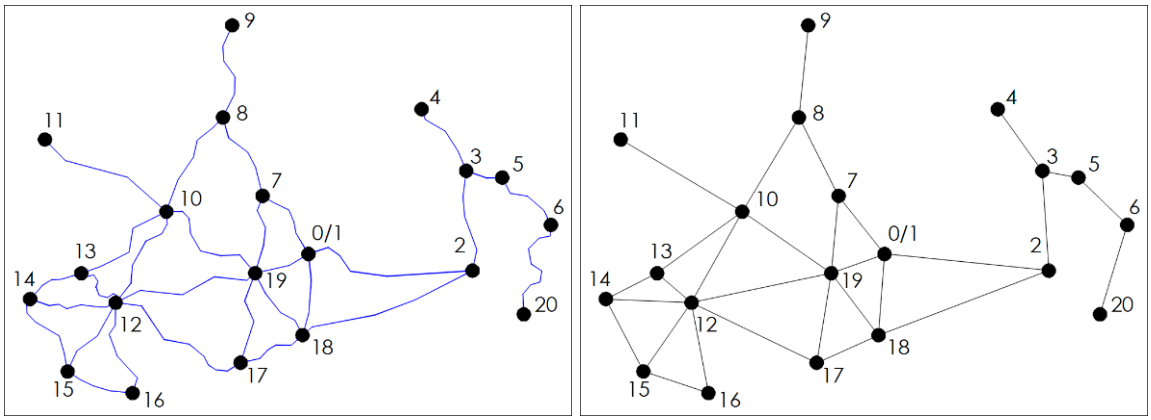

Figure 12: Original input CV network and Graph representation

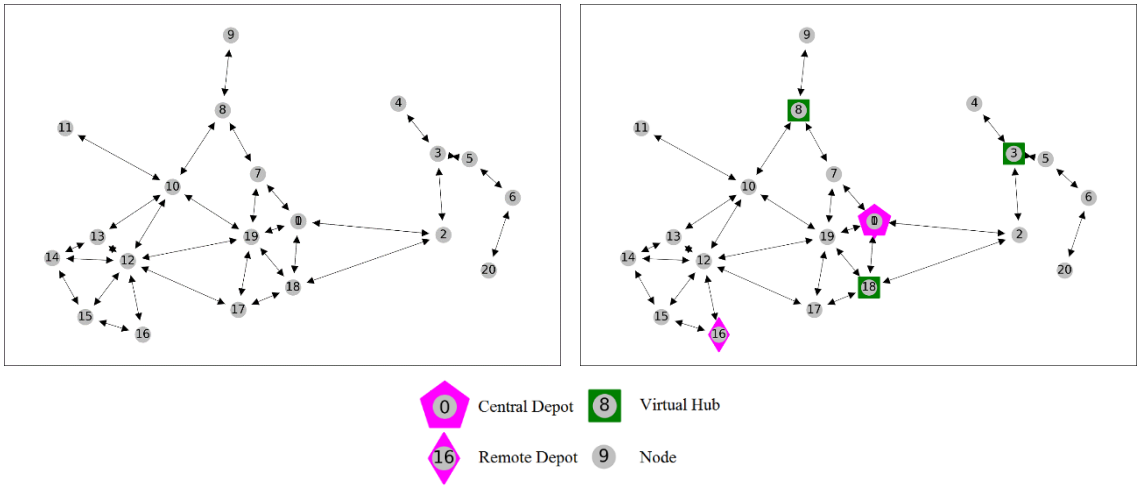

Figure 13: CV network and Node Types

Table 5: Actual length (L^{CV}_{ij}, m) of CV Network links

L_{ij}	0	1	2	3	4	5	6	7	8	9	10	11	12	13	14	15	16	17	18	19	20
0	0	0	23899	inf	inf	inf	inf	10611	inf	inf	inf	inf	inf	inf	inf	inf	inf	inf	11133	7752	inf
1	0	0	23899	inf	inf	inf	inf	10611	inf	inf	inf	inf	inf	inf	inf	inf	inf	inf	11133	7752	inf
2	23899	23899	0	13880	inf	inf	inf	inf	inf	inf	inf	inf	inf	inf	inf	inf	inf	inf	24885	inf	inf
3	inf	inf	13880	0	10717	5038	inf	inf	inf	inf	inf	inf	inf	inf	inf	inf	inf	inf	inf	inf	inf
4	inf	inf	inf	10717	0	inf	inf	inf	inf	inf	inf	inf	inf	inf	inf	inf	inf	inf	inf	inf	inf
5	inf	inf	inf	5038	inf	0	9870	inf	inf	inf	inf	inf	inf	inf	inf	inf	inf	inf	inf	inf	inf
6	inf	inf	inf	inf	inf	9870	0	inf	inf	inf	inf	inf	inf	inf	inf	inf	inf	inf	inf	inf	16017
7	10611	10611	inf	inf	inf	inf	inf	0	12358	inf	inf	inf	inf	inf	inf	inf	inf	inf	inf	11020	inf
8	inf	inf	inf	inf	inf	inf	inf	12358	0	13583	15285	inf	inf	inf	inf	inf	inf	inf	inf	inf	inf
9	inf	inf	inf	inf	inf	inf	inf	inf	13583	0	inf	inf	inf	inf	inf	inf	inf	inf	inf	inf	inf
10	inf	inf	inf	inf	inf	inf	inf	inf	15285	inf	0	19703	15115	15413	inf	inf	inf	inf	inf	16914	inf
11	inf	inf	inf	inf	inf	inf	inf	inf	inf	inf	19703	0	inf	inf	inf	inf	inf	inf	inf	inf	inf
12	inf	inf	inf	inf	inf	inf	inf	inf	inf	inf	15115	inf	0	8641	12129	11621	13828	21266	inf	20338	inf
13	inf	inf	inf	inf	inf	inf	inf	inf	inf	inf	15413	inf	8641	0	8088	inf	inf	inf	inf	inf	inf
14	inf	inf	inf	inf	inf	inf	inf	inf	inf	inf	inf	inf	12129	8088	0	12523	inf	inf	inf	inf	inf
15	inf	inf	inf	inf	inf	inf	inf	inf	inf	inf	inf	inf	11621	inf	12523	0	9433	inf	inf	inf	inf
16	inf	inf	inf	inf	inf	inf	inf	inf	inf	inf	inf	inf	13828	inf	inf	9433	0	inf	inf	inf	inf
17	inf	inf	inf	inf	inf	inf	inf	inf	inf	inf	inf	inf	21266	inf	inf	inf	inf	0	9629	12908	inf
18	11133	11133	24885	inf	inf	inf	inf	inf	inf	inf	inf	inf	inf	inf	inf	inf	inf	9629	0	10852	inf
19	7752	7752	inf	inf	inf	inf	inf	11020	inf	inf	16914	inf	20338	inf	inf	inf	inf	12908	10852	0	inf
20	inf	inf	inf	inf	inf	inf	16017	inf	inf	inf	inf	inf	inf	inf	inf	inf	inf	inf	inf	inf	0

Table 6: Edge weights as travel time (ct_{ij}, sec) along CV Network links

ct_{ij}	0	1	2	3	4	5	6	7	8	9	10	11	12	13	14	15	16	17	18	19	20
0	0	0	2151	inf	inf	inf	inf	955	inf	inf	inf	inf	inf	inf	inf	inf	inf	inf	1002	698	inf
1	0	0	2151	inf	inf	inf	inf	955	inf	inf	inf	inf	inf	inf	inf	inf	inf	inf	1002	698	inf
2	2151	2151	0	1249	inf	inf	inf	inf	inf	inf	inf	inf	inf	inf	inf	inf	inf	inf	2240	inf	inf
3	inf	inf	1249	0	965	453	inf	inf	inf	inf	inf	inf	inf	inf	inf	inf	inf	inf	inf	inf	inf
4	inf	inf	inf	965	0	inf	inf	inf	inf	inf	inf	inf	inf	inf	inf	inf	inf	inf	inf	inf	inf
5	inf	inf	inf	453	inf	0	888	inf	inf	inf	inf	inf	inf	inf	inf	inf	inf	inf	inf	inf	inf
6	inf	inf	inf	inf	inf	888	0	inf	inf	inf	inf	inf	inf	inf	inf	inf	inf	inf	inf	inf	1442
7	955	955	inf	inf	inf	inf	inf	0	1112	inf	inf	inf	inf	inf	inf	inf	inf	inf	inf	992	inf
8	inf	inf	inf	inf	inf	inf	inf	1112	0	1222	1376	inf	inf	inf	inf	inf	inf	inf	inf	inf	inf
9	inf	inf	inf	inf	inf	inf	inf	inf	1222	0	inf	inf	inf	inf	inf	inf	inf	inf	inf	inf	inf
10	inf	inf	inf	inf	inf	inf	inf	inf	1376	inf	0	1773	1360	1387	inf	inf	inf	inf	inf	1522	inf
11	inf	inf	inf	inf	inf	inf	inf	inf	inf	inf	1773	0	inf	inf	inf	inf	inf	inf	inf	inf	inf
12	inf	inf	inf	inf	inf	inf	inf	inf	inf	inf	1360	inf	0	778	1092	1046	1244	1914	inf	1830	inf
13	inf	inf	inf	inf	inf	inf	inf	inf	inf	inf	1387	inf	778	0	728	inf	inf	inf	inf	inf	inf
14	inf	inf	inf	inf	inf	inf	inf	inf	inf	inf	inf	inf	1092	728	0	1127	inf	inf	inf	inf	inf
15	inf	inf	inf	inf	inf	inf	inf	inf	inf	inf	inf	inf	1046	inf	1127	0	849	inf	inf	inf	inf
16	inf	inf	inf	inf	inf	inf	inf	inf	inf	inf	inf	inf	1244	inf	inf	849	0	inf	inf	inf	inf
17	inf	inf	inf	inf	inf	inf	inf	inf	inf	inf	inf	inf	1914	inf	inf	inf	inf	0	867	1162	inf
18	1002	1002	2240	inf	inf	inf	inf	inf	inf	inf	inf	inf	inf	inf	inf	inf	inf	867	0	977	inf
19	698	698	inf	inf	inf	inf	inf	992	inf	inf	1522	inf	1830	inf	inf	inf	inf	1162	977	0	inf
20	inf	inf	inf	inf	inf	inf	1442	inf	inf	inf	inf	inf	inf	inf	inf	inf	inf	inf	inf	inf	0

Delivery Locations of items are introduced. In our case, one of them (item '11') must be delivered outside the CV Network and a new node is introduced (No '21'). Allowed Launch Sites are selected among the CD, RDs, VHs ans DLs. Here, the selection is random, but, in the real world it would be associated with operational constraints.

Table 7: Items and Delivery Locations

Item (k)	x	y	Node (d_k)
1	26209.829	10341.626	5
2	32795.242	3940.702	6
3	-6200.316	7871.878	7
4	-10318.214	30943.160	9

5	-19235.476	5729.837	10
6	-26081.454	-6588.331	12
7	-30736.252	-2595.080	13
8	-37656.441	-6082.275	14
9	-32594.951	-15883.915	15
10	29121.346	-8156.159	20
11	-21798.415	26453.613	21

Delivery Locations [DL]: ‘5’, ‘6’, ‘7’, ‘9’, ‘10’, ‘12’, ‘13’, ‘14’, ‘15’, ‘20’, ‘21’

Launch Sites [LS]: ‘0’, ‘1’, ‘2’, ‘8’, ‘10’, ‘12’, ‘14’, ‘16’

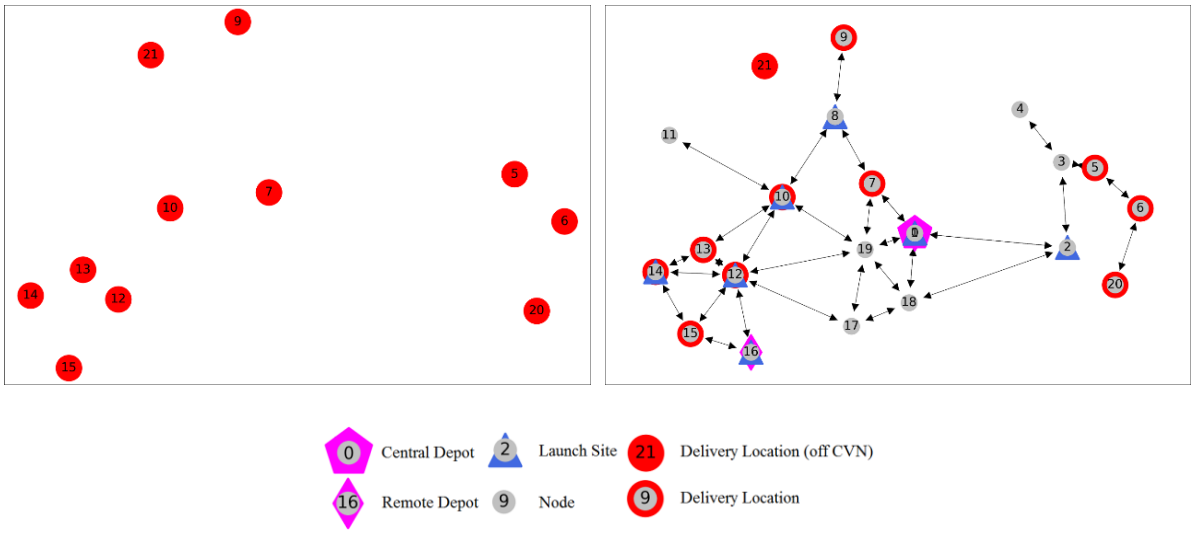

Figure 14: Delivery Locations and final allowed Launch Sites

Certain specs for the CV and the UAV are selected*:

$S^{CV} = 40km/h$, $H^{UAV} = 120m$, $S^{UAV} = 14.45\ m/sec$

$S^{UAV}_{asc} = 4.25\ m/sec$ ($tta = 28.2\ sec$, for $H^{UAV} = 120m$)

$S^{UAV}_{des} = 3.4\ m/sec$ ($ttd = 35.3\ sec$, for $H^{UAV} = 120m$)

$R^{UAV} = 40min\ (2400sec)$

Service and transshipment times are assumed:

$st = 60\ sec$, $tc = 300\ sec\ (5min)$

** The specifications for the UAV resemble today’s advanced commercial UAVs and are naturally expected to improve in the future.*

(for examples, see (DJI, 2023) (Flying Basket, 2023) (Matternet, 2023))

3.4.2 Preliminary Analysis

In the context of the Preliminary Analysis, feasibility of UAV connections is determined and the respective Graph $F = (A, V)$ is formed. Next, we examine which Launch Sites are within range for the Delivery Locations, forming the set LS^{DL} for each one. Then, the Service Nodes Pool (SN_k) is shaped for each item. If the DL is in the CV Network, its own node can be included in the SN_k. For instance, in our case, item no '11', on node '21' is outside the CVN, hence node "21" cannot be included.

Table 8: Edge costs as total flight time for UAV (tft_{ij}, sec), including take-off and landing

tft_{ij}	0	1	2	3	4	5	6	7	8	9	10	11	12	13	14	15	16	17	18	19	20	21
0	0	0	inf	inf	inf	inf	inf	757	inf	inf	inf	inf	inf	inf	inf	inf	inf	inf	825	594	inf	inf
1	0	0	inf	inf	inf	inf	inf	757	inf	inf	inf	inf	inf	inf	inf	inf	inf	inf	825	594	inf	inf
2	inf	inf	0	1000	inf	978	913	inf	inf	inf	inf	inf	inf	inf	inf	inf	inf	inf	inf	inf	693	inf
3	inf	inf	1000	0	776	406	1004	inf	inf	inf	inf	inf	inf	inf	inf	inf	inf	inf	inf	inf	inf	inf
4	inf	inf	inf	776	0	1053	inf	inf	inf	inf	inf	inf	inf	inf	inf	inf	inf	inf	inf	inf	inf	inf
5	inf	inf	978	406	1053	0	699	inf	inf	inf	inf	inf	inf	inf	inf	inf	inf	inf	inf	inf	inf	inf
6	inf	inf	913	1004	inf	699	0	inf	inf	inf	inf	inf	inf	inf	inf	inf	inf	inf	inf	inf	938	inf
7	757	757	inf	inf	inf	inf	inf	0	886	inf	978	inf	inf	inf	inf	inf	inf	inf	inf	791	inf	inf
8	inf	inf	inf	inf	inf	inf	inf	886	0	931	1093	inf	inf	inf	inf	inf	inf	inf	inf	inf	inf	962
9	inf	inf	inf	inf	inf	inf	inf	inf	931	0	inf	inf	inf	inf	inf	inf	inf	inf	inf	inf	inf	917
10	inf	inf	inf	inf	inf	inf	inf	978	1093	inf	0	inf	1039	1046	inf	inf	inf	inf	inf	1075	inf	inf
11	inf	inf	inf	inf	inf	inf	inf	inf	inf	inf	inf	0	inf	inf	inf	inf	inf	inf	inf	inf	inf	inf
12	inf	inf	inf	inf	inf	inf	inf	inf	inf	inf	1039	inf	0	488	865	849	924	inf	inf	inf	inf	inf
13	inf	inf	inf	inf	inf	inf	inf	inf	inf	inf	1046	inf	488	0	600	992	inf	inf	inf	inf	inf	inf
14	inf	inf	inf	inf	inf	inf	inf	inf	inf	inf	inf	inf	865	600	0	827	inf	inf	inf	inf	inf	inf
15	inf	inf	inf	inf	inf	inf	inf	inf	inf	inf	inf	inf	849	992	827	0	705	inf	inf	inf	inf	inf
16	inf	inf	inf	inf	inf	inf	inf	inf	inf	inf	inf	inf	924	inf	inf	705	0	1114	inf	inf	inf	inf
17	inf	inf	inf	inf	inf	inf	inf	inf	inf	inf	inf	inf	inf	inf	inf	inf	1114	0	698	913	inf	inf
18	825	825	inf	inf	inf	inf	inf	inf	inf	inf	inf	inf	inf	inf	inf	inf	inf	698	0	794	inf	inf
19	594	594	inf	inf	inf	inf	inf	791	inf	inf	1075	inf	inf	inf	inf	inf	inf	913	794	0	inf	inf
20	inf	inf	693	inf	inf	inf	938	inf	inf	inf	inf	inf	inf	inf	inf	inf	inf	inf	inf	inf	0	inf
21	inf	inf	inf	inf	inf	inf	inf	inf	962	917	inf	inf	inf	inf	inf	inf	inf	inf	inf	inf	inf	0

Table 9: Adjacency matrix for UAV (x^{UAV}_{ij})

x^{UAV}_{ij}	0	1	2	3	4	5	6	7	8	9	10	11	12	13	14	15	16	17	18	19	20	21
0	-	-	-	-	-	-	-	1	-	-	-	-	-	-	-	-	-	-	1	1	-	-
1	-	-	-	-	-	-	-	1	-	-	-	-	-	-	-	-	-	-	1	1	-	-
2	-	-	-	1	-	1	1	-	-	-	-	-	-	-	-	-	-	-	-	-	1	-
3	-	-	1	-	1	1	1	-	-	-	-	-	-	-	-	-	-	-	-	-	-	-
4	-	-	-	1	-	1	-	-	-	-	-	-	-	-	-	-	-	-	-	-	-	-
5	-	-	1	1	1	-	1	-	-	-	-	-	-	-	-	-	-	-	-	-	-	-
6	-	-	1	1	-	1	-	-	-	-	-	-	-	-	-	-	-	-	-	-	1	-
7	1	1	-	-	-	-	-	-	1	-	1	-	-	-	-	-	-	-	-	1	-	-
8	-	-	-	-	-	-	-	1	-	1	1	-	-	-	-	-	-	-	-	-	-	1
9	-	-	-	-	-	-	-	-	1	-	-	-	-	-	-	-	-	-	-	-	-	1
10	-	-	-	-	-	-	-	1	1	-	-	-	1	1	-	-	-	-	-	1	-	-
11	-	-	-	-	-	-	-	-	-	-	-	-	-	-	-	-	-	-	-	-	-	-
12	-	-	-	-	-	-	-	-	-	-	1	-	-	1	1	1	1	-	-	-	-	-
13	-	-	-	-	-	-	-	-	-	-	1	-	1	-	1	1	-	-	-	-	-	-
14	-	-	-	-	-	-	-	-	-	-	-	-	1	1	-	1	-	-	-	-	-	-

Table 10: Potential Launch Sites and Final Service Nodes Pool for Items

Item (k)	Node (d_k)	Potential Launch Sites [LS^{DL}]	Service Nodes Pool [SN_k]	$\lvert SN_k \rvert$

1	5	2				5	2				(2)
2	6	2				6	2				(2)
3	7	0	1	8	10	7	0	1	8	10	(5)
4	9	8				9	8				(2)
5	10	8	12			10	8	12			(3)
6	12	10	14	16		12	10	14	16		(4)
7	13	10	12	14		13	10	12	14		(4)
8	14	12				14	12				(2)
9	15	12	14	16		15	12	14	16		(4)
10	20	2				20	2				(2)
11	21	8					8				(1)

Judging from the available Service Nodes for all items and having no additional constraints going forward, all possible assignment solutions amount to the total number of N = 30720.

3.4.3 Experiments and Results

Our sample network is of moderate size; thus, we chose to execute Analysis "s2" (Shortest Path calculation and Shell Edges Graph construction) for all candidate mandatory nodes, namely DL and LS and the CD with its duplicate. This is purely done for computational simplicity and for using an existing, "static" matrix of all possible shortest paths and associated costs as a reference as explained in section 3.3.3.3. Since mandatory nodes only emerge after each assignment iteration, shortest paths between pairs would also be calculated each time anew. However, many of these pairs are possibly met in other iterations, thus directly retrieving the shortest path information from a single source rather than recalculating could be computationally favorable. This may not be true if the full matrix containing all possible pairs is very large. In this case, working with sub-sets in each iteration is expected to be better.

For example:

Shell Edge : ('20', '16')

Path Cost, $ct^{M}_{20,16}$: 9956.1 sec

Nodes Path, $\widehat{S_{20,16}}$: ['20', '6', '5', '3', '2', '0', '19', '12', '16']

Edge Sequence, $\widehat{S_{(20,16)}}$: [('20', '6'), ('6', '5'), ('5', '3'), ('3', '2'), ('2', '0'), ('0', '19'), ('19', '12'), ('12', '16')]

There are cases where the path is the original edge itself since no other nodes interfere.

Shell Edge : ('19', '7')

Path Cost, $ct^{M}_{19,7}$: 991.8 sec

Nodes Path, $\widehat{S_{19,7}}$: ['19', '7'],

Edge Sequence, $\widehat{S_{(19,7)}}$: [('19', '7')]

The next step is to seek the best solution, namely the one that yields the lowest value of TOT. The nested-GA process described in section 3.3.3 is initiated. Several experiments are conducted for calibrating the GA parameters.

For the assignment GA (outer), the chromosome consists of 11 genes (equal to the number of items), each one being able to bear a discrete value among the respective gene space, SN_k. After extensive experimentation, certain parameters were further selected for calibration. We select a random mutation method, picking permitted values from each gene's gene space. Single point crossover and ranking parent selection are used. A total of 100 generations are produced. Crossover and mutation probabilities are set at 0.1 and 0.2 and population size is set at 10 and 20 and several combinations of the parameters are tested.

For the routing GA (inner), the chromosome each time is of different size ($|T^{v}_{Mc}|$), depending on the mandatory nodes resulting from assignment. Each gene takes up random, continuous values between -100 and 100 and then the mandatory nodes are ordered according to their respective gene's value. Single point crossover and ranking parent selection are used. A total of 100 generations are produced. Crossover and mutation probabilities are both set at 0.1. Population size is set at 5 and 10. Several combinations of Routing and Assignment GA settings are tested.

Table 11: Parameter combinations for nested-GA calibration experiments

	Assignment GA			**Routing GA**		
Exp. No	**Pop Size**	**Cross P**	**Mut P**	**Pop size**	**Cross P**	**Mut P**
Exp. 1	10	0.1	0.1	5	0.1	0.1
Exp. 2	10	0.1	0.2	5	0.1	0.1
Exp. 3	10	0.2	0.1	5	0.1	0.1
Exp. 4	10	0.2	0.2	5	0.1	0.1
Exp. 5	10	0.2	0.2	10	0.2	0.2
Exp. 6	10	0.2	0.4	10	0.2	0.2
Exp. 7	10	0.4	0.2	10	0.2	0.2
Exp. 8	10	0.4	0.4	10	0.2	0.2

Exp. 9	20	0.2	0.2	10	0.2	0.2
Exp. 10	20	0.2	0.4	10	0.2	0.2

Summary results of the above experiments are presented in Table 12. Increasing population size and crossover or mutation probabilities seems to have little effect on the best achievable result and computing time is increased without benefit. Results show that a specific solution (solution *1) is dominantly suggested as the best, yielding a TOT of 19942.7 sec (5h32'23"). Figure 15 and Figure 16 illustrate the evolution of results for Experiment 1, Run 2 (occurrence of best solution).

Table 12: Summary results of nested-GA calibration experiments

	Run 1			Run 2			Run 3		
Exp. No	**TOT (sec)**	**TMa**	**S^{M}_{ij}**	**TOT (sec)**	**TMa**	**S^{M}_{ij}**	**TOT (sec)**	**TMa**	**S^{M}_{ij}**
Exp. 1	20003	['2', '7', '8', '10', '12']	['0', '2', '12', '10', '8', '7', '1']	**19943*¹**	**['0', '2', '8', '10', '12']**	**['0', '8', '10', '12', '2', '1']**	19943	['0', '2', '8', '10', '12']	['0', '2', '12', '10', '8', '1']
Exp. 2	20445	['0', '2', '8', '12']	['0', '2', '8', '12', '1']	19943	['0', '2', '8', '10', '12']	['0', '2', '8', '10', '12', '1']	19943	['0', '2', '8', '10', '12']	['0', '2', '12', '10', '8', '1']
Exp. 3	19943	['0', '2', '8', '10', '12']	['0', '2', '12', '10', '8', '1']	19943	['0', '2', '8', '10', '12']	['0', '2', '8', '10', '12', '1']	20445	['0', '2', '8', '12']	['0', '12', '8', '2', '1']
Exp. 4	19943	['0', '2', '8', '10', '12']	['0', '8', '10', '12', '2', '1']	19943	['0', '2', '8', '10', '12']	['0', '8', '10', '12', '2', '1']	21849	['2', '7', '8', '10', '14']	['0', '2', '14', '10', '8', '7', '1']
Exp. 5	20360	['0', '2', '8', '10', '12', '13', '14', '15']	['0', '2', '8', '10', '13', '14', '15', '12', '1']	19943	['0', '2', '8', '10', '12']	['0', '2', '12', '10', '8', '1']	19943	['0', '2', '8', '10', '12']	['0', '2', '12', '10', '8', '1']
Exp. 6	19943	['0', '2', '8', '10', '12']	['0', '12', '10', '8', '2', '1']	19943	['0', '2', '8', '10', '12']	['0', '2', '12', '10', '8', '1']	19943	['0', '2', '8', '10', '12']	['0', '2', '12', '10', '8', '1']
Exp. 7	21910	['0', '2', '8', '13', '14', '15', '16']	['0', '8', '13', '14', '15', '16', '2', '1']	19943	['0', '2', '8', '10', '12']	['0', '2', '12', '10', '8', '1']	19943	['0', '2', '8', '10', '12']	['0', '2', '12', '10', '8', '1']
Exp. 8	19943	['0', '2', '8', '10', '12']	['0', '12', '10', '8', '2', '1']	19943	['0', '2', '8', '10', '12']	['0', '2', '12', '10', '8', '1']	19943	['0', '2', '8', '10', '12']	['0', '2', '12', '10', '8', '1']
Exp. 9	20445	['0', '2', '8', '12']	['0', '12', '8', '2', '1']	19943	['0', '2', '8', '10', '12']	['0', '2', '12', '10', '8', '1']	19943	['0', '2', '8', '10', '12']	['0', '2', '12', '10', '8', '1']
Exp. 10	19943	['0', '2', '8', '10', '12']	['0', '8', '10', '12', '2', '1']	19943	['0', '2', '8', '10', '12']	['0', '2', '12', '10', '8', '1']	19943	['0', '2', '8', '10', '12']	['0', '2', '12', '10', '8', '1']

**¹ Solution *1: best solution*

Pop Size: Population Size, Cross P: Probability of Crossover, Mut P: Probability of Mutation, TMa: Mandatory Nodes with Action, S^{M}_{ij}: Order of visit of mandatory nodes (coded in Python 3.9)

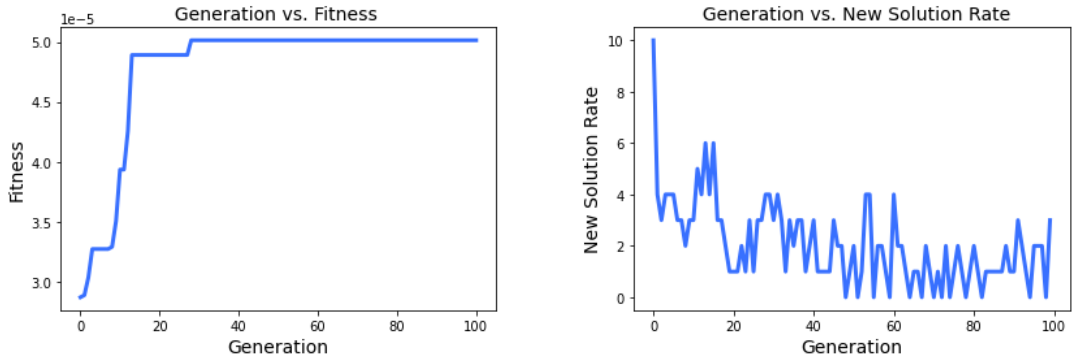

Figure 15: Evolution of Fitness and Solutions through Generations (Experiment 1, Run 2, Solution *1)

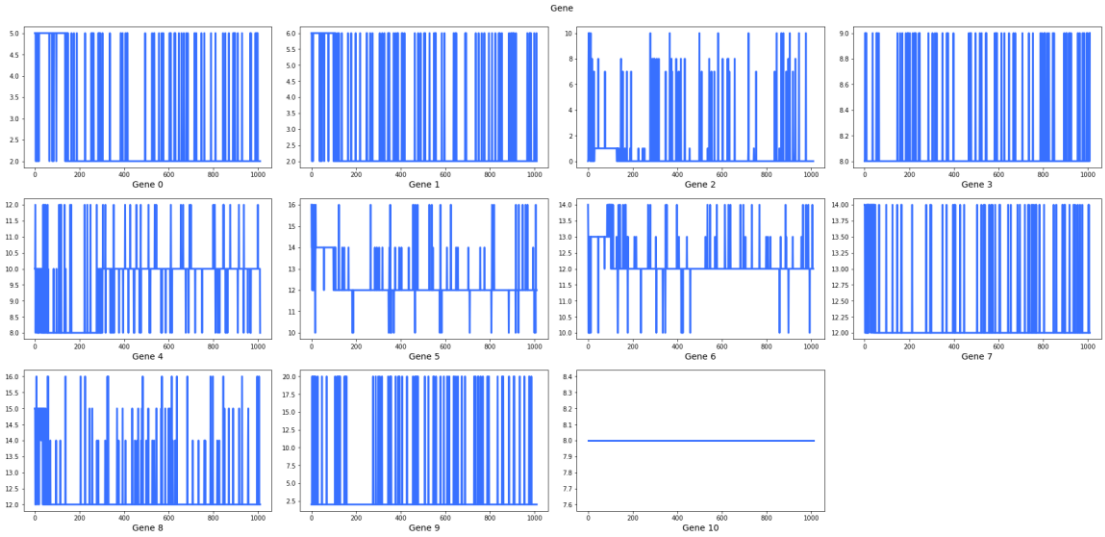

Figure 16: Gene selection process through Generations (Experiment 1, Run 2, Solution *1)

The following figures represent the best solution (Solution *1) found throughout the experiments.

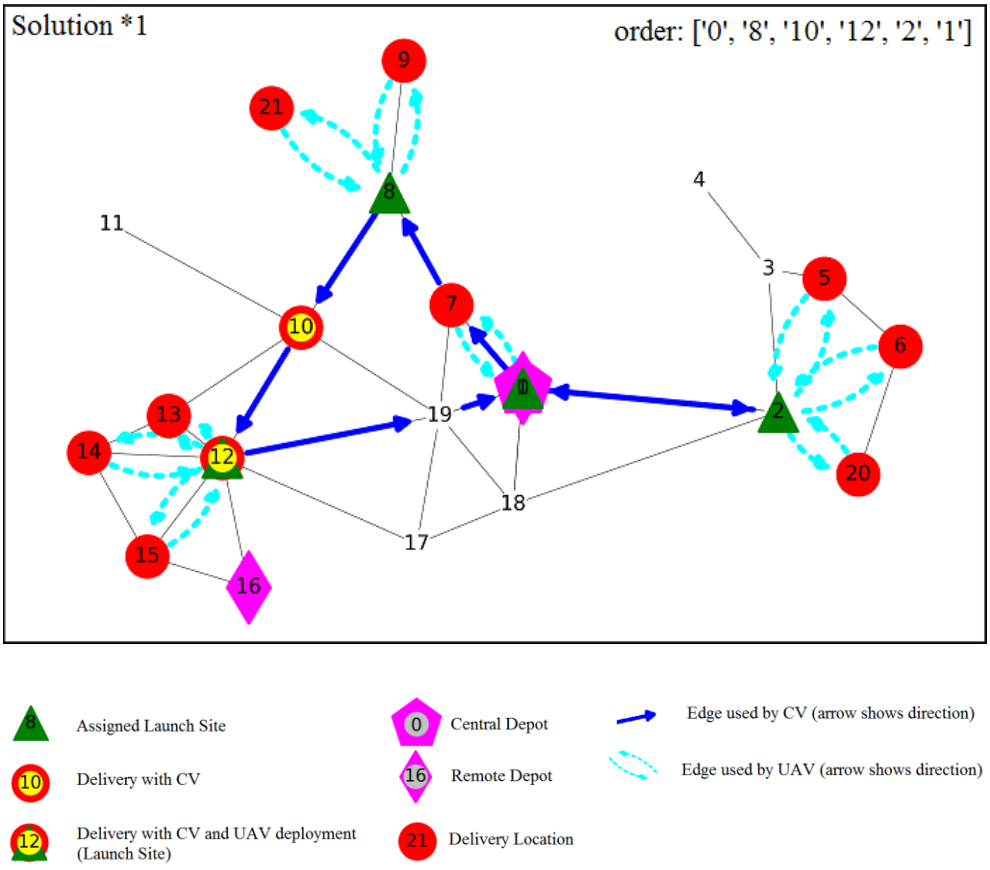

Figure 17: Illustration of assignment and routing for Solution *1

We further examine Solution *1 to see the calculations involved.

Table 13: Potential Launch Sites and Final Service Nodes Pool for Items

Item (k)	Node (d_k)	Service Nodes Pool [SN_k]					Assigned Service Node (l_k)	Mode (final)
1	5	5	2				2	UAV
2	6	6	2				2	UAV
3	7	7	0	1	8	10	0	UAV
4	9	9	8				8	UAV
5	10	10	8	12			10	CV
6	12	12	10	14	16		12	CV
7	13	13	10	12	14		12	UAV
8	14	14	12				12	UAV
9	15	15	12	14	16		12	UAV
10	20	20	2				2	UAV
11	21		8				8	UAV

The following information describes the path of the CV:

Table 14: Routing information (solution *1)

T_{Ma}^{v}	['0', '2', '8', '10', '12']	Mandatory nodes with action
T_{M}^{v}	['0', '1', '2', '8', '10', '12']	Mandatory nodes

$\widehat{S_v^M}$	['0', '8', '10', '12', '2', '1'	Path of mandatory nodes
$\widehat{S_{(e)}^M}$	[('0', '8'), ('8', '10'), ('10', '12'), ('12', '2'), ('2', '1')]	Sequence of shell edges, through mandatory nodes
$\widehat{S_v}$	[['0', '7', '8'], ['8', '10'], ['10', '12'], ['12', '19', '0', '2'], ['2', '1']]	Full path of nodes
$\widehat{S_{(e)}}$	[('0', '7'), ('7', '8'), ('8', '10'), ('10', '12'), ('12', '19'), ('19', '0'), ('0', '2'), ('2', '1')]	Full sequence of edges

Calculations resulting from the actions taken on mandatory nodes are shown in Table 15, below.

Table 15: Calculations for mandatory nodes with action(s) (*TMa*) (solution *1)

Service Nodes	Assigned Items (k)				Nodes (dk)				|Li|	dth_{ij}			max dth_{ij}	w_i	st (sum)	tc (sum)
0		3				7			1	1574.0			1574.0	0.0	0.0	300*
8		4	11			9	21		2	1921.6	1983.2		1983.2	2583.2	0.0	600.0
10	*5*				*10*				0	-			0.0	60.0	60.0	0.0
12	*6*	7	8	9	*12*	13	14	15	3	1035.9	1790.7	1758.1	1790.7	2750.7	60.0	900.0
2		1	2	10		5	6	20	3	2015.6	1885.2	1446.7	2015.6	2915.6	0.0	900.0
	CV	UAV			*CV*	UAV										

**Launch from Central Depot, CV does not wait*

The path of the CV, actions along the way and performance results are presented in Table 16, below.

Table 16: Path, actions, and time evolution (sec) (solution *1)

Order	*1 (CD)*	*2*	*3*	*4*	*5*	*6 (CD/RD)*
Mandatory Node	**'0'**	**'8'**	**'10'**	**'12'**	**'2'**	**'1'**
Pass Through	*'7'*			*'19', '0'*		
Action	Launch	Launch	Delivery	Delivery Launch	Launch	
$\mathbf{t^{app}}$	-	2067.2	6026.1	7446.5	14876.2	**19942.7**
$\boldsymbol{ct_{ij}^M}$	0.0	2067.2	1375.7	1360.4	4679.1	2150.9
$\mathbf{w_i}$	0.0	2583.2	60.0	2750.7	2915.6	0.0
$\mathbf{t^{dep}}$	0.0	4650.4	6086.1	10197.1	17791.8	-
$\mathbf{t^{ret}}$	**1874.0**	0.0	0.0	0.0	0.0	0.0
TOT (sec)						**19942.7**

Table 17: Items delivery information

Item (k)	Node (d_k)	Assigned Service Node (l_k)	Mode (final)	Delivery Time (dt_k) (sec)
1	5	2	UAV	16814.0
2	6	2	UAV	16748.8
3	7	0	UAV	1117.0
4	9	8	UAV	3658.1

5	10	10	CV	6086.1
6	12	12	CV	7506.5
7	13	12	UAV	8954.4
8	14	12	UAV	9331.8
9	15	12	UAV	9315.5
10	20	2	UAV	16529.5
11	21	8	UAV	3688.8

The following charts (Figure 18, Figure 19) illustrate the evolution of time along the path of solution *1.

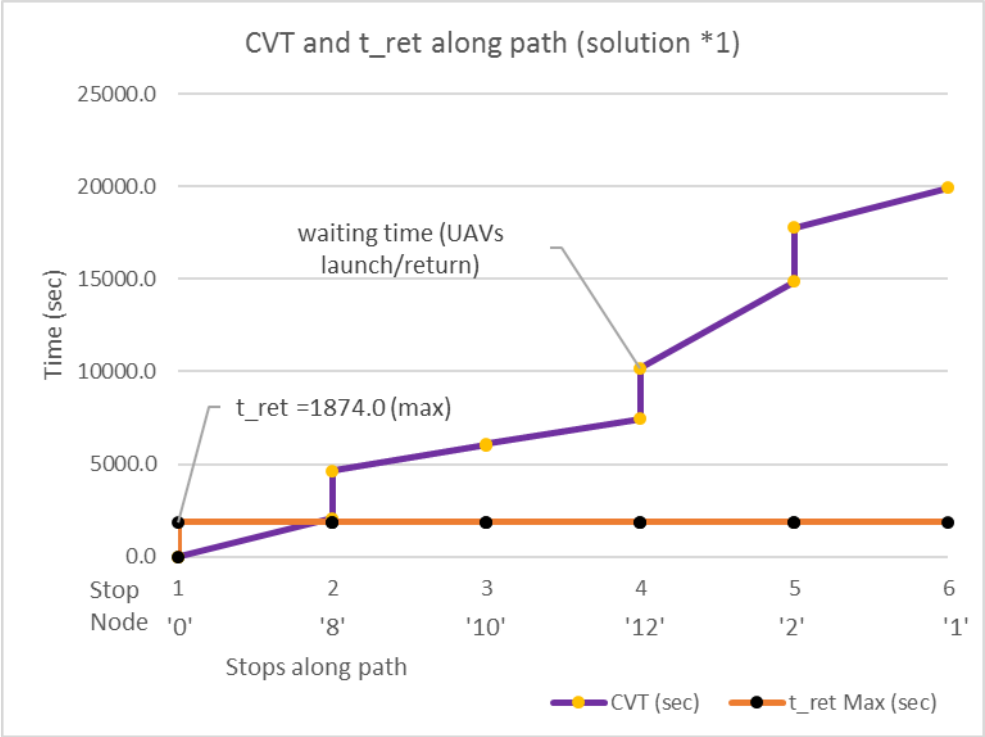

Figure 18: CVT and max t^{ret} evolution along path (solution *1)

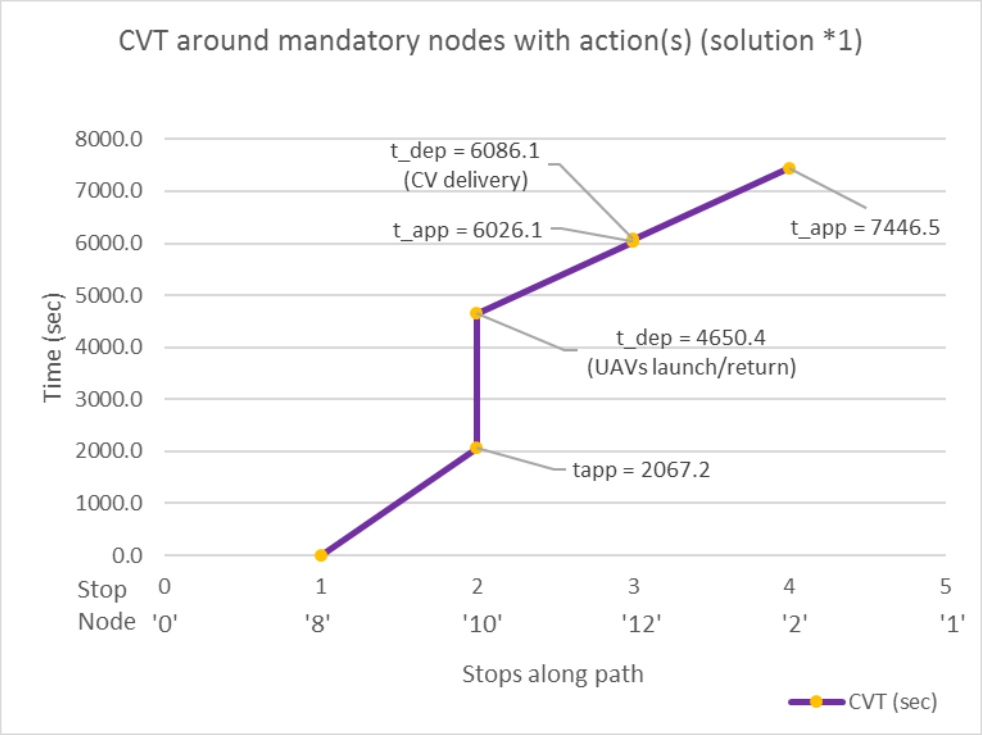

Figure 19: Close-up view of CVT evolution before and after mandatory node with action (solution *1)

It is worth noting that in operations throughout such a network with considerable distances to cover, some parameters such as time to ascend/descend or transshipment only amount for a small fraction of the total time. However, their inclusion in our framework ensures more accurate estimations for smaller networks and more deliveries, adding to the versatility we intended to achieve.

Before proceeding to more complex cases, we opted to compare our framework against simple, CV-based operations. To test that, we used our core methodology again, adjusting available infrastructure for UAV deployment. By just removing all Launch Sites, no UAV can be used, and all deliveries must be executed by CV, provided the Delivery Location is within the CVN. In the nested-GA optimization process, assignment no longer plays a role, since all DLs in the CVN are assigned to CV. Thus, only the routing (inner) part is used, seeking the best visiting order by the CV through mandatory nodes. Figure 20 below illustrates the best solution.

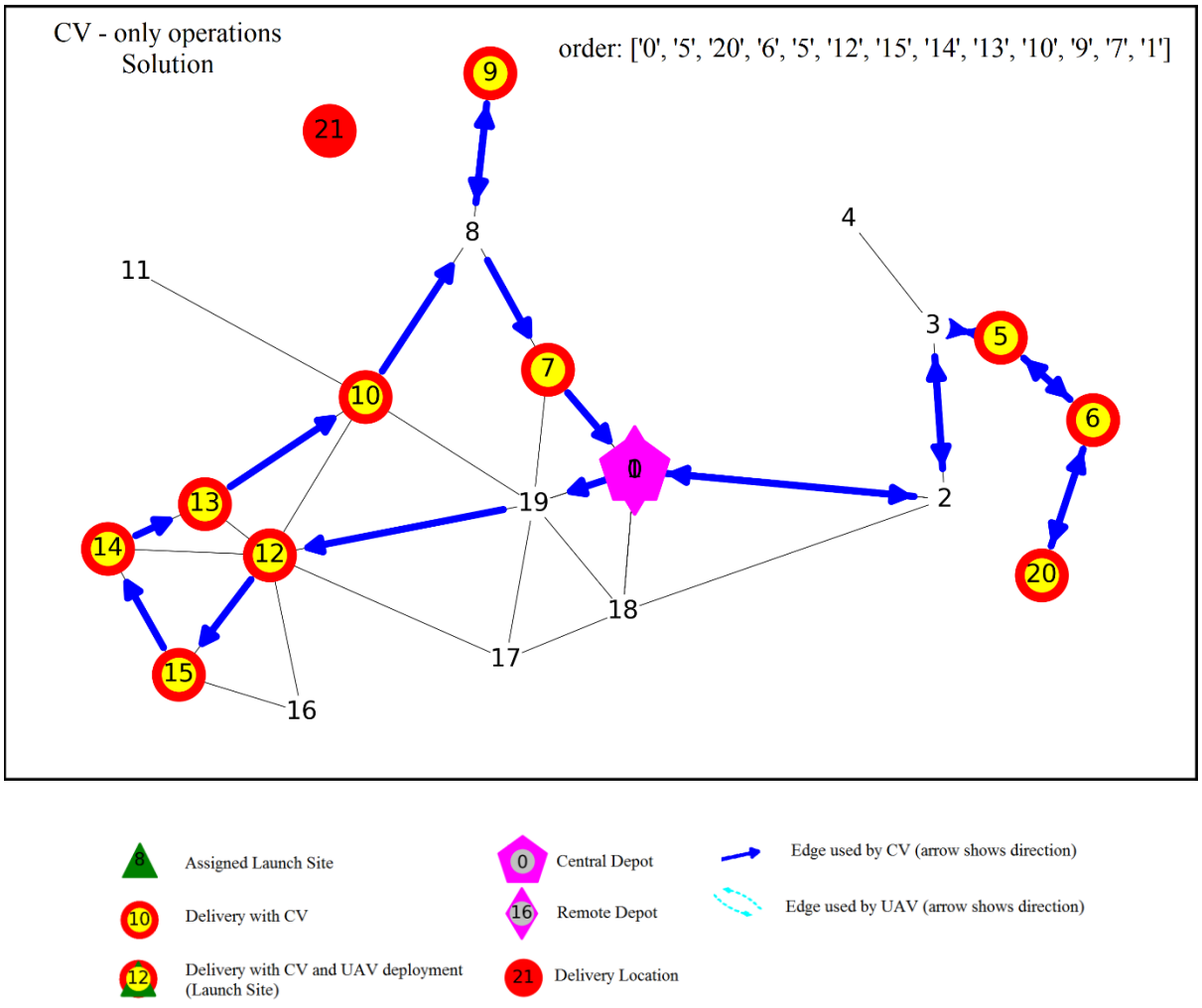

Figure 20: Illustration of assignment and routing for best solution in CV - only operations

All operations are finished in CVT = TOT = 25730.9 sec, or 7h8'51". Solution*1 obtained under combined CV-UAV operations yielded a TOT = 19942.7 sec (5h32'23"), which is 5788.2 sec, or 1h36'28", or an impressive 22.5% faster. It must be noted that DL at node 21 cannot be served under CV-only operations. Despite serving node 21 too, the combined CV-UAV operations fare significantly better than CV – only.

Table 18: Routing information (CV – only operations solution)

T_{Ma}^{v}	['5', '6', '7', '9', '10', '12', '13', '14', '15', '20']	Mandatory nodes with action
T_{M}^{v}	['0', '1', '5', '6', '7', '9', '10', '12', '13', '14', '15', '20'	Mandatory nodes
$\widehat{S_{v}^{M}}$	['0', '5', '20', '6', '5', '12', '15', '14', '13', '10', '9', '7', '1']	Path of mandatory nodes
$\widehat{S_{(e)}^{M}}$	[('0', '5'), ('5', '20'), ('20', '6'), ('6', '5'), ('5', '12'), ('12', '15'), ('15', '14'), ('14', '13'), ('13', '10'), ('10', '9'), ('9', '7'), ('7', '1')]	Sequence of shell edges, through mandatory nodes

$\widehat{S_v}$	[['0', '2', '3', '5'], ['5', '6', '20'], ['20', '6'], ['6', '5'], ['5', '3', '2', '0', '19', '12'], ['12', '15'], ['15', '14'], ['14', '13'], ['13', '10'], ['10', '8', '9'], ['9', '8', '7'], ['7', '1']]	Full path of nodes
$\widehat{S_{(e)}}$	[('0', '2'), ('2', '3'), ('3', '5'), ('5', '6'), ('6', '20'), ('20', '6'), ('6', '5'), ('5', '3'), ('3', '2'), ('2', '0'), ('0', '19'), ('19', '12'), ('12', '15'), ('15', '14'), ('14', '13'), ('13', '10'), ('10', '8'), ('8', '9'), ('9', '8'), ('8', '7'), ('7', '1')]	Full sequence of edges

It is also important that this additional analysis was performed using the same methodology, by just removing the "Launch Site" label from all nodes. This highlights the methodology's responsiveness to infrastructure changes and its convenient front-end structure for practical use and experimentation.

3.4.3.1 Sensitivity Analysis

We have further explored the responsiveness of our framework to different infrastructure and equipment parameters. Guided by trends shown in preceding experiments and for the same delivery locations, we assume the establishment of new Remote Depots at critical nodes, namely Nodes 2, 8 and 12, removing the one at Node 16. This is Infrastructure Setup 2 (the original one is named Setup 1). Another Setup (named Setup 3) is devised, featuring the minimum number of launch sites of the lowest specs, namely a single Virtual Hub at Node 8, which at least ensures the delivery at Node 21 (outside the CVN).

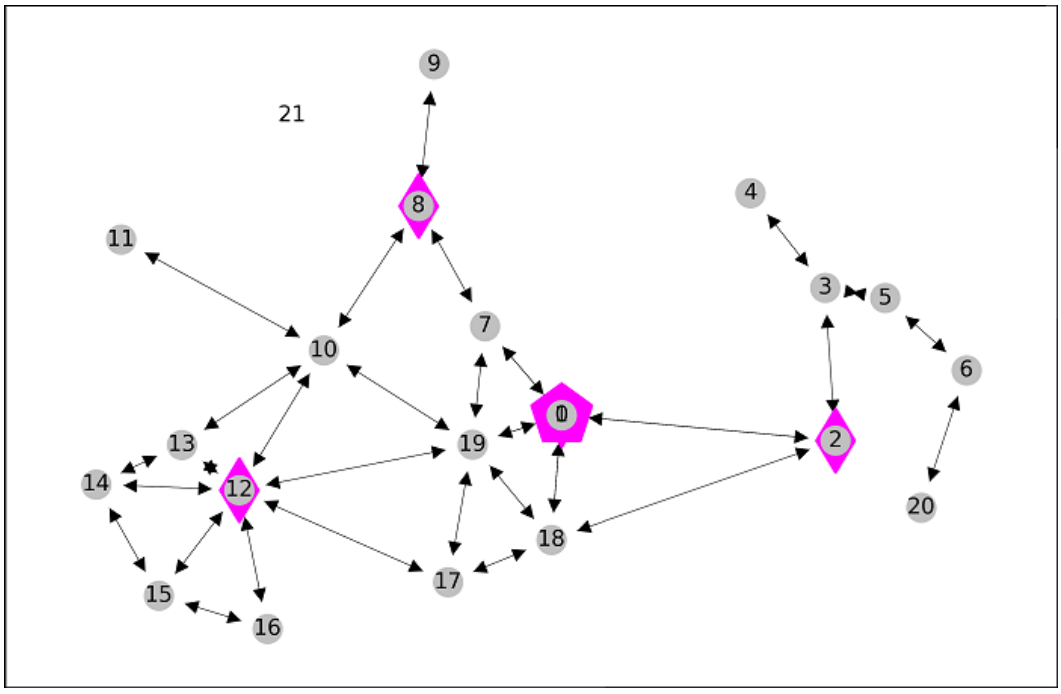

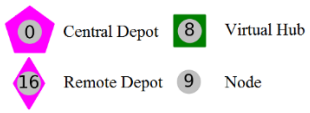

Figure 21: CV network and Node Types for Setup 2

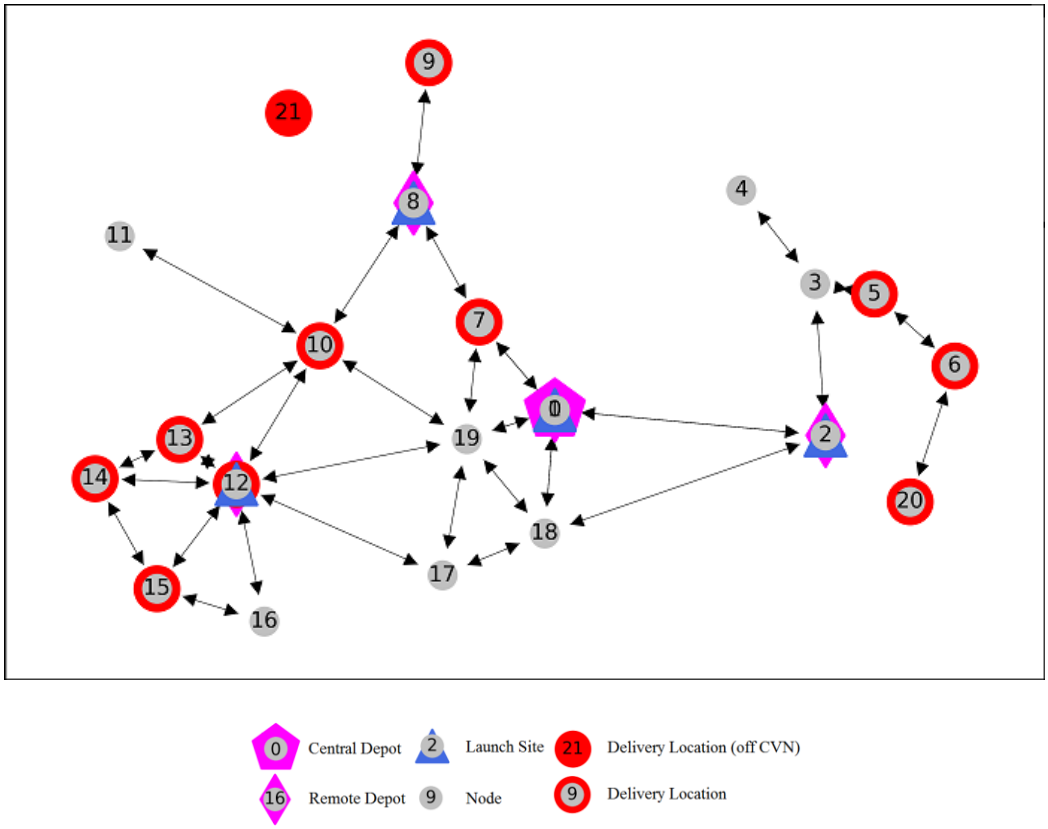

Figure 22: Delivery Locations and final allowed Launch Sites for Setup 2

Central Depot [CD]: '0'

Remote Depots [RD]: '2', '8', '12'

Virtual Hubs [VH]: (none)

Delivery Locations [DL]: '5', '6', '7', '9', '10', '12', '13', '14', '15', '20', '21'

Launch Sites [LS]: '2', '8', '12'

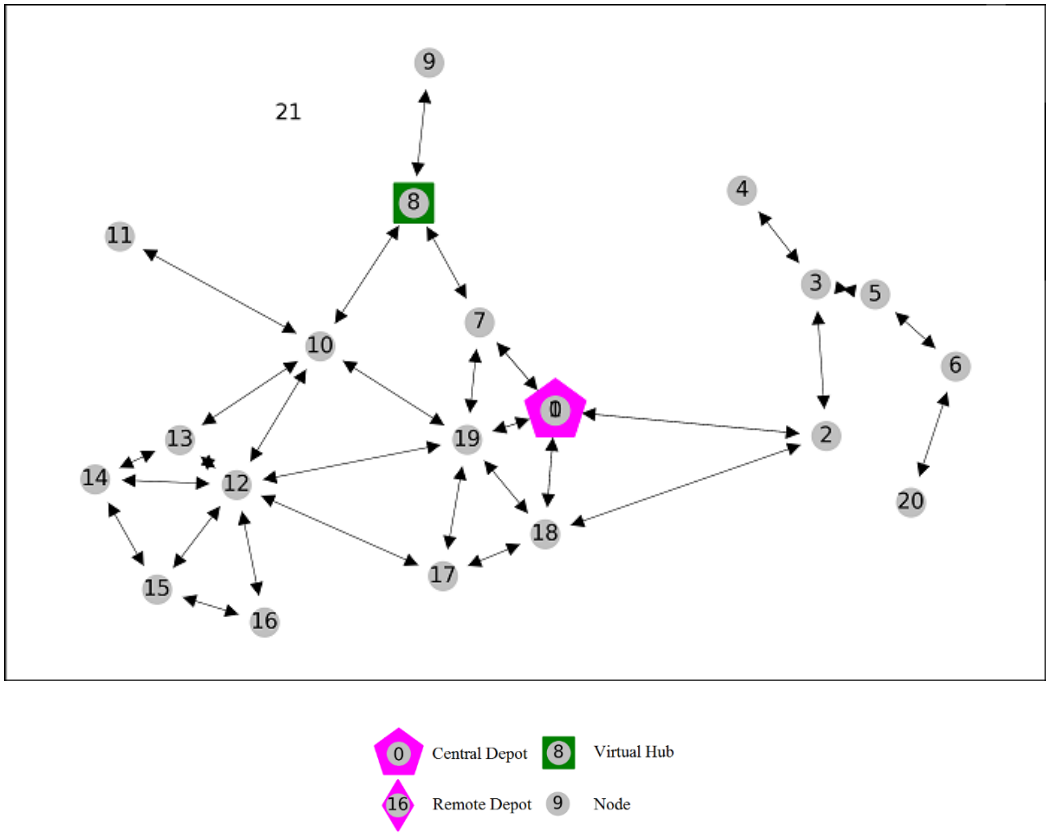

Figure 23: CV network and Node Types for Setup 3

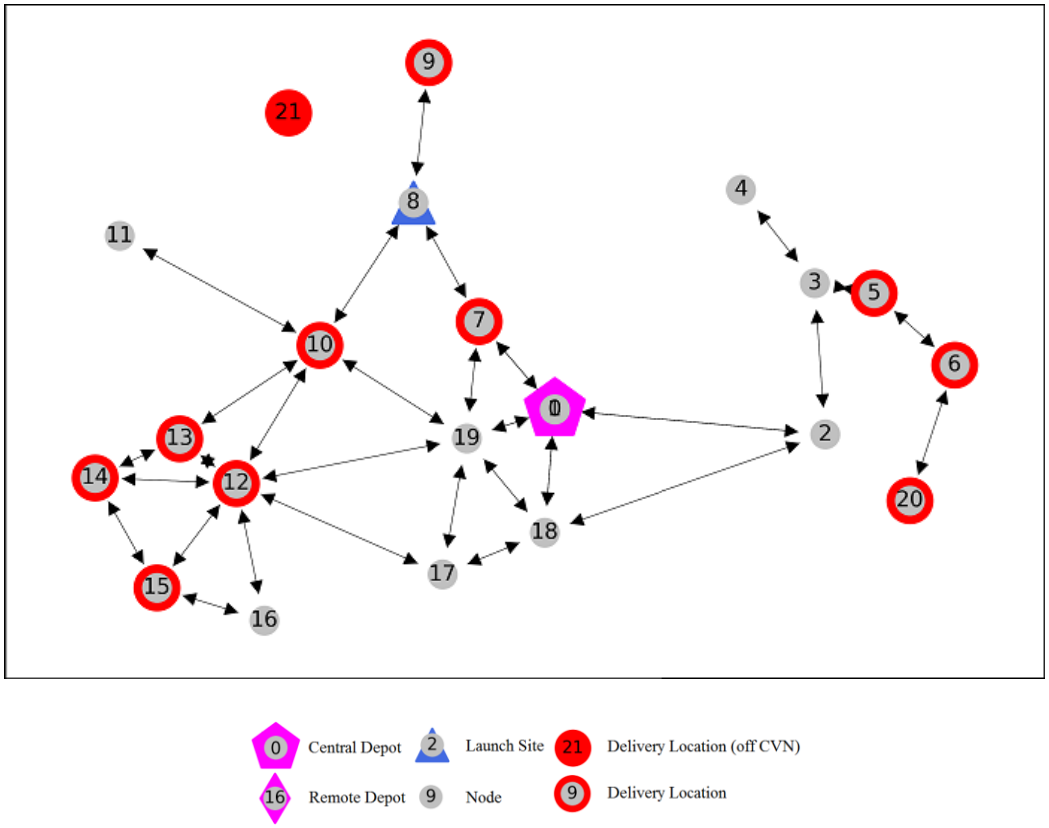

Figure 24: Delivery Locations and final allowed Launch Sites for Setup 3

Central Depot [CD]: '0'

Remote Depots [RD]: (none)

Virtual Hubs [VH]: '8'

Delivery Locations [DL]: '5', '6', '7', '9', '10', '12', '13', '14', '15', '20', '21'

Launch Sites [LS]: '8'

Additionally, different specifications for the UAV and CV are considered: UAV range, which may be a result of battery technology or communication reliability, and CV mean speed, which may be a result of traffic conditions or vehicle technology.

Table 19: Alternative equipment specifications for sensitivity analysis

Specification	*Values*		
S^{CV} *(km/h)*	20	40	60
R^{UAV} *(min)*	40	60	80

For each setup all different combinations of the above specifications have been tested. The edge costs and adjacency matrices are updated based on each scenario.

After several runs, each experiment yielded a best result as listed in Table 20 below. The best performance (5958.8 sec, or 1h39'19") was achieved under Setup 2, Experiment 9 (UAV Range: 80 min, CV speed: 60 km/h). The worst one (59934.2 sec, or 16h38'54") appeared under Setup 3, Experiment 1 (UAV Range: 40 min, CV speed: 20 km/h).

Table 20: Sensitivity experiment parameters and results

SETUP	Experiment	R_UAV (min)	S_CV (km/h)	TOT (sec)	TMa	S^{M}_{ij}
SETUP 1	**Exp1**	40	20	31576.0	['0', '2', '8', '10', '12']	['0', '8', '10', '12', '2', '1']
	Exp2	**40**	**40**	19942.7	['0', '2', '8', '10', '12']	['0', '8', '10', '12', '2', '1']
	Exp3	40	60	16065.0	['0', '2', '8', '10', '12']	['0', '2', '12', '10', '8', '1']
	Exp4	60	20	31516.0	['0', '2', '8', '12']	['0', '12', '8', '2', '1']
	Exp5	60	40	19861.1	['0', '2', '8', '16']	['0', '8', '16', '2', '1']
	Exp6	60	60	16005.0	['0', '2', '8', '12']	['0', '2', '8', '12', '1']
	Exp7	80	20	13483.8	['0', '10']	['0', '10', '1']
	Exp8	80	40	9043.9	['0', '10']	['0', '10', '1']
	Exp9	80	60	7563.9	['0', '10']	['0', '10', '1']
SETUP 2	**Exp1**	40	20	23866.6	['0', '2', '8', '12']	['0', '2', '12', '8', '1']

	Exp2	**40**	**40**	12395.8	['0', '2', '8', '12']	['0', '2', '8', '12', '1']
	Exp3	40	60	9360.8	['0', '2', '8', '12']	['0', '2', '8', '12', '1']
	Exp4	60	20	23806.6	['0', '2', '8', '12']	['0', '8', '12', '2', '1']
	Exp5	60	40	12335.8	['0', '2', '8', '12']	['0', '2', '8', '12', '1']
	Exp6	60	60	9300.8	['0', '2', '8', '12']	['0', '2', '8', '12', '1']
	Exp7	80	20	10934.9	['0', '12']	['0', '12', '1']
	Exp8	80	40	7511.4	['0', '8', '12'	['0', '8', '12', '1']
	Exp9	80	60	*5958.8*	['0', '7', '8', '12']	['0', '8', '12', '1']
SETUP 3	**Exp1**	40	20	59934.2	['5', '6', '7', '8', '12', '13', '14', '15', '20']	['0', '8', '7', '20', '5', '6', '14', '15', '12', '13', '1']
	Exp2	**40**	**40**	33024.6	['5', '6', '7', '8', '12', '13', '14', '15', '20']	['0', '12', '6', '5', '20', '8', '13', '14', '15', '1']
	Exp3	40	60	21157.3	['5', '6', '7', '8', '12', '13', '14', '15', '20']	['0', '15', '13', '14', '12', '8', '5', '6', '20', '7', '1']
	Exp4	60	20	56359.1	['5', '6', '8', '12', '13', '14', '15', '20']	['0', '8', '5', '20', '6', '12', '14', '13', '15', '1']
	Exp5	60	40	28925.3	['5', '6', '7', '8', '12', '13', '14', '15', '20']	['0', '5', '6', '20', '7', '15', '12', '13', '14', '8', '1']
	Exp6	60	60	20333.1	['5', '6', '7', '8', '12', '13', '14', '15', '20']	['0', '10', '13', '14', '15', '12', '8', '20', '5', '6', '1']
	Exp7	80	20	52918.9	['5', '6', '8', '10', '12', '13', '14', '15', '20']	['0', '6', '20', '5', '14', '12', '15', '13', '10', '8', '1']
	Exp8	80	40	27242.6	['5', '6', '8', '12', '13', '14', '15', '20']	['0', '5', '6', '20', '15', '14', '13', '12', '8', '1']
	Exp9	80	60	19710.6	['5', '6', '8', '12', '13', '14', '15', '20']	['0', '20', '6', '5', '12', '14', '15', '13', '8', '1']

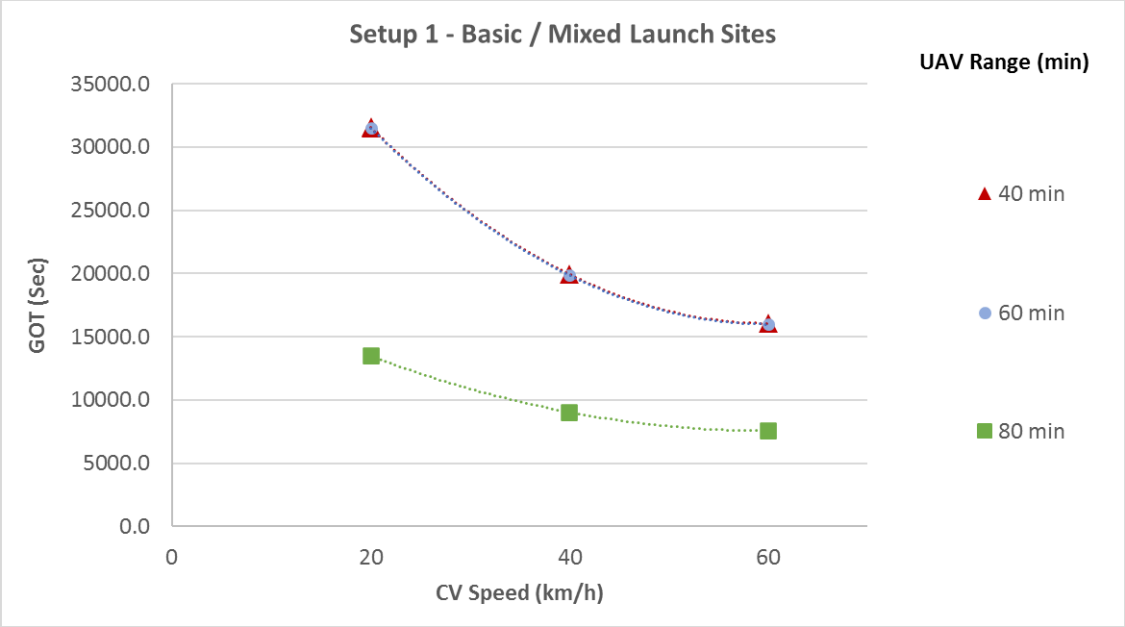

Figure 25: Illustration of sensitivity experiment results for Setup 1

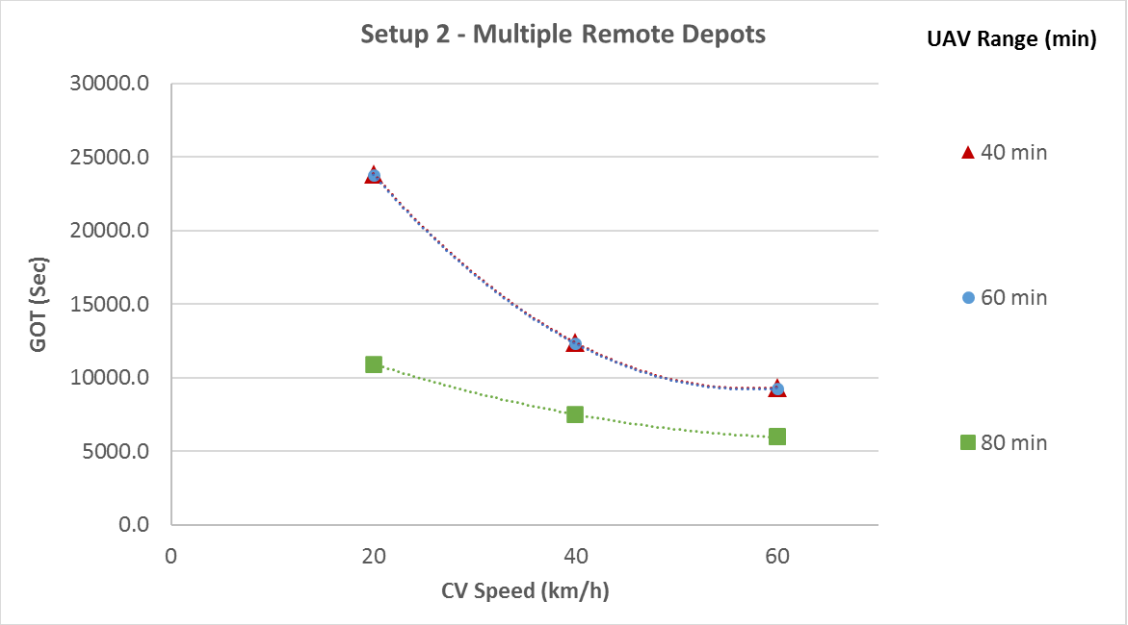

Figure 26: Illustration of sensitivity experiment results for Setup 2

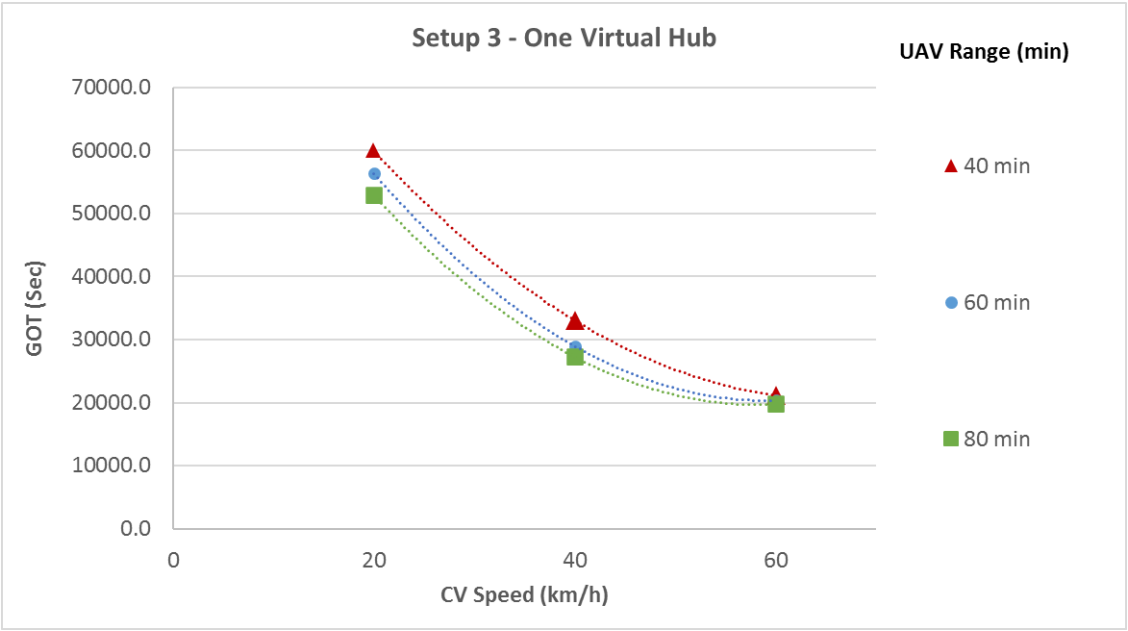

Figure 27: Illustration of sensitivity experiment results for Setup 3

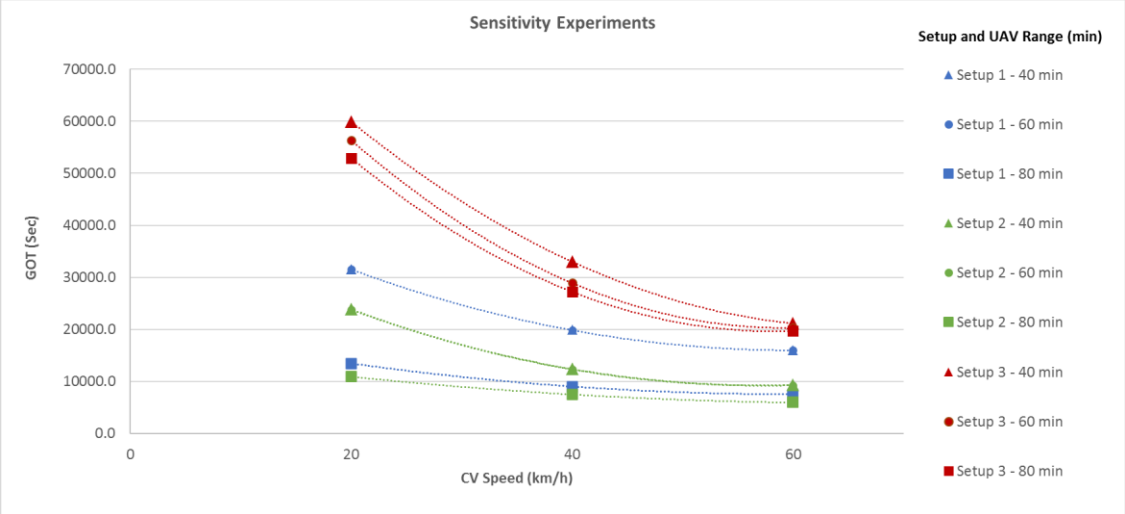

Figure 28: Comparative illustration of sensitivity experiment results

The experiments have shown that the proposed framework, its model, and the solution methodology respond well against changes in infrastructure and equipment. The adaptation is easy, and the proposed solution is clearly described for implementation.

It is reasonable to expect better performance as UAV range and CV speed increase. However, it is not as simple as "more is better". The positioning of Remote Depots, Virtual Hubs and the final allocation of potential Launch Sites greatly affect performance. Creating Remote Depots closer to areas with multiple delivery requests (Setup 2) is a good strategy, however a wise mix of Remote Depots, Virtual Hubs, and pop-up Launch Sites (e.g., at delivery locations) (Setup 1) is also a strong combination if such heavy infrastructure is not available. Under Setup 1 and Setup 2, the increase of UAV range from 40 min to 60 min does not offer big gains; because of the geographic position of the DLs and LSs, there is little change in the Service Nodes Pool. This changes drastically with the 80 min range. It is also worth noting that longer UAV ranges are not always taken advantage of, since a faster CV or the increased time for the preparation and repackaging of multiple UAVs may lead to a counter-intuitive (but better) solution.

We illustrate the assignment and routing solutions of certain experiments, showing how everything changes depending on infrastructure and equipment.

Under Setup 1, Experiment 9 it is clear how the increased UAV range unleashes potential for clustered long-distance deliveries with UAVs, using just the CD and an LS

elsewhere. The CV just travels between nodes '0' and '10', without executing any in-person delivery (see Figure 29).

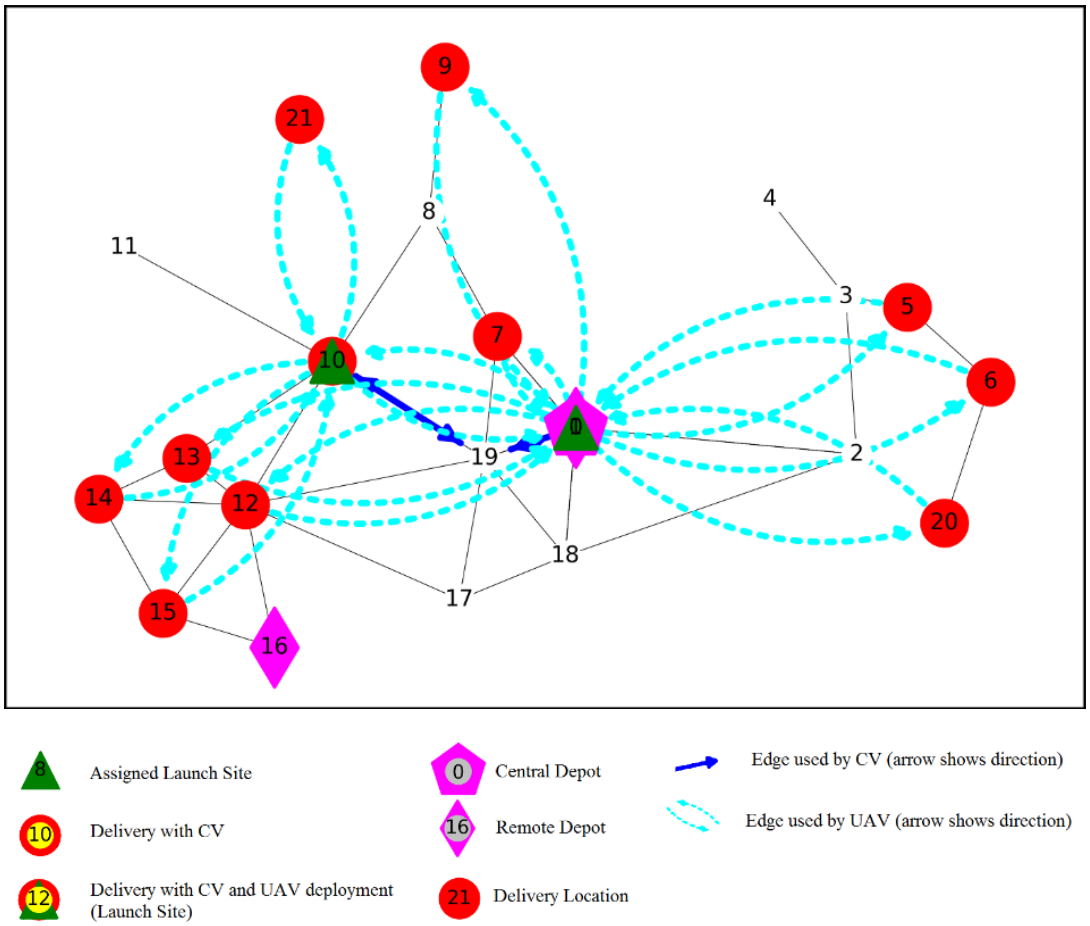

Figure 29: Illustration of Solution for Setup 1, Experiment 9 (R_UAV: 80 min, S_CV: 60 km/h, TOT = 7563.9 sec)

The following experiment (Setup 2, Experiment 2) yields very similar assignment and routing compared to the base case (Setup 1, Experiment 2). However, this time all LSs are also RDs, so that the CV does not have to wait for the UAVs to return. The gains are significant compared to the similar case in the basic setup (Setup 1) (12395.8 sec vs 19942.7 sec, or 3h26'36" vs 5h32'23") (see Figure 30).

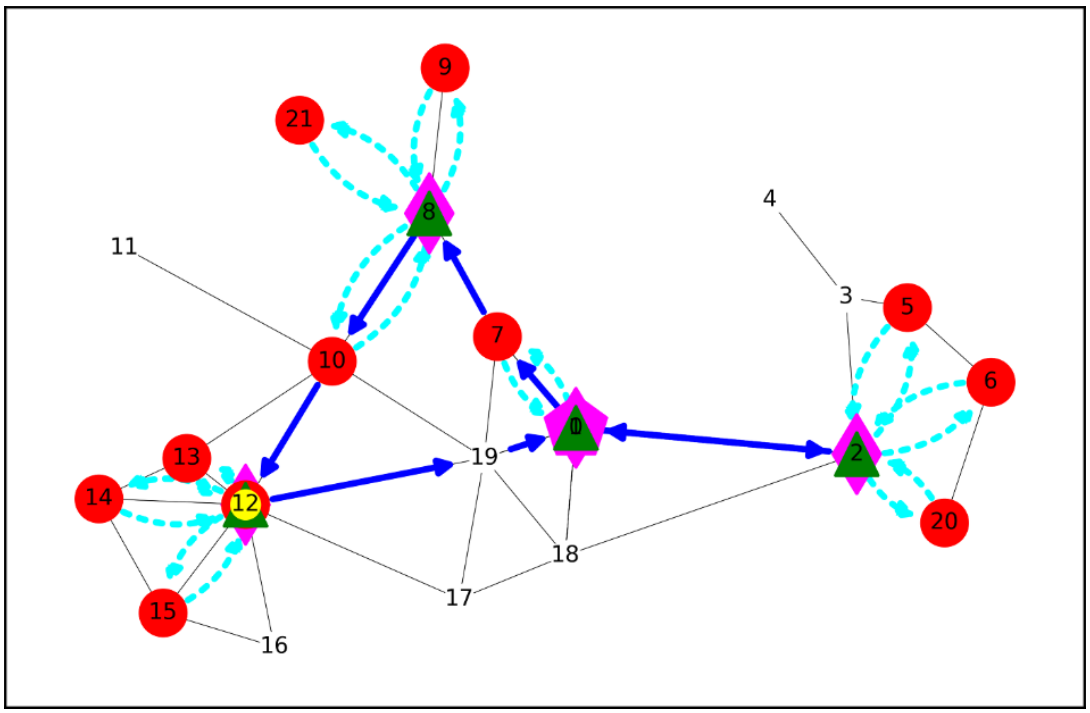

Figure 30: Illustration of Solution for Setup 2, Experiment 2 (R_UAV: 40 min, S_CV: 40 km/h, TOT = 12395.8 sec)

Under the severe constraint of only one available Launch Site (at Node '8'), the CV must travel to most of the DLs for in-person deliveries (Setup 3). The LS at Node '8' primarily exists to serve Node "21", which is outside the CVN, but through the optimization process other DLs (nodes '9' and '10') are served by it as well (see Figure 31).

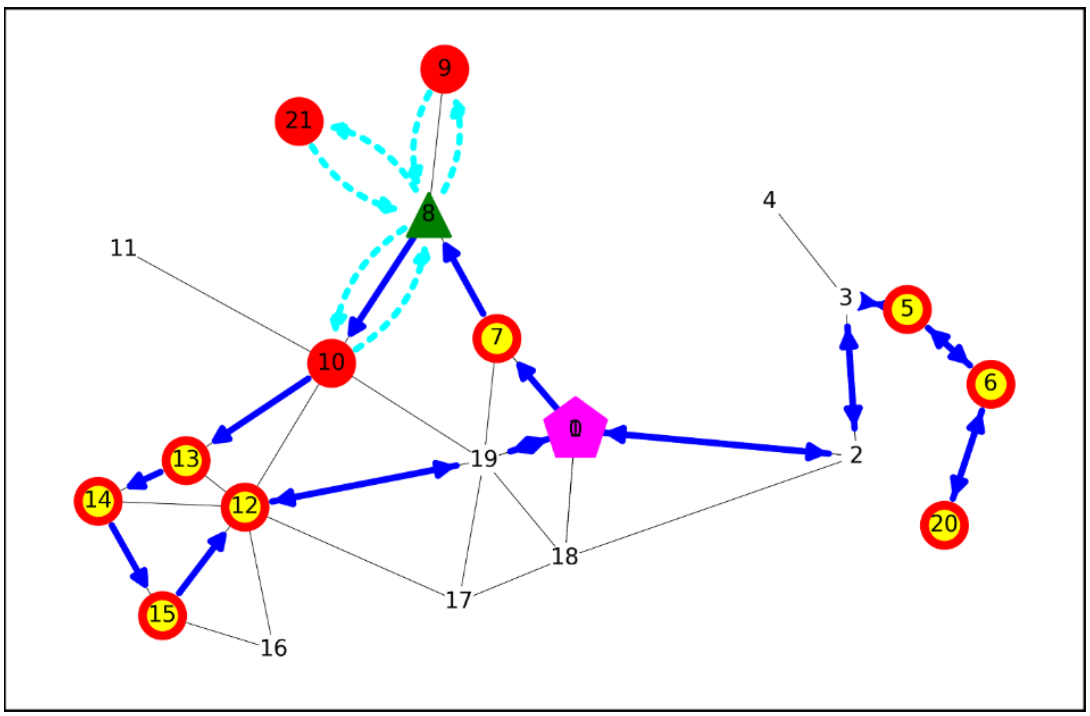

Figure 31: Illustration of Solution for Setup 3, Experiment 2 (R_UAV: 40 min, S_CV: 40 km/h, TOT = 33024.6 sec)

Other interesting results also appear under Setup 2. The order of visit through the mandatory nodes is ['0', '2', '8', '12', '1'] and DLs of '13', '14' and '15' are assigned via UAV to '12', which is now an RD but also a DL (a delivery is made at the RD, before leaving the other items to the personnel for UAV delivery). The CV, running at a high speed of 60 km/h, returns to the CD before the last UAV returns to its base ('12'), meaning TOT (9300.8 sec) and CVT (8295.5 sec) do not coincide (see Figure 32).

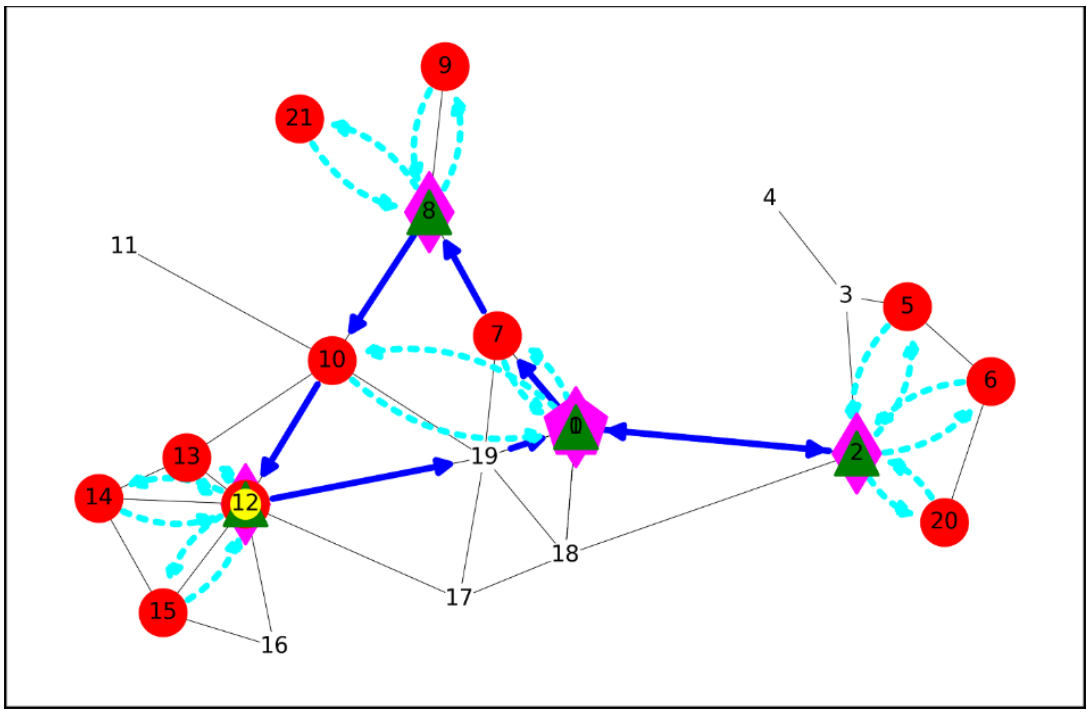

Figure 32: Illustration of Solution for Setup 2, Experiment 6 (R_UAV: 60 min, S_CV: 60 km/h, TOT = 9300.8 sec, CVT = 8295.5 sec)

Again, TOT and CVT do not coincide under Setup 2, Experiment 7 (TOT = 10934.9 sec, CVT = 10292.6 sec). The CV is used just for reaching the LS (RD) at '12' and all deliveries are made with UAVs (see Figure 33).

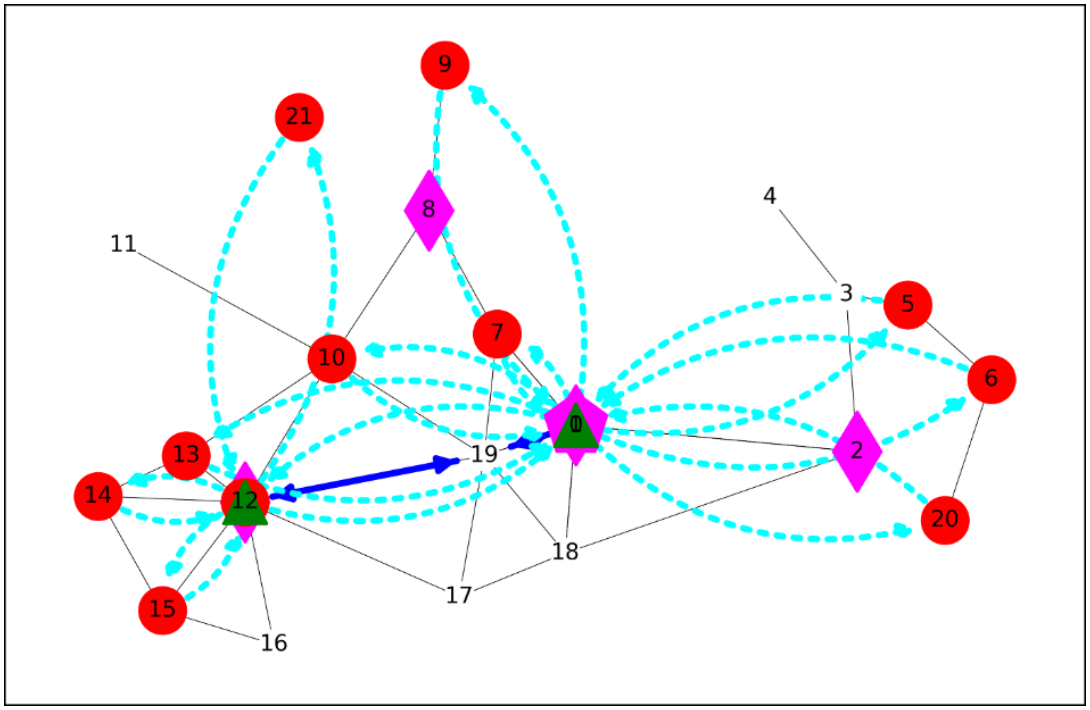

Figure 33: Illustration of Solution for Setup 2, Experiment 7 (R_UAV: 80 min, S_CV: 20 km/h, TOT = 10934.9 sec, CVT = 10292.6 sec)

3.4.4 Discussion

We have introduced a framework for planning item delivery consisting of a single Conventional Vehicle and multiple UAVs, using the physical network of the Conventional Vehicle and a given infrastructure of Virtual Hubs and Depots (a Central and several Remote ones). Choices are inspired by real-world applications and constraints, enriched by the experience of actual UAV operations. The formulation and the solution methodology proposed offer flexibility in adaptation to infrastructure (links, nodes, types of facilities) and equipment (vehicle specs) but also a wide spectrum of network characteristics (missing links, dead-ends, butterfly routes). Each step, from inputs to final optimization, is part of a modular workflow which allows for preference-based solutions (e.g., constraints for certain locations, shortage in equipment, priority in deliveries, routing). We have developed a tailored nested-GA scheme for the two-level optimization of assignment and routing. Since not all nodes and edges of the physical network are necessarily visited, a shell network resulting from mandatory nodes and shortest path total costs between them is created, deconstructing, and simplifying the problem. Our model was implemented on a test network and delivery locations with benchmark characteristics. We have presented detailed calculations regarding

the best solution obtained under the basic scenario and have conducted sensitivity analysis under alternative network setups and equipment parameters. Substantial gains in performance (total time of operations) can be achieved with wise infrastructure choices and improved equipment specifications. Experiments have shown the robustness of the formulation and general methodology from preliminary analysis to final solution optimization.

4 Stage 2 - Design under Restricted Airspace

4.1 Background

Although it is reasonable to expect that UAVs will claim more space against controlled air traffic in the future, depending on their market penetration and range of applications, safety and operational concerns are likely to keep them away from certain areas for some time.

Air traffic rules are implemented for the efficiency and safety of air transport. Airspace is apportioned by altitude for various types of aircrafts. Current air traffic regulations in the US and the EU contain commercial UAV flights at altitudes below 400 ft/120 m (ICAO, 2018) (EASA, 2022). Most commercial and freight airplanes are fixed-wing structures and take-off, and landing procedures require certain free corridors around the airports, as the aircrafts approach and leave the ground at an angle, for a long distance. Such design standards are followed around the world and require obstacle-free zones for airport operations. (ICAO, 2022). Forbidden areas are commonly distinguished into the following categories: Prohibited Areas – P (usually military), Restricted Areas – R (monuments, environmental, military flight areas), Danger Areas – D (usually training flights), Controlled Firing Areas – C (military exercises). (ICAO, 2005) (EASA, 2022)[2] (FAA, 2016) (FAA, 2022) (HCAA, 2023). We will be referring to all forbidden areas as Restricted Zones (RZ). Figure 34 shows how airspace is segregated and controlled by airport class in the United States, according to current regulations (FAA, 2016) (FAA, 2022).

[2] *Implementing Rules: Regulation (EU) 2019/947 (Initial issue, 31/12/2020), Amendments: 2020/639, 2020/746, 2021/1166, 2022/425*

Delegated Rules: Regulation (EU) 2019/945 (Initial issue, 1/7/2019), Amendment 2020/1058

Decisions: ED Decision 2019/021/R Issue 1, 11/10/2019, 2020/022/R (Issue 1, Amendment 1, 18/12/2020), 2022/002/R (Issue 1, Amendment 2, 10/2/2022)

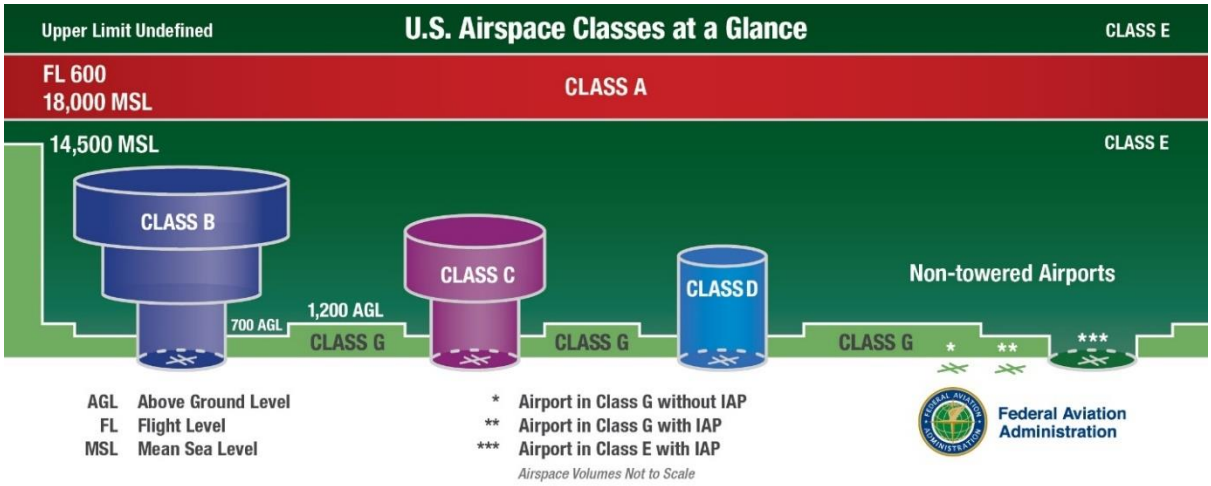

Figure 34: Illustration of airspace classification according to the FAA, USA (FAA, 2016)

Figure 35 is an example of no-fly zones for UAVs in Central Greece on an actual day (June 2023), according to the maps issued by the Hellenic Civil Aviation Authority (HCAA), as seen on the special UAS real-time information system for Greece (Drone Aware - GR (DAGR)) (HCAA, 2023).

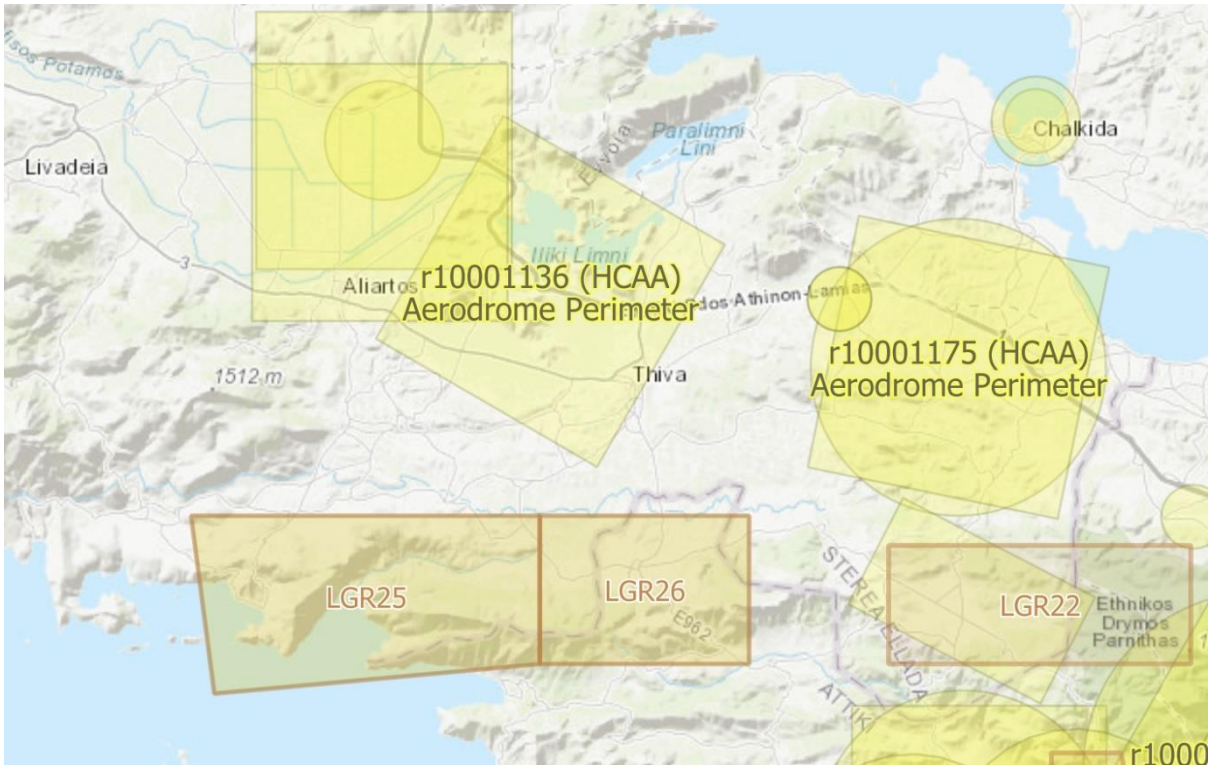

Figure 35: Example of Restricted Zones in Central Greece, June 2023 (HCAA, 2023).

Based on the above, even if the UAVs claim more dedicated free airspace in the foreseeable future, they will still not be allowed to always travel at a straight line while at

cruising altitude; they will have to navigate around RZs, following an optimal path. We will be treating such areas as obstacles in a path planning process.

Several methods have been proposed for acquiring a path around obstacles. We refer to some of them with considerable value for our case. Algorithms Bug 1 and Bug 2 were developed by Lumelsky & Stepanov (Lumelsky & Stepanov, 1987). With the Bug 1 method, the path starts with an original straight line from start to finish as a reference, it then goes around an obstacle's perimeter and then leaves when at the closest point to the target. Bug 2 differs from the previous method, by keeping the original m-line and leaving each obstacle's perimeter when the m-line is crossed again. When encountering simple obstacles, the greedy strategy employed by Bug2 offers immediate benefits, whereas in the presence of complex obstacles, the cautious approach taken by Bug1 often leads to superior performance (Choset, et al., 2005). Figure 36 and Figure 37 illustrate the way Bug 1 and Bug 2 work while tackling randomly shaped obstacles.

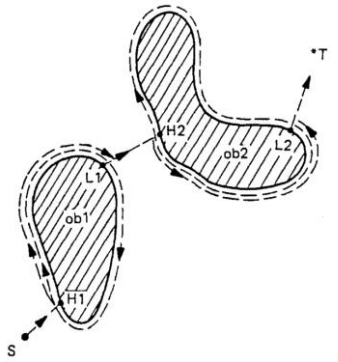

Figure 36: Automaton's path (dotted lines), Algorithm Bug1 (ob1, ob2, obstacles; H1, H2, hit points; L1, L2, leave points) (Lumelsky & Stepanov, 1987)

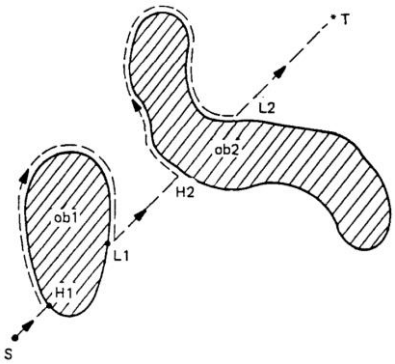

Figure 37: Automaton's path (dotted line) under Algorithm Bug2 (Lumelsky & Stepanov, 1987)

The Tangent Bug Algorithm which is a range-sensor based globally convergent navigation algorithm for two degrees of freedom mobile robots was developed by Kamon et al (Kamon, Rimon, & Rivlin, 1998), (Kamon, Rivlin, & Rimon, 1996). The Tangent Bug uses a 360 degree infinite orientation resolution and is an improvement on the Bug 2 algorithm in acquiring an optimal (shortest) path; however it needs infinite range to work properly, thus may raise high computational demands.

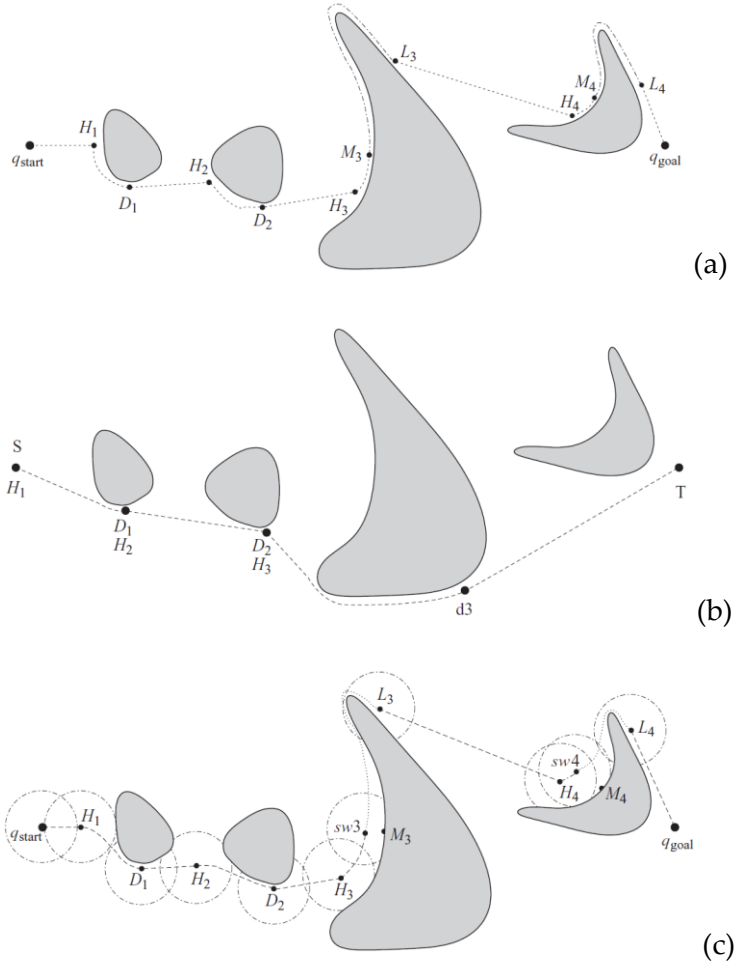

Figure 38: Implementation of the Tangent Bug Algorithm with: (a) zero sensor range, (b) finite sensor range, (c) infinite sensor range (Choset, et al., 2005)

An Artificial Potential Field method was proposed by Khatib (Khatib, 1985). The potential function approach guides a robot as though it were a particle navigating through a gradient vector field. Gradients can be perceived as forces exerted on a positively charged robot particle, drawing it towards the negatively charged goal. Similarly, obstacles possess a positive charge that generates a repulsive force, steering the robot away from obstacles. By

combining these repulsive and attractive forces, the robot is ideally guided from its starting position to the goal location while effectively avoiding obstacles.

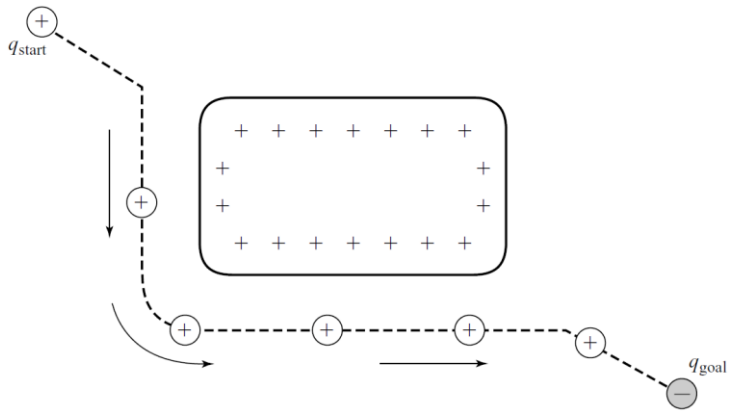

Figure 39: Example of Potential Field method (Choset, et al., 2005)

Others have used combined methods, for example Rashid et al employed a tangent visibility graph and then the Dijkstra method among possible paths (Rashid, Ali, Frasca, & Fortuna, 2017).

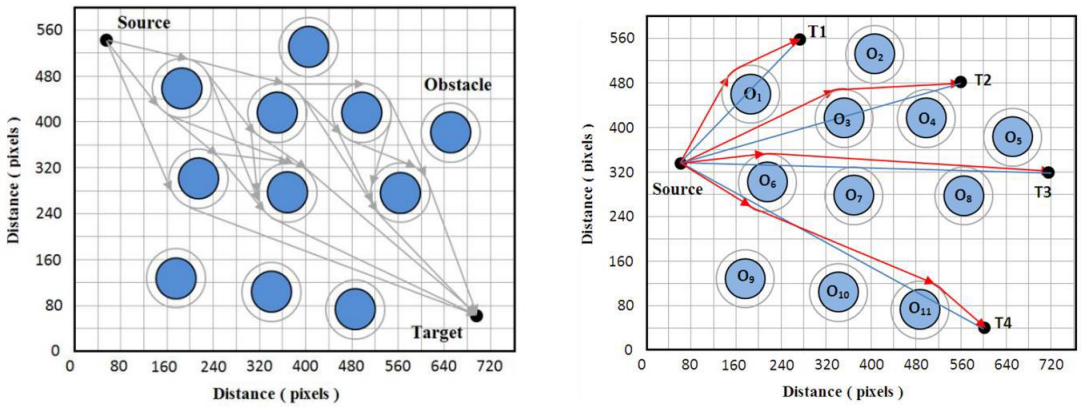

(a) (b)

Figure 40: Examples of using the tangent visibility graph algorithm (a) Trajectories from source to target (b) Shortest paths for different target locations (Rashid, Ali, Frasca, & Fortuna, 2017)

Modern advanced tools use a variety of methods for obtaining the optimal path around obstacles or on cost-weighted surfaces. Accumulated cost surface and slopeline (Douglas, 1994) is used as a basis for such tools in commercial GIS software. An original distance accumulation raster is created, including forbidden areas as barriers. The generated back direction raster illustrates the direction required to exit a cell and return to the source. The directional values in the output are represented within a compass range of 0 to 360 degrees.

The selection of analysis cell size defines the desired precision. The created raster maps are the basis for calculating the optimal line.

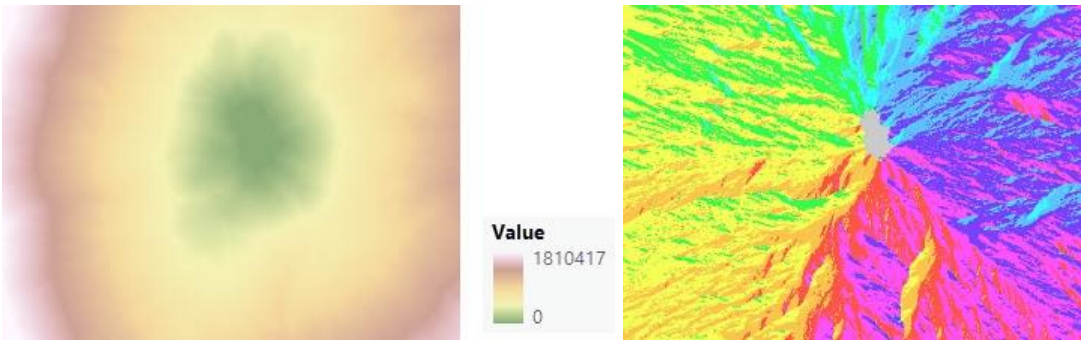

Figure 41: Rasters created to obtain optimal paths in ArcGIS Pro: (a) output distance accumulation raster (b) output back direction raster (ESRI, 2023)

The calculations are carried out through a D8 flow direction algorithm (ESRI, 2023), using D8 (Jenson & Domingue, 1988), Multiple Flow Direction (MFD) (Qin, et al., 2007) or D-Infinity (DINF) (Tarboton, 1997) methods. The Multiple Flow Direction (MFD) algorithm (Qin, et al., 2007) divides the flow from a cell among its downslope neighbors. To determine the portion of flow directed to each downslope neighbor, an adaptive approach is employed, considering the local terrain conditions, and creating a flow-partition exponent. The D-Infinity (DINF) flow algorithm (Tarboton, 1997) calculates the direction of flow by identifying the most pronounced downward slope among eight triangular facets formed within a 3x3 cell window centered on the focal cell. The resulting flow direction is represented as a floating-point raster, denoting a specific angle in degrees, which progresses in a counterclockwise manner from 0 (representing due east) to 360 (also denoting due east). The D8 method (Jenson & Domingue, 1988) assumes 8 valid output directions from each cell and determines the direction of flow based on the steepest descent.

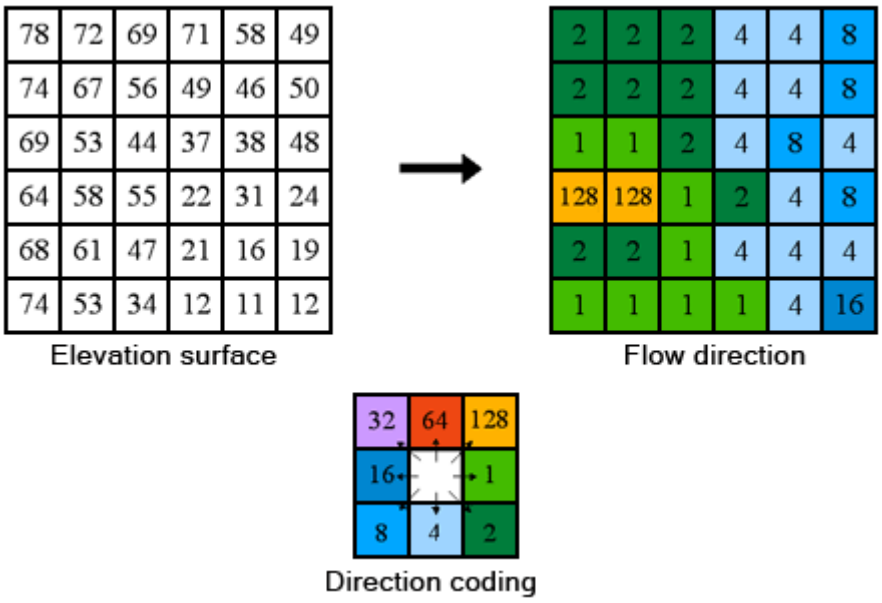

Figure 42: Coding of the direction of flow (ESRI, 2023)

Each method has its own merits and drawbacks. In our case, it is important to choose based on the desired level of precision and computational effort, depending on the size of network and the complexity of no-fly areas. Since we are dealing with macroscopic planning but also considerable distances (operations in big cities or between cities), the most important criterion for selecting a path planning method is the consistency in good line choices, which would not see their errors magnified along with the scale of operations. Also, depending on the input data format, it is favorable in terms of convenience and consistency to use dedicated tools which are developed for said format. The UAV size is assumed negligible and thus ensuring a free corridor width is not crucial, occasional contact with the edges of obstacles is allowed and a macroscopic smoothing of paths is preferable.

Based on the above, we believe it is important to add this aspect to our original design, by developing a suitable workflow. UAVs do not necessarily fly straight when at cruising altitude, thus the actual length of the path traveled between two locations may exceed the straight distance between them. Some locations may fall out of UAV range when non-straight paths are considered, while other may be well inside RZs and take-off or landing is impossible. We take advantage of the modular setup of the original design and develop an updated workflow which includes such provisions and proposes a methodology of optimizing under restricted airspace. We decided to also take advantage of developed advanced tools and techniques, aligning our research with modern trends. Geographic

Information Systems (GIS) are commonly used for database management and network analysis purposes. We opt to merge our workflow with GIS interpretations and exploit spatial analysis and optimal line generation tools included in relevant specialized software packages. This way, our core methodology is also streamlined for implementation by practitioners.

4.2 Methodology

This section explains the expansion on the fundamental design, assuming the presence of no-fly zones for UAVs.

4.2.1 Core Analysis and Solution Workflow

Taking advantage of the modular character of our framework, we dig further into analysis "a2" (see section 3.3.1 and Figure 10). We explore how the formulation is changed to care for non-straight flight paths and no-fly zones avoidance.

The updated workflow is shown in Figure 43, below.

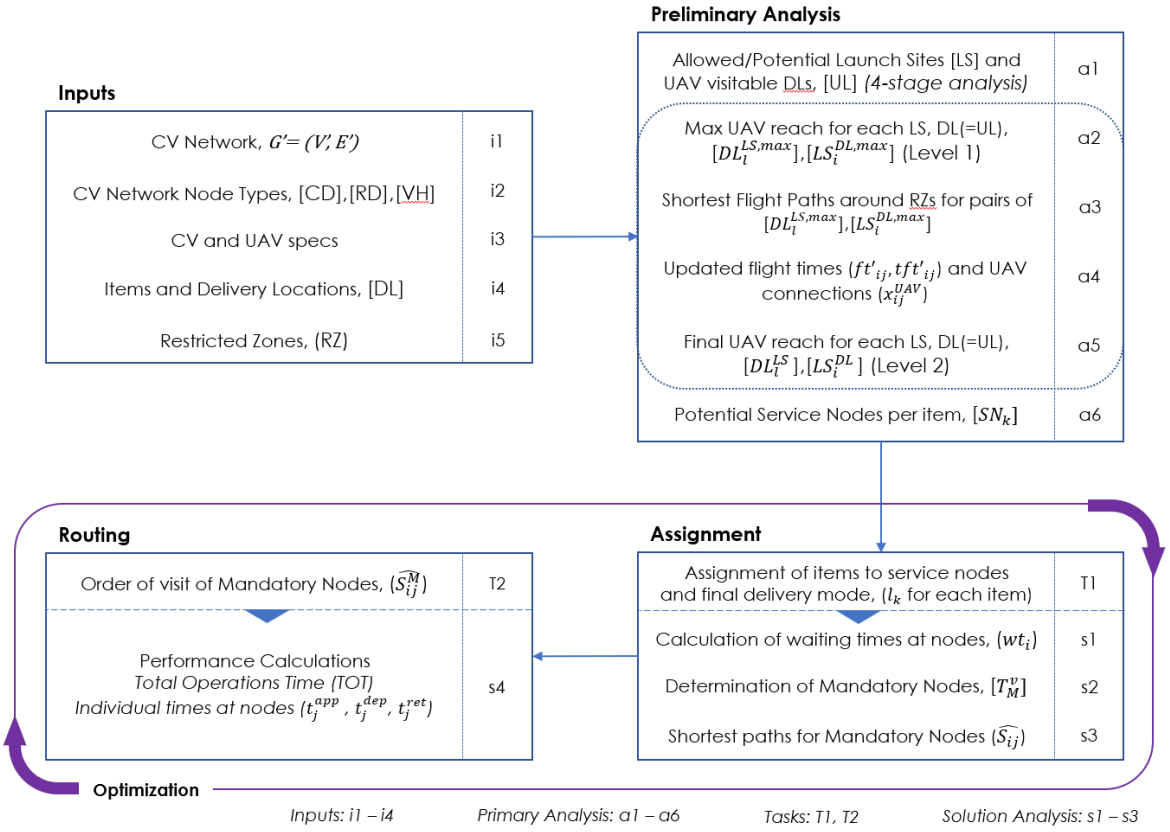

Figure 43: General methodology workflow, considering Restricted Zones

This time, Preliminary Analysis first defines which sites are initially allowed for UAV deployment (Launch Sites -LS, selected from CD, RDs, VHs and some of the DLs) and which pairs of DLs and LSs are within maximum UAV range (straight flight path) to each other ($DL_l^{LS,max}$, $LS_i^{DL,max}$). Then, for the above pairs, actual optimal paths around RZs are estimated and UAV feasible connections are again filtered based on the UAV's range. Each item is then associated with potential service nodes (Service Nodes Pool - SN_k).

4.2.2 Mathematical Formulation

One of the most important processes within the proposed workflow is the identification of the allowed UAV Launch Sites and UAV-visitable Delivery Locations. This is executed in stages, as new information emerges:

- Stage 0: Initial Infrastructure (CD, RDs, VHs)
- Stage 1: Physical constraints on emerged DLs (e.g., area characteristics, obstacles, safe room for take-off/landing)
- Stage 2: Operational constraints (e.g., maintenance, time of day, customer choices)
- Stage 3: RZ constraints (an LS or DL falls within an RZ)

Stage 3 analysis assumes that any location "i" falling within an RZ cannot be an LS or UL, thus $x_i^{LS} = x_i^{UL} = 0$.

Based on the above analysis, for each Launch Site and Delivery Location a set of reachable nodes is formed. The analysis is performed at two levels. First, the maximum reachable DLs and LSs are identified, assuming no air space restrictions and straight-line paths between node pairs.

$$DL_l^{LS,max} = \left[A \subseteq V \mid x_{li}^{UAV} = 1, \quad i \in UL, l \in LS\right]$$

(Delivery Locations, visitable by UAV, within range of Launch Site) (Eq. 44)

$$LS_i^{DL,max} = \left[B \subseteq V \mid x_{il}^{UAV} = 1, \quad i \in UL, l \in LS\right]$$

(Launch Sites within range of Delivery Location, which is visitable by UAV) (Eq. 45)

Then the actual flight paths around RZs are calculated. This is done only for the pairs resulting from the first level of filtering for DLs and LSs ($DL_l^{LS,max}$, $LS_i^{DL,max}$), since there is no

possibility for other pairs to have feasible UAV connections. Acquiring optimal paths around obstacles is an intensive process. By first applying the Level 1 filter, which is simple and quick, the overall computational effort is significantly reduced.

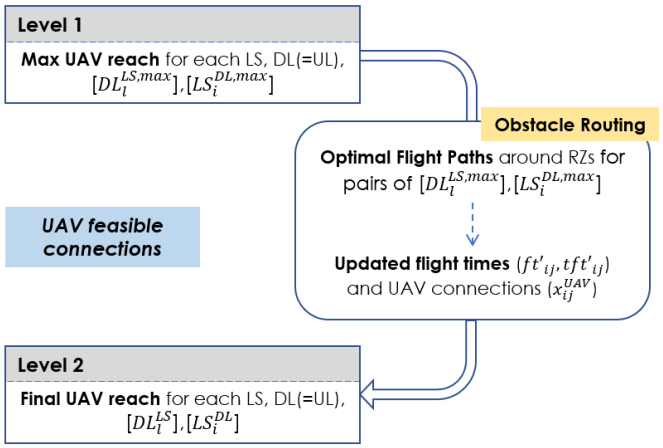

Figure 44: 2-level Identification process of UAV feasible connections between LSs and DLs

A suitable algorithm is selected to obtain optimal paths around the RZs. Source and target nodes are feasible LS and DL pairs which have resulted from the 1st Level analysis.

New values for flight time and total flight time (ft'_{ij} and tft'_{ij}, respectively) emerge, based on the length of the new flight paths. The edges *a(i,j)* of graph $F = (V, A)$ are updated, responding to tft'_{ij}. The values of x_{ij}^{UAV} are also updated based on the new flight times between nodes:

$$x_{ij}^{UAV} = \begin{cases} 0, & tft'_{ij} + tft'_{ji} > R^{UAV} \\ 1, & 0 < tft'_{ij} + tft'_{ji} \leq R^{UAV} \end{cases} \qquad i,j \in V, i,j \in UL, i \neq j$$

(Eq. 46)

The final lists of reachable LSs and DLs are calculated:

$$DL_l^{LS} = \left[A \subseteq V \mid x_{li}^{UAV} = 1, \quad i \in UL, l \in LS\right]$$

(Delivery locations, visitable by UAV, within range of launch site) (Eq. 47)

$$LS_i^{DL} = \left[B \subseteq V \mid x_{il}^{UAV} = 1, \quad i \in UL, l \in LS\right]$$

(Launch sites within range of delivery location, which is visitable by UAV) (Eq. 48)

Since all UAV-related calculations will be based on the actual flight paths around obstacles, we can substitute respective values as $ft_{ij} = ft'_{ij}$, $tft_{ij} = tft'_{ij}$.

The Service Pool Nodes, SN_k, are then calculated based on the above analysis:

$$SN_k = LS_{d_k}^{DL} \cup d_k, \ k \in K, d_k \in V' \quad \text{(Eq. 49)}$$

4.3 Case Study

We test the updated methodology with a case study. This time, we use the geometry of the previously devised network, although with some changes in infrastructure and demand for added solution alternatives and we also introduce a randomly generated set of Restricted Zones for UAVs.

4.3.1 Input data

A 60-min UAV range and a 40-km/h CV speed are selected, and RDs are placed at critical locations, based on the experience gained by previous experimentation.

As such, the following specs are assumed:

$S^{CV} = 40$ *km/h,* $H^{UAV} = 120$ *m,* $S^{UAV} = 14.45$ *m/sec*

$S^{UAV}_{asc} = 4.25$ *m/sec (tta = 28.2 sec, for* $H^{UAV} = 120$ *m)*

$S^{UAV}_{des} = 3.4$ *m/sec (ttd = 35.3 sec, for* $H^{UAV} = 120$ *m)*

$R^{UAV} = 60$ *min (2400sec)*

Service and transshipment times are again: *st = 60 sec (1 min), tc = 300 sec (5 min)*

The network is transformed into GIS format and Restricted Zones (RZ) of various types and shapes are introduced. RZ sizes and shapes resemble common cases met in airspace no-fly zones (E.g., ATZs usually cover a range of 3000 – 8000 m around the airport.). Such Zones are commonly archived and updated in GIS databases, thus we believe it makes sense to include such an approach in our framework.

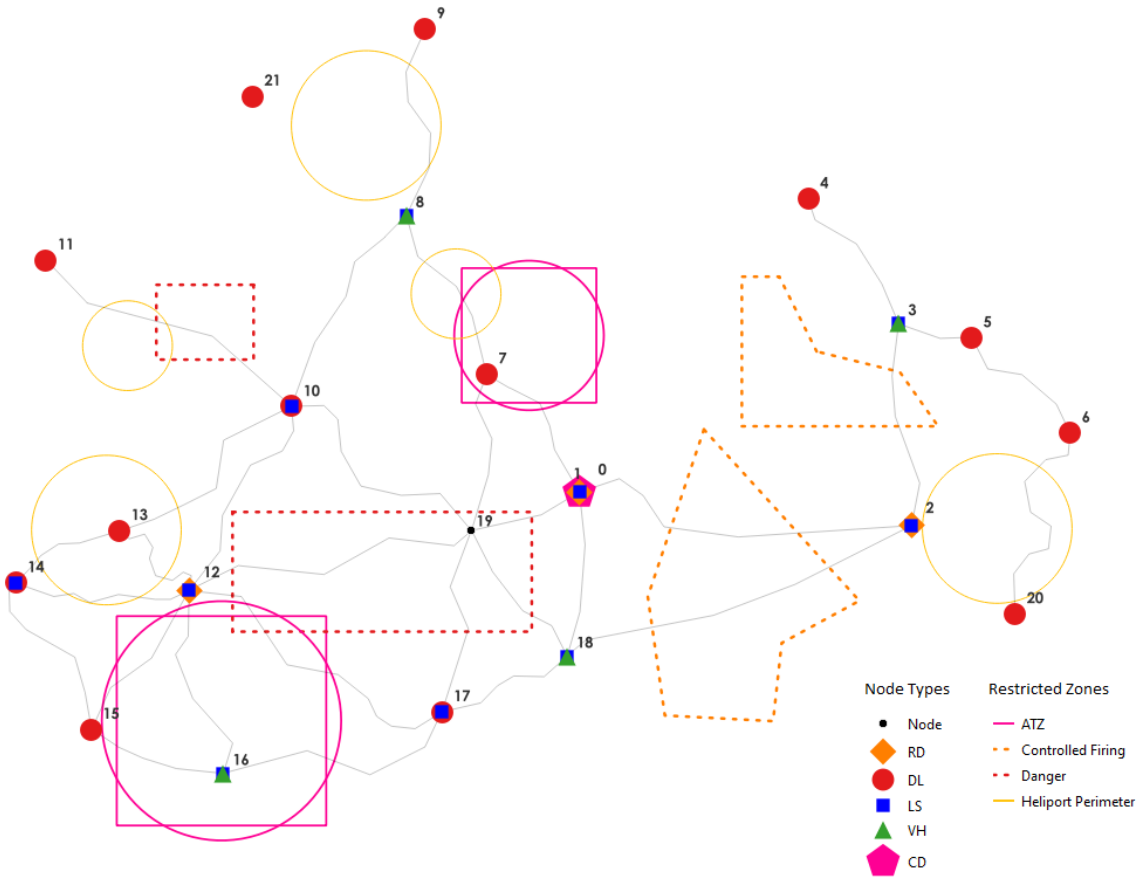

Figure 45: Illustration of introduced Restricted Zones

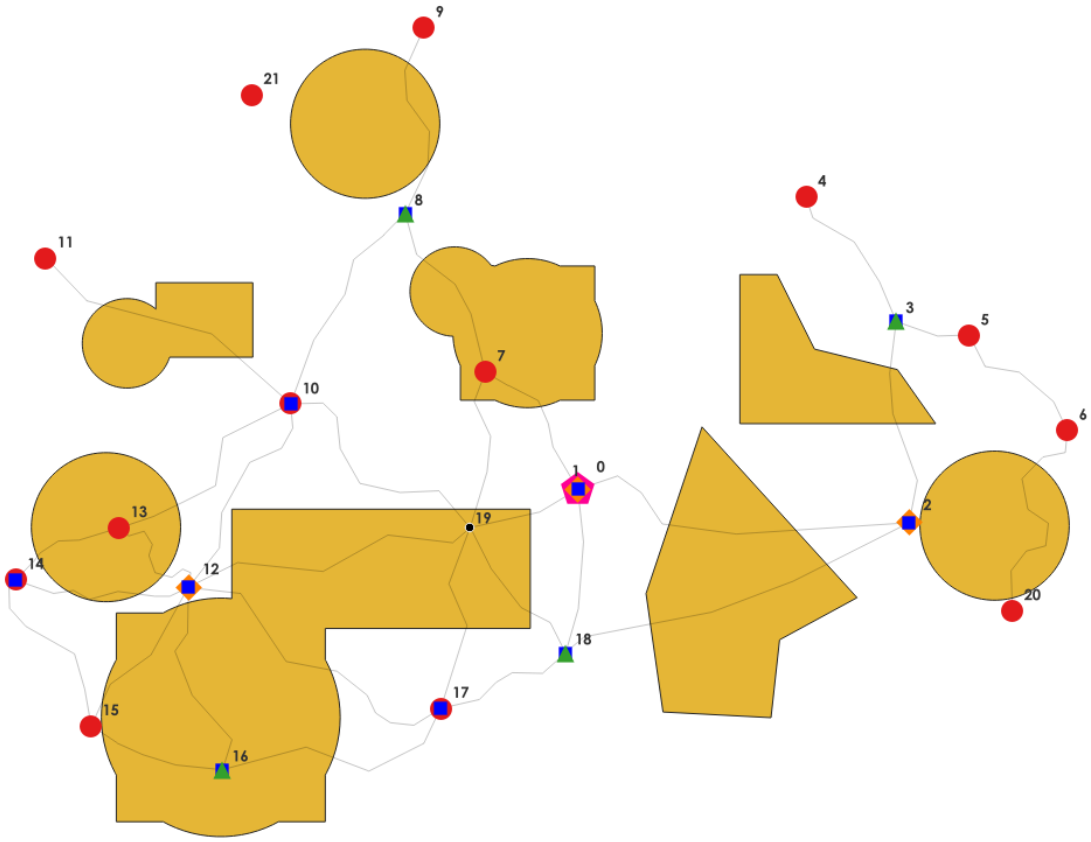

Figure 46: Dissolving Restricted Zones into integrated no-fly areas

4.3.2 Analysis and Experiments

DLs and potential LSs which fall within the RZs are removed from the UAV operations. For each DL and its maximum potential LSs, optimal UAV paths around the RZs are calculated. For this purpose, we make use of existing optimal line tools built within GIS software.

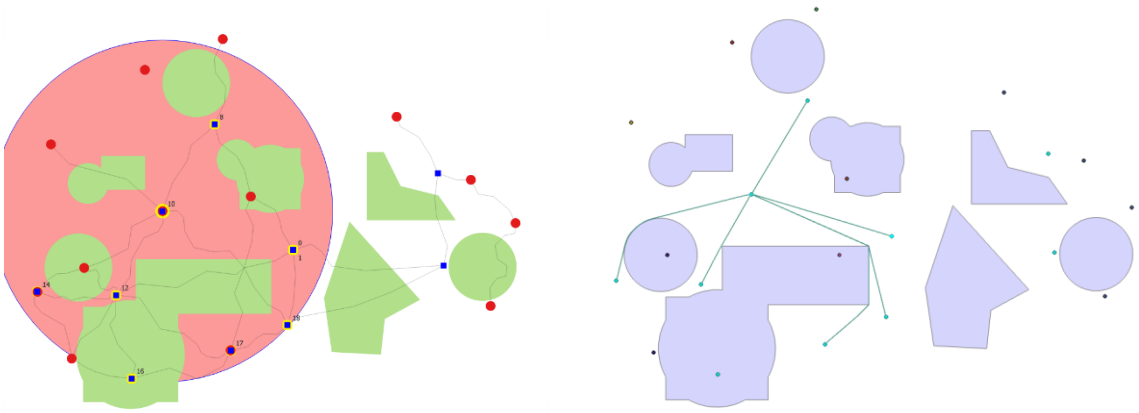

Figure 47: Example of optimal paths between a DL and its feasible LSs within max UAV range

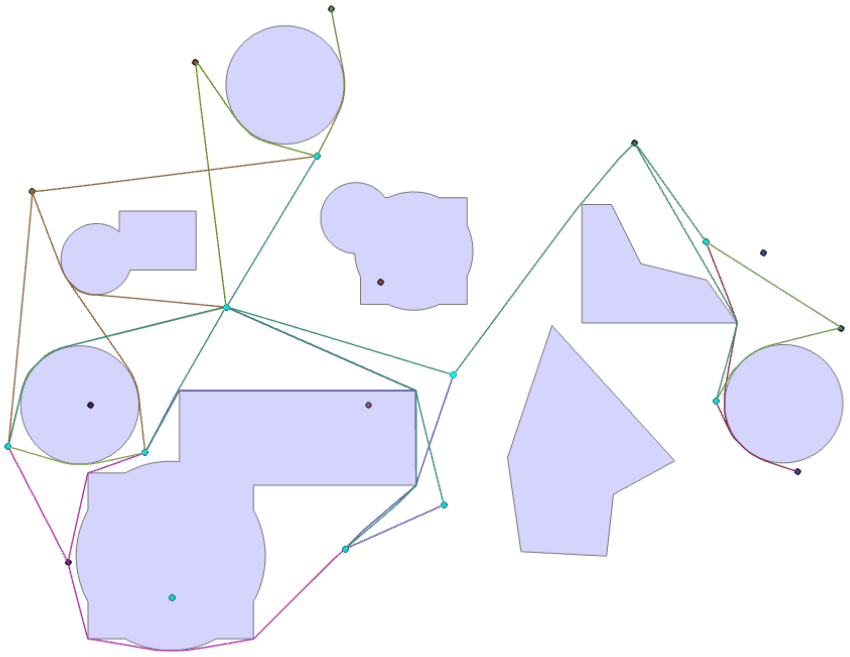

Figure 48: All UAV optimal paths between DLs and potential LSs within max UAV range

We construct the new resulting edge weight and adjacency matrix for UAV connections.

Table 21: Updated UAV edge costs (tft_{ij}, sec), considering RZs

tft_{ij}	0	1	2	3	4	5	6	7	8	9	10	11	12	13	14	15	16	17	18	19	20	21
0	0	0	inf	inf	1785	inf	inf	inf	inf	inf	1452	inf	inf	inf	inf	inf	inf	1305	inf	inf	inf	inf
1	0	0	inf	inf	inf	inf	inf	inf	inf	inf	inf	inf	inf	inf	inf	inf	inf	inf	inf	inf	inf	inf
2	inf	inf	0	inf	1752	979	965	inf	inf	inf	inf	inf	inf	inf	inf	inf	inf	inf	inf	inf	731	inf
3	inf	inf	inf	0	777	406	1002	inf	inf	inf	inf	inf	inf	inf	inf	inf	inf	inf	inf	inf	1692	inf
4	1785	inf	1752	777	0	inf	inf	inf	inf	inf	inf	inf	inf	inf	inf	inf	inf	inf	inf	inf	inf	inf
5	inf	inf	979	406	inf	0	inf	inf	inf	inf	inf	inf	inf	inf	inf	inf	inf	inf	inf	inf	inf	inf
6	inf	inf	965	1002	inf	inf	0	inf	inf	inf	inf	inf	inf	inf	inf	inf	inf	inf	inf	inf	inf	inf
7	inf	inf	inf	inf	inf	inf	inf	0	inf	inf	inf	inf	inf	inf	inf	inf	inf	inf	inf	inf	inf	inf
8	inf	inf	inf	inf	inf	inf	inf	inf	0	969	1094	1743	inf	inf	inf	inf	inf	inf	inf	inf	inf	1006
9	inf	inf	inf	inf	inf	inf	inf	inf	969	0	inf	inf	inf	inf	inf	inf	inf	inf	inf	inf	inf	inf
10	1452	inf	inf	inf	inf	inf	inf	inf	1094	inf	0	1584	1038	inf	1751	inf	inf	2389	1966	inf	inf	1509
11	inf	inf	inf	inf	inf	inf	inf	inf	1743	inf	1584	0	1758	inf	1565	inf	inf	inf	inf	inf	inf	inf
12	inf	inf	inf	inf	inf	inf	inf	inf	inf	inf	1038	1758	0	inf	885	957	inf	2976	inf	inf	inf	inf
13	inf	inf	inf	inf	inf	inf	inf	inf	inf	inf	inf	inf	inf	0	inf	inf	inf	inf	inf	inf	inf	inf
14	inf	inf	inf	inf	inf	inf	inf	inf	inf	inf	1751	1565	885	inf	0	826	inf	inf	inf	inf	inf	inf
15	inf	inf	inf	inf	inf	inf	inf	inf	inf	inf	inf	inf	957	inf	826	0	inf	2257	inf	inf	inf	inf
16	inf	inf	inf	inf	inf	inf	inf	inf	inf	inf	inf	inf	inf	inf	inf	inf	0	inf	inf	inf	inf	inf
17	1305	inf	inf	inf	inf	inf	inf	inf	inf	inf	2390	inf	2976	inf	inf	2257	inf	0	698	inf	inf	inf
18	inf	inf	inf	inf	inf	inf	inf	inf	inf	inf	1966	inf	inf	inf	inf	inf	inf	698	0	inf	inf	inf
19	inf	inf	inf	inf	inf	inf	inf	inf	inf	inf	inf	inf	inf	inf	inf	inf	inf	inf	inf	0	inf	inf
20	inf	inf	731	1692	inf	inf	inf	inf	inf	inf	inf	inf	inf	inf	inf	inf	inf	inf	inf	inf	0	inf
21	inf	inf	inf	inf	inf	inf	inf	inf	1006	inf	1509	inf	inf	inf	inf	inf	inf	inf	inf	inf	inf	0

Table 22: Adjacency matrix for UAV (x^{UAV}_{ij}), considering RZs

x^{UAV}_{ij}	0	1	2	3	4	5	6	7	8	9	10	11	12	13	14	15	16	17	18	19	20	21
0	-	-	-	-	1	-	-	-	-	-	1	-	-	-	-	-	-	1	-	-	-	-
1	-	-	-	-	-	-	-	-	-	-	-	-	-	-	-	-	-	-	-	-	-	-
2	-	-	-	-	1	1	1	-	-	-	-	-	-	-	-	-	-	-	-	-	1	-

3	-	-	-	-	1	1	1	-	-	-	-	-	-	-	-	-	-	-	-	-	1	-
4	1	-	1	1	-	-	-	-	-	-	-	-	-	-	-	-	-	-	-	-	-	-
5	-	-	1	1	-	-	-	-	-	-	-	-	-	-	-	-	-	-	-	-	-	-
6	-	-	1	1	-	-	-	-	-	-	-	-	-	-	-	-	-	-	-	-	-	-
7	-	-	-	-	-	-	-	-	-	-	-	-	-	-	-	-	-	-	-	-	-	-
8	-	-	-	-	-	-	-	-	-	1	1	1	-	-	-	-	-	-	-	-	-	1
9	-	-	-	-	-	-	-	-	1	-	-	-	-	-	-	-	-	-	-	-	-	-
10	1	-	-	-	-	-	-	-	1	-	-	1	1	-	1	-	-	-	-	-	-	1
11	-	-	-	-	-	-	-	-	1	-	1	-	1	-	1	-	-	-	-	-	-	-
12	-	-	-	-	-	-	-	-	-	-	1	1	-	-	1	1	-	-	-	-	-	-
13	-	-	-	-	-	-	-	-	-	-	-	-	-	-	-	-	-	-	-	-	-	-
14	-	-	-	-	-	-	-	-	-	-	1	1	1	-	-	1	-	-	-	-	-	-

After establishing the shortest paths around the RZs, a further filter is applied excluding paths which now exceed the UAV range and the Service Nodes pool is updated for each DL.

Table 23: Potential Launch Sites and Final Service Nodes Pool for Items, considering RZs

Item (k)	Node (d_k)	Potential Launch Sites [LS^{DL}]				Service Nodes Pool [SN_k]					$\|SN_k\|$
1	4	0	2	3		4	0	2	3		(4)
2	5	2	3			5	2	3			(3)
3	6	2	3			6	2	3			(3)
4	7					7					(1)
5	9	8				9	8				(2)
6	10	0	8	12	14	10	0	8	12	14	(5)
7	11	8	10	12	14	11	8	10	12	14	(5)
8	13					13					(1)
9	14	10	12			14	10	12			(3)
10	15	12	14			15	12	14			(3)
11	17	0	18			17	0	18			(3)
12	20	2	3			20	2	3			(3)
13	21	8	10				8	10			(2)

After running the algorithm and the optimization workflow, we have obtained the following results:

TOT = 16340.8 sec, CVT = 16340.8 sec

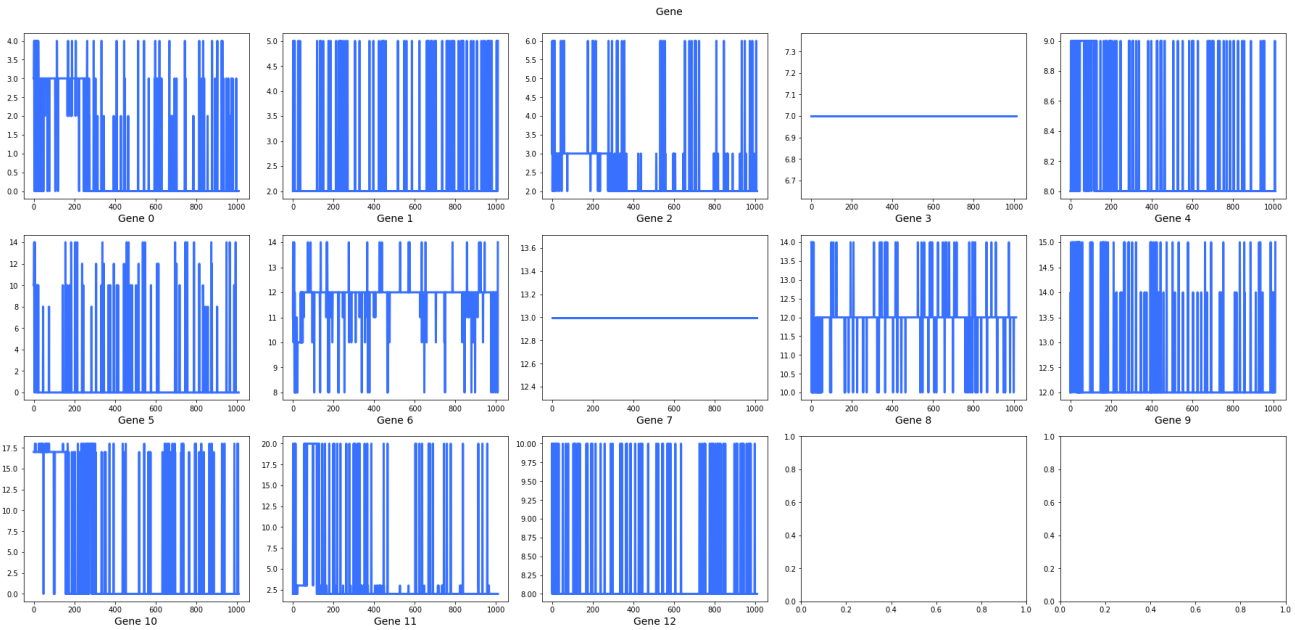

Figure 49: Nested GA mode assignment solutions (outer GA genes)

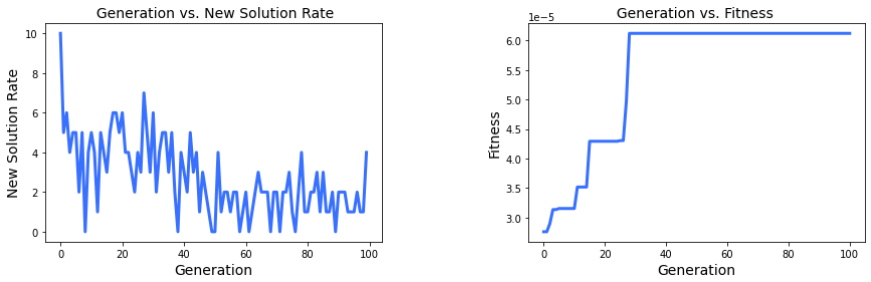

(a) **(b)**

Figure 50: Nested GA results evolution: (a) generation vs new solution rate; (b) Generation vs fitness

Table 24: Potential Launch Sites and Final Service Nodes Pool for Items

Item (k)	Node (d_k)	Service Nodes Pool [SN_k]					Assigned Service Node (l_k)	Mode (final)
1	4	4	0	2	3		0	UAV
2	5	5	2	3			2	UAV
3	6	6	2	3			2	UAV
4	7	7					7	CV
5	9	9	8				8	UAV
6	10	10	0	8	12	14	0	UAV
7	11	11	8	10	12	14	12	UAV
8	13	13					13	CV
9	14	14	10	12			12	UAV
10	15	15	12	14			12	UAV
11	17	17	0	18			0	UAV
12	20	20	2	3			2	UAV
13	21		8	10			8	UAV

The following information describes the path of the CV:

Table 25: Routing information

T_{Ma}^{v}	['0', '2', '7', '8', '12', '13']	Mandatory nodes with action
T_{M}^{v}	['0', '1', '2', '7', '8', '12', '13']	Mandatory nodes
$\widehat{S_{v}^{M}}$	['0', '2', '13', '12', '8', '7', '1']	Path of mandatory nodes
$\widehat{S_{(e)}^{M}}$	[('0', '2'), ('2', '13'), ('13', '12'), ('12', '8'), ('8', '7'), ('7', '1')]	Sequence of shell edges, through mandatory nodes
$\widehat{S_{v}}$	[['0', '2'], ['2', '0', '19', '12', '13'], ['13', '12'], ['12', '10', '8'], ['8', '7'], ['7', '1']]	Full path of nodes
$\widehat{S_{(e)}}$	[('0', '2'), ('2', '0'), ('0', '19'), ('19', '12'), ('12', '13'), ('13', '12'), ('12', '10'), ('10', '8'), ('8', '7'), ('7', '1')]	Full sequence of edges

Table 26: Path, actions, and time evolution (sec) (solution *1)

Order	**1 (CD)**	**2**	**3**	**4**	**5**	**6**	**7 (CD/RD)**
Mandatory Node	0	2	13	12	8	7	1
Pass Through		0, 9, 12		10			
Action	Launch	Delivery Launch		Launch	Launch	Delivery	(end)
$\mathbf{T^{APP}}$	0.0	2150.9	7787.7	8625.5	2736.0	15325.8	16340.8
$\boldsymbol{ct_{ij}^{M}}$	0.0	2150.9	5456.8	777.7	2736.0	1112.3	955.0
$\mathbf{W_I}$	0.0	180.0	60.0	180.0	2672.1	60.0	0.0
$\mathbf{T^{DEP}}$	0.0	2330.9	7847.7	8805.5	14213.6	15385.8	16340.8
$\mathbf{T^{RET}}$	4530.3	5248.7	0.0	13281.0	0.0	0.0	0.0
TOT (SEC)							**16340.8**

Figure 51, below illustrates the solution.

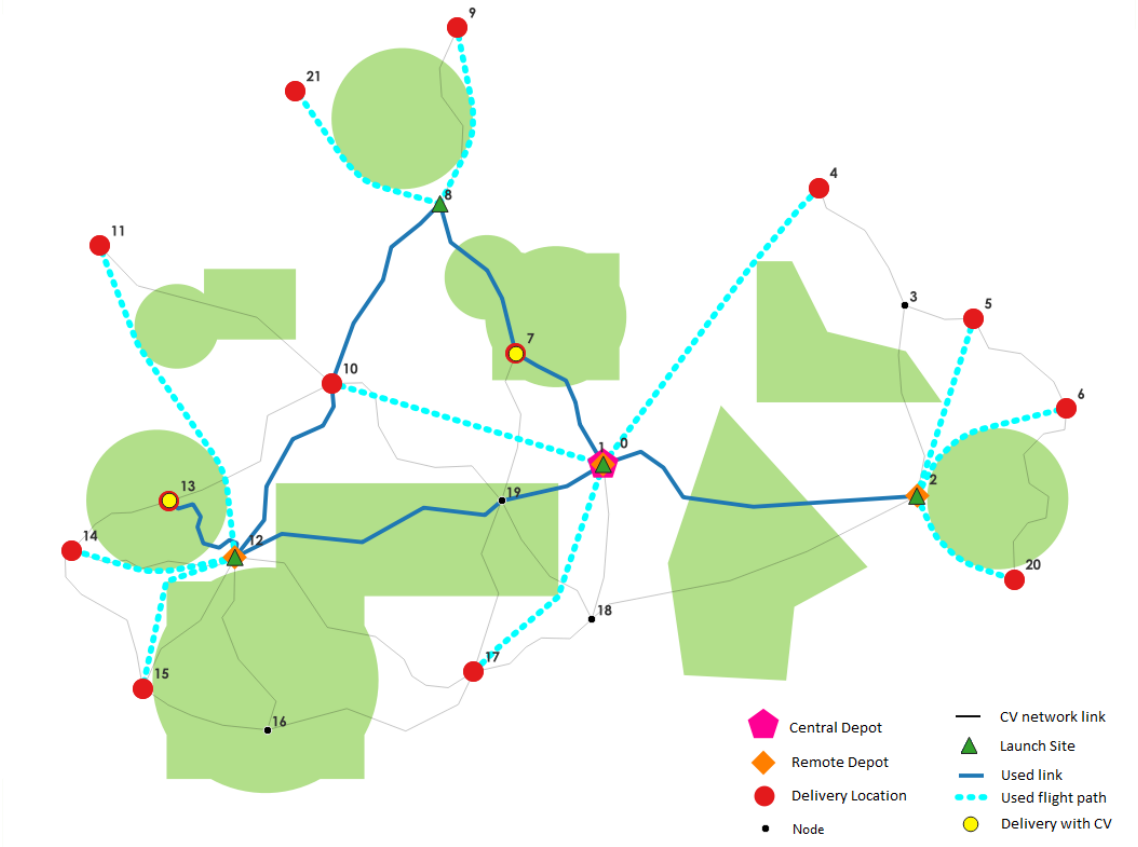

Figure 51: GIS-based illustration of best solution under constrained airspace

We have recalculated the optimal solution excluding the RZs, to compare the results. A TOT = 14756.5 sec has been obtained. Under the presence of RZs, the TOT (16340.8 sec) was significantly higher (9.7%) and different assignment and routing options were selected. The two solutions are depicted side by side in a similar simplistic manner for easier direct comparison.

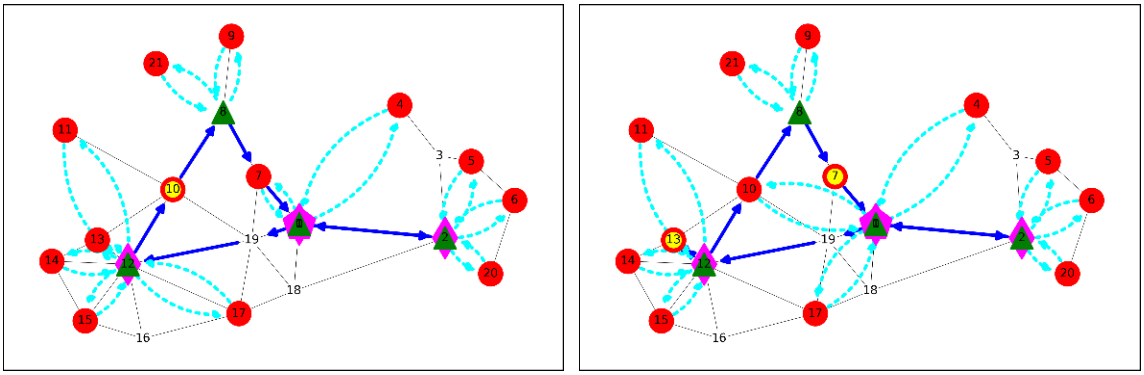

(a) (b)

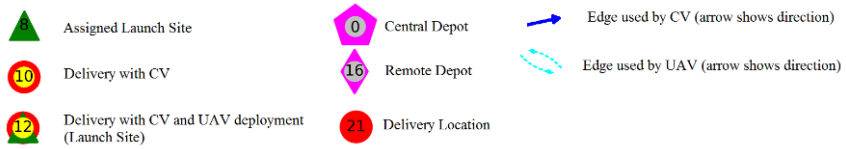

Figure 52: Simplified illustration of assignment and routing solutions: (a) without RZs; (b) with RZs

4.4 Discussion

The presence of Restricted Zones significantly alters the potential solutions and is worth considering for a more realistic approach. It is reasonable to expect that larger and more complicated shapes of RZs further hinder UAV flights and force longer paths. This leads to less feasible UAV connections and thus LS options, while TOTs are higher. The preliminary analysis highlighting the initial maximum feasible UAV connections is a step worth taking, since it is a very quick and simple distance analysis, whereas optimal path design around obstacles is a heavy computational process and should only be executed where there is a chance of a flight within the UAV's range. We have incorporated spatial and optimal path analysis in a GIS environment, offering a path to exploit our methodology in a modern database and software environment.

5 Stage 3 - Stochastic Planning

5.1 Background

This section offers more insight on the parameter of uncertainty, highlighting the need for consideration of stochastic conditions both for the CVN and airspace. Relevant background in each field is presented.

5.1.1 Stochastic Conditions

5.1.1.1 Conventional Vehicle Network

In terms of vehicle routing alone, research on seeking a robust solution under uncertainty is not new. Gendreau et al (Gendreau, Laporte, & Séguin, 1996) have sampled several stochastic VRP cases, citing uncertainty sources in demand, travel times and customers or combinations of the above. Bertsimas and Simchi-Levi (Bertsimas & Simchi-Levi, 1996) highlighted the importance of including congestion and stochasticity in the VRP problems and evaluated relevant heuristics algorithms for obtaining near-optimal solutions. For the case of a VRP with time windows and stochastic travel times, Wu and Hifi (Wu & Hifi, 2020) propose a scenario-based optimization process through a custom robust model, also using a guided neighborhood search-based heuristic to evaluate the results. Erbao and Mingyong (Erbao & Mingyong, 2009) tackle uncertainty in demand by building a fuzzy chance-constraint model, including a differential evolution algorithm. A chance-constraint approach is also followed by Kepaptsoglou et al (Kepaptsoglou, Fountas, & Karlaftis, 2015), who assume stochastic weather conditions and affected travel times for ships, attempting to optimize containership routing.

In our case, we assume that conditions through the Conventional Vehicle Network (CVN) are uncertain, but historical patterns help with prediction. Link travel times are stochastic variables, based on the link's respective CV travel speed; this refers to the representative average speed throughout the entire link length, observed at a mesoscopic level. Historical values are used to extract a distribution of mean speed for each link. While planning the operations, it is assumed that conditions at each link will fall within an expected range and according to its observed speed distribution. Such a distribution is randomly generated and used as an example in Figure 53.

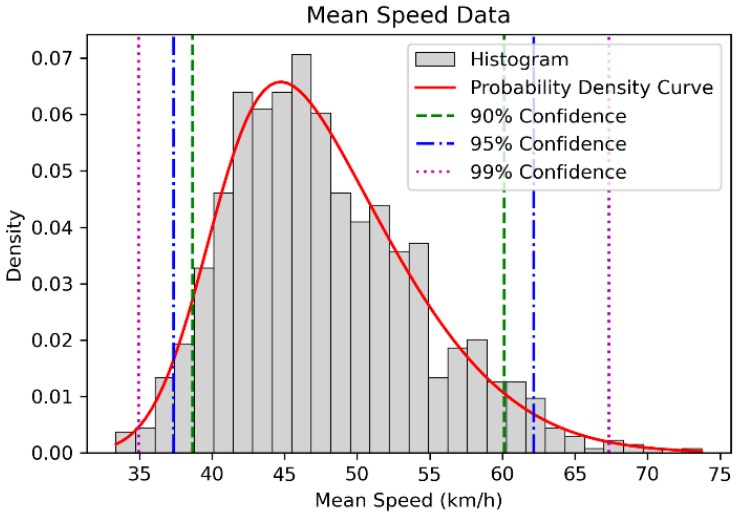

Figure 53: Generated example of historical data concerning observed mean link speed.

By selecting a certain confidence level, the planner decides how far from an expected mean value actual conditions may occur, in terms of average speed over a CVN link. A higher confidence level means that roads are likely to offer a very predictable average speed for the CV to travel on, while going lower implies bigger variations.

5.1.1.2 Weather Forecast

Weather forecasting is a notoriously complex task with no guaranteed success. The information on projected conditions can be conveyed in various forms and levels of certainty. When delivering a forecast, there are two options to consider. The first option is a deterministic forecast, where the forecaster provides a single value that represents their best estimate of the most probable outcome. Although this forecast is unlikely to be completely accurate, the goal is to choose the most precise option among multiple forecasts.

The second option involves breaking down the potential outcomes into ranges or bins and assigning a probability of occurrence to each bin. This is known as a probability forecast. Instead of predicting future weather conditions with a specific value, the objective of the probabilistic forecaster is to accurately describe the probabilities of the outcome falling within each bin.

A contingency table can be constructed including forecast and observed events. For the case of dichotomous forecasts and dichotomous events, it is a simple 2 x 2 table. We can do the same for forecasted events: we predict that the event will happen or will not happen (an

analogy with “observed” or “not observed”) under various probabilities. The occurrence of an event is assigned a value of 1, while the non-occurrence is assigned a value of 0. In the case of dichotomous forecasts, these values also represent the presence or absence of the event. When dealing with polychotomous forecasts (such as probabilities with multiple categories) and a dichotomous event (e.g., measurable rain or no rain), the table size becomes m x 2, where m is the number of probability categories. If both the event and the forecast are polychotomous, with k categories each, the table size becomes m x k. The sums along the margins provide information about the distribution of forecasts and observations within their respective categories. It is evident how the table can be generalized to accommodate polychotomous forecasts and/or events. A conditional probability is defined as the probability of one event occurring given that another event has already occurred. Using "p" to denote probability, the conditional probability of event x given event y is represented as p(x|y) (Doswell & Brooks, 2023).

In our case, Weather Forecast is given in the form of a probabilistic prediction on whether a certain threshold is surpassed. For instance, this could be rain intensity or wind speed exceeding UAV capabilities at any time within the expected duration of operations. We are thus referring to a dichotomous event (e.g., rain exceeds a certain value or not), given as a forecast at *m* categories of probability, namely polychotomous forecasts (Doswell & Brooks, 2023). To acquire a probability forecast we are dividing the potential outcomes into ranges or bins and assigning a probability of occurrence to each bin. Instead of aiming to predict specific future weather conditions, the probabilistic forecaster focuses on accurately describing the probabilities of the outcome falling within each bin. This information does not tell us precisely what i.e., the rain intensity will be, but simply that it is highly likely to be above or below a certain value (World Climate Service, 2021). The following Figure 54 depicts an example or such forecast.

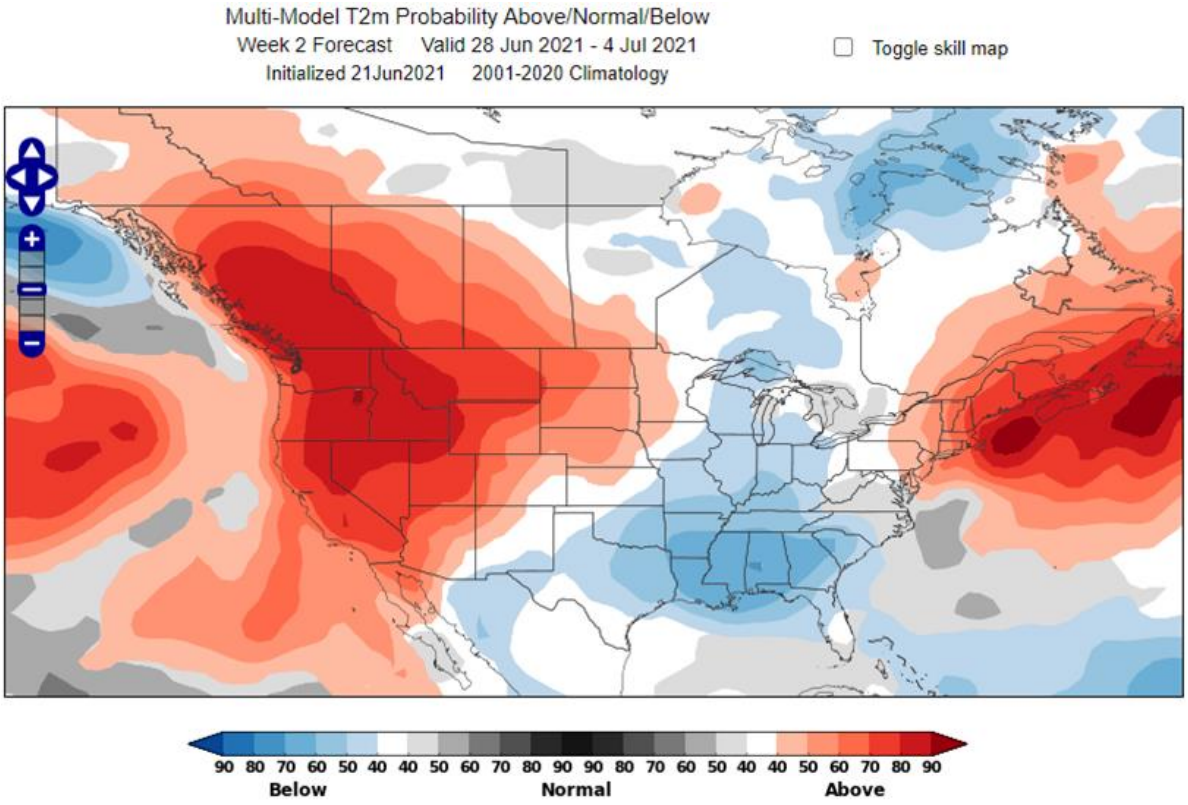

Figure 54: WCS surface temperature probability map with a week 2 lead time; source: (World Climate Service, 2021)

More information on probabilistic forecasting can be found in relevant literature (Doswell & Brooks, 2023) (Doswell, Duncomb, & Brooks, 1996) (Murphy & Winkler, 1984) (Murphy & Winkler, 1987) (Murphy, 1991).

5.1.2 Relevant research and methods

Real-life limitations in terms of infrastructure and conditions, as well as the stochastic nature of such operations and inherent risk have received comparatively little attention when considering combined CV-UAV operations.

5.2 Methodology

We intervene to the entire fundamental design, incorporating elements of uncertainty and risk level choice. The goal is shifted from finding an optimal solution under known conditions towards a global, robust solution for prior planning under uncertainty.

5.2.1 Core Analysis and Solution Workflow

A robust optimization process, using benchmark scenario solutions for reference is developed. Although several components are similar to the fundamental design, we will be describing the entire process (instead of just the differences) to better demonstrate the interrelations of all packages and the workflow rationale.

Initial Input includes basic information on the Conventional Vehicle Network (CVN) geometry, the node types, available infrastructure, and equipment specifications. Also, there are historical data on the mean speed of CVN links, Restricted Zones (RZ) which cannot be traversed by the UAVs and a probabilistic weather forecast. Then, there is the demand for delivery of items at certain Delivery Locations (DL).

For the formulation of a Scenario, SC_{TW}, CVN and Weather data is used *(indicators "T" for CVN seed and "W" for weather accepted probability)*.

Concerning the weather, an accepted level of prediction certainty is selected. Areas exceeding the safe conditions threshold at a probability above certain value, P_W, are excluded and therefore named adverse weather zones, or AWZs. In this phase of our research, the exceedance of a weather event is perceived regarding the entire expected timeframe of operations. This means that if the wind is higher at a certain area during any time until the operations are expected to finish, the area inherits the no-fly character for the entire timeframe. Selecting a higher probability implies more certainty about the prediction and more risk. A lower probability threshold excludes more areas and leans towards the safe side. Weather Forecast is given as a probabilistic prediction on whether a certain threshold is surpassed. The information is further transformed into a Digital Elevation Model (DEM)-like background for further analysis with GIS tools.

For the CVN, historical data of mean speeds over the network links are used to estimate projected conditions. Each link holds its own database and an associated distribution of said speeds. A certain level of confidence, "α_T" is selected. Several possible values for speed (and resulting travel times) for each link are produced, based on the abovementioned distribution and level of confidence. Each seed, *"T"*, features a certain value for each link and represents a possible CVN state. Together with the flight conditions resulting from the selected weather risk, it forms a Scenario, SC_{TW}.

Preliminary Analysis defines which sites are finally allowed for UAV deployment (LS) and which pairs of DLs and LSs are within maximum UAV range (assuming a straight flight path) to each other ($DL_l^{LS,max}$, $LS_i^{DL,max}$). For the above pairs, actual optimal paths around RZs and AWZs are estimated, and UAV feasible connections are updated based on the UAV's range. Each item is then associated with potential service nodes (Service Nodes Pool (SN_k)). A service node for an item may be its own DL node (if within the CVN, implying in-person service by the CV) or any allowed LS which is reachable by UAV (implying a UAV-assisted delivery).

A final transport mode assignment for each item and the routing of the CV is needed. For obtaining the optimal Solution we are setting up a nested GA, two-level optimization process, hereby named Assignment and Routing Optimization nested Genetic Algorithm (AROnGA). Each time an assignment iteration is produced, a set of mandatory nodes ($T^v{}_M$) for visit emerges. At each of these nodes, waiting times (wt_i) for the CV are calculated based on the actions required (e.g., in-person delivery, UAV launch and recover, items delivered to an RD for UAV deployment by the personnel). Shortest paths ($\widehat{S_{ij}}$) between mandatory nodes are calculated, using given CVN link travel times. Routing for the CV is then a matter of selecting the best order of visit ($\widehat{S_{ij}^M}$) across mandatory nodes.

First, a benchmark solution for each produced Scenario must be found. For each Scenario, the target is to minimize the Total Operations Time (TOT_{TW}), namely the time needed for all vehicles (CV and deployed UAVs) to complete their tasks and return to their intended base. The Scenario Solution Optimization (SSO) process is executed using the AROnGA, by setting the TOT_{TW} minimization as its target.

The benchmark solutions are then used as a comparison database for a scenario-based robust optimization process under uncertainty, hereby named Global Solution Optimization (GSO). The AROnGA is again used in a modified form. For each candidate solution, the *TOT* is calculated using each Scenario's conditions and then it is compared to the Scenario's benchmark TOT_{TW}^{min} previously calculated. The target is minimizing the mean difference of the solution's TOT to the benchmark solution for all Scenarios. The Global Solution proposes final mode assignment for each item, its service node, and the order of visit of mandatory nodes.

A summarized illustration of the workflow is shown in Figure 10, below.

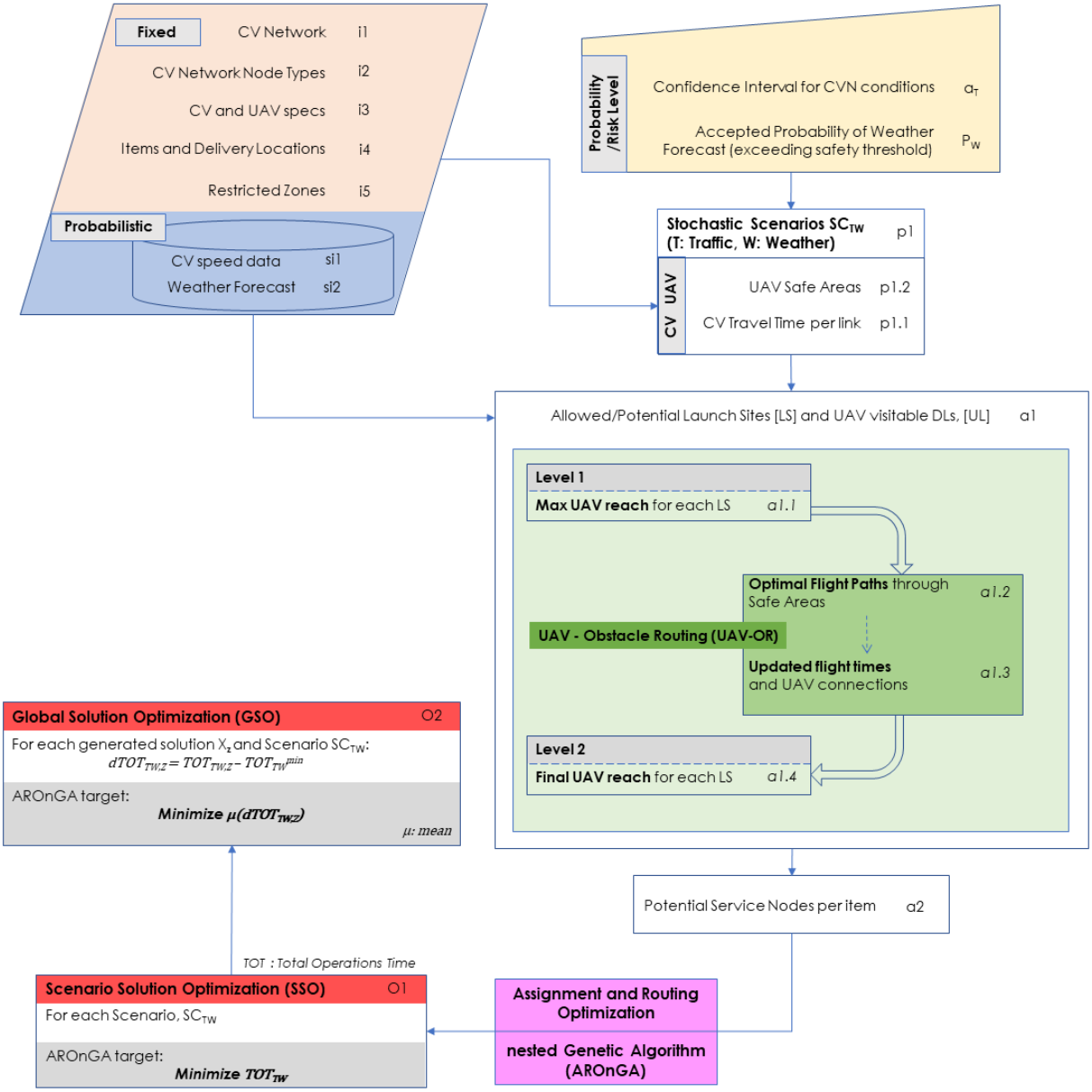

Figure 55: General workflow

5.2.2 Solution under known conditions (Scenario Solution Optimization - SSO)

For each generated Scenario SC_{TW} the best solution is sought by using the AROnGA. Here, the optimization target is to minimize the TOT for each scenario:

$$SSO\ target:\ Minimize\ (TOT_{TW}) \qquad \text{(Eq. 50)}$$

Each scenario is then characterized by is best solution, $X^*_{TW,}$ which is described by the results as:

$$X^*_{TW} = \{TOT_{TW}^{min}, C, \widehat{S_v^M}, \widehat{S_{(e)}^M}, \widehat{S_v}, \widehat{S_{(e)}}\} \quad \text{(Eq. 51)}$$

TOT_{TW}^{min} will later be used as benchmark for each candidate solution during the GSO process.

5.2.3 Global Solution (Global Solution Optimization - GSO)

Here, a solution which fares well against all possible scenarios is sought. The AROnGA is modified to be used for the generation of candidate solutions and their evaluation. Every time a candidate solution, Z, is produced, its performance is calculated based on each Scenario's conditions and then compared to the Scenario's benchmark. We obtain the difference as:

$$dTOT_{TW,Z} = TOT_{TW,Z} - TOT_{TW}^{min} \quad \text{(Eq. 52)}$$

The mean, $\mu(dTOT_{TW,Z})$, of all said differences is calculated. Here, the AROnGA target is to minimize this mean value:

$$GSO\ target: Minimize\ \mu(dTOT_{TW,Z}) \quad \text{(Eq. 53)}$$

The global solution, X^*_Z, is then described as:

$$X^*_Z = \{\mu(TOT_{TW,Z}), C, \widehat{S_v^M}\} \quad \text{(Eq. 54)}$$

It is important to highlight that every candidate solution is run under each scenario's conditions are the associated shortest paths between mandatory nodes. It is not the same TOT value that we compare with each scenario's benchmark TOT_{TW}^{min}.

5.3 Case Study

5.3.1 Input data

5.3.1.1 Network

An artificial network is created, along with infrastructure and demand information. The setup should have certain features, to be able to test our proposed framework and solution methodology. The basic features of the network are previously described in Section 3.4.1 and its fundamental geometry remains the same. The network's geometry and node types are shown in Figure 56 and Figure 57, below.

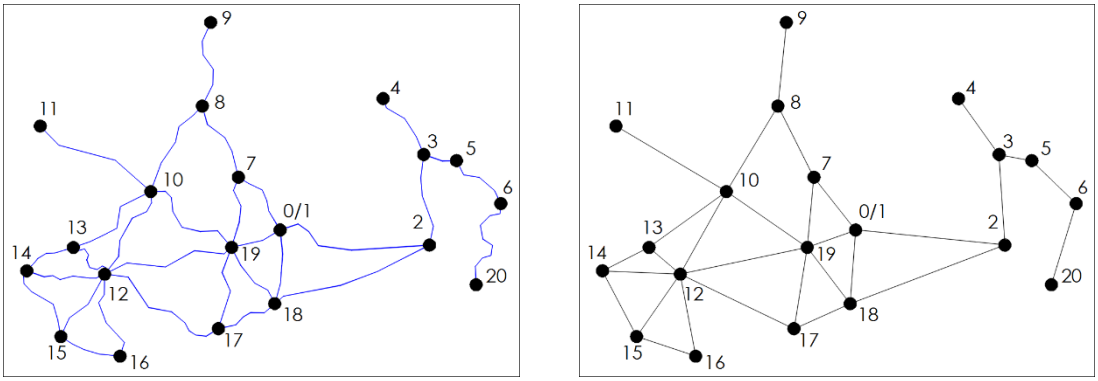

Figure 56: Original input CV network and Graph representation

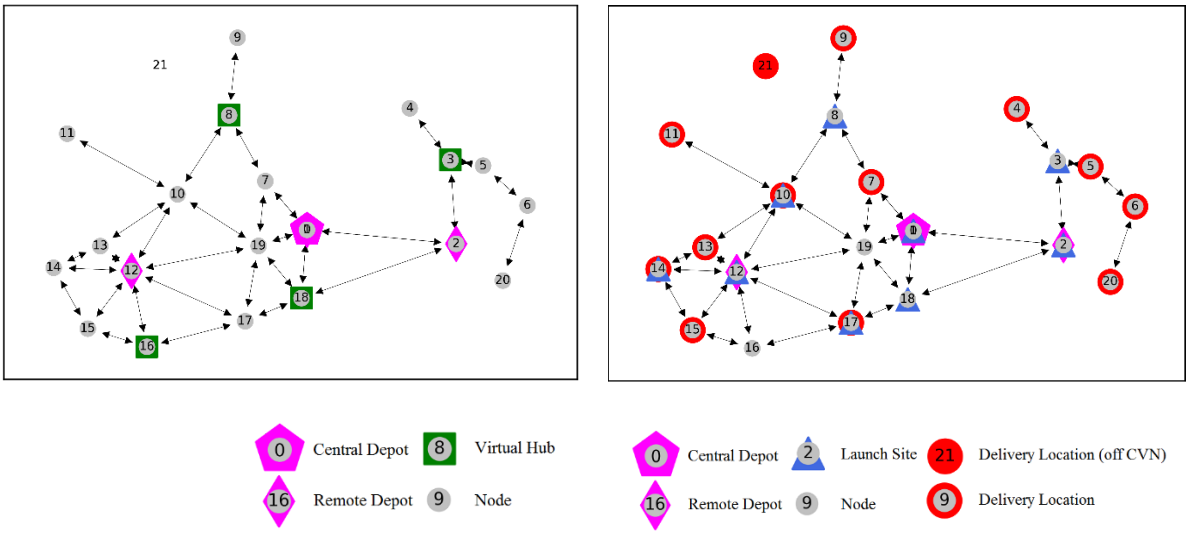

Figure 57: CV network and Node Types

5.3.1.2 *Stochastic Conditions*

For each CVN link, a historical database of observed mean CV travel speed, expressed through a normal distribution with a different mean and standard deviation is assumed. The probability density function for each link's travel speed would be:

$$P(x)_{ij} = \frac{1}{\sigma\sqrt{2\pi}} e^{-\frac{1}{2}\left(\frac{x-\mu}{\sigma}\right)^2} \quad \text{(Eq. 55)}$$

where μ and σ^2 are the mean and variance for variate $x = S_{ij}^{CV}$.

The mean and standard deviation for each link's average speed are random values, as presented in Table 27.

Table 27: Mean and standard deviation of average speed on each link

Origin	Destination	μ	σ	Origin	Destination	μ	σ
20	6	26.00	4.63	6	20	22.00	5.59

6	5	60.00	13.68	5	6	42.00	6.80
5	3	26.00	4.63	3	5	34.00	11.49
3	4	32.00	10.94	4	3	38.00	6.61
3	2	57.00	7.75	2	3	43.00	5.16
2	18	58.00	21.81	18	2	30.00	3.42
18	17	49.00	9.51	17	18	34.00	10.00
17	12	32.00	9.98	12	17	37.00	7.40
12	16	32.00	12.61	16	12	33.00	5.35
16	15	40.00	13.68	15	16	29.00	6.44
15	14	45.00	12.51	14	15	51.00	6.02
12	14	20.00	2.92	14	12	26.00	9.83
14	13	20.00	7.44	13	14	57.00	15.05
12	19	47.00	7.99	19	12	20.00	5.20
19	0	39.00	15.60	0	19	49.00	17.15
0	7	36.00	8.50	7	0	30.00	6.30
7	19	31.00	4.96	19	7	49.00	12.94
7	8	25.00	5.35	8	7	28.00	9.74
19	10	56.00	10.86	10	19	56.00	11.65
10	13	27.00	7.29	13	10	46.00	10.12
13	12	43.00	15.31	12	13	49.00	8.82
12	10	27.00	5.99	10	12	55.00	20.02
10	11	54.00	5.94	11	10	59.00	17.46
10	8	53.00	5.83	8	10	59.00	9.91
8	9	39.00	12.87	9	8	30.00	7.92
19	17	48.00	15.94	17	19	43.00	13.24
19	18	54.00	7.13	18	19	23.00	5.24
0	18	47.00	7.71	18	0	53.00	11.34
0	2	43.00	8.51	2	0	46.00	10.12
12	15	32.00	5.63	15	12	41.00	8.86
16	17	20.00	2.52	17	16	24.00	6.38

At a selected confidence level, $\alpha_T = 90\%$, a total of 30 seeds ("T") are created, every time assigning a generated mean CV travel speed ($S_{ij,T}^{CV}$) and the resulting travel time ($ct_{ij,T}$) to each CVN link. The generated seeds are presented in Table 28, below.

Table 28: Generated link speeds, $S_{ij,T}^{CV}$ (km/h) by seed, T

	Seed	1	2	3	4	5	6	7	8	9	10	11	12	13	14	15
O	D															
20	6	27.2	26.7	24.9	25.8	27.0	25.5	25.8	25.7	26.0	26.0	25.8	26.9	27.2	27.1	26.4
6	5	60.6	62.8	63.4	58.9	62.6	61.7	63.9	61.0	57.9	56.3	60.3	56.1	60.1	56.1	61.1
5	3	24.8	25.0	26.9	24.9	25.1	27.0	25.7	26.6	26.9	27.4	25.9	25.5	26.7	25.1	24.7
3	4	32.1	34.0	33.7	31.7	33.9	29.2	31.9	35.2	33.5	34.0	31.6	33.5	30.4	29.8	30.7
3	2	55.7	55.4	57.2	59.2	57.7	58.5	55.7	54.9	58.3	57.5	56.6	58.3	57.9	56.9	55.9
2	18	61.9	56.7	58.0	59.2	63.0	61.2	60.3	54.7	51.5	53.9	59.2	56.8	57.3	55.9	56.3
18	17	48.8	49.3	46.2	48.3	46.2	47.8	49.5	51.0	46.9	48.0	51.6	49.3	49.1	47.2	49.6
17	12	29.1	32.1	30.9	29.7	33.1	30.5	33.4	29.1	32.1	29.1	32.6	30.1	31.9	31.8	32.0
12	16	33.5	35.2	35.5	28.3	30.5	31.3	29.6	33.2	33.0	34.8	34.9	32.8	29.7	33.1	32.0
16	15	40.1	40.1	36.0	38.7	40.3	43.2	40.8	39.6	36.3	38.8	37.2	43.1	38.7	42.3	41.7
15	14	46.5	48.0	47.0	47.4	43.8	43.6	44.4	45.6	47.8	43.7	42.8	47.0	43.6	45.5	46.2
12	14	19.7	20.2	19.5	19.8	19.2	20.3	20.1	19.8	20.2	20.9	20.7	19.9	19.4	19.4	19.3
14	13	21.1	21.5	21.1	20.1	18.8	21.9	21.6	21.8	20.6	21.7	17.9	18.9	19.4	19.6	19.9
12	19	47.6	48.6	45.0	48.7	48.5	48.0	47.9	49.3	46.1	46.5	44.7	46.1	48.6	44.8	45.1
19	0	38.9	41.7	40.9	37.4	39.5	40.4	42.0	41.1	39.0	38.0	43.1	43.3	40.0	39.3	40.5
0	7	34.3	34.5	37.4	38.3	38.2	35.8	35.5	38.2	36.9	38.3	34.7	34.2	33.9	35.1	37.2
7	19	29.6	30.6	31.0	31.8	31.7	32.0	32.4	30.5	29.9	31.7	30.7	30.5	32.2	32.1	32.4
7	8	23.8	25.1	26.5	26.3	25.2	23.6	26.0	26.1	24.6	24.5	24.1	24.4	23.7	24.0	25.9
19	10	54.5	55.7	56.9	55.6	56.8	53.6	52.9	56.2	57.1	52.9	54.0	54.3	57.5	56.3	55.6
10	13	27.1	26.3	29.0	26.7	25.5	28.2	28.3	28.6	27.0	28.7	27.8	25.6	25.3	26.6	26.9
13	12	39.5	44.4	46.4	44.7	46.7	44.0	41.5	45.5	47.6	46.8	46.4	38.8	42.4	39.5	42.3
12	10	26.1	27.5	28.1	28.1	27.3	28.0	25.6	25.7	25.5	26.6	28.0	26.2	28.8	27.7	27.3
10	11	54.7	53.8	54.9	52.4	55.4	53.1	54.1	52.5	52.7	55.4	53.9	55.7	53.7	55.7	54.5
10	8	54.0	54.3	53.1	53.1	51.4	53.7	51.5	52.0	54.2	51.7	54.7	53.5	53.4	53.9	53.4
8	9	37.3	38.9	36.7	36.9	38.0	39.2	35.7	41.5	37.2	38.8	42.8	37.0	38.6	41.8	38.9
19	17	47.8	46.9	49.4	52.0	49.7	43.6	43.6	44.9	45.9	45.6	50.4	45.6	49.5	45.4	50.1
19	18	52.3	56.0	55.6	54.3	55.0	55.4	53.2	52.4	55.1	53.0	52.5	55.0	53.6	55.9	55.3
0	18	47.8	47.9	46.6	47.4	49.1	49.1	47.0	47.5	48.9	44.8	45.3	47.0	45.4	48.0	47.4
0	2	43.1	44.7	41.9	41.1	40.6	42.4	43.4	44.9	45.1	43.1	42.5	41.0	41.2	43.8	44.5
12	15	30.6	32.7	32.2	32.6	30.6	33.6	31.2	30.4	30.9	32.0	33.0	32.0	30.4	31.4	32.5
16	17	20.7	20.0	19.5	20.0	20.1	20.1	20.5	20.6	20.2	20.6	19.4	19.3	20.3	20.1	20.7
6	20	23.3	21.6	23.2	20.4	23.6	21.4	21.4	22.1	21.6	21.4	22.5	22.6	21.7	20.4	21.1
5	6	41.4	40.6	41.7	41.7	42.6	43.6	40.6	43.4	41.0	40.6	42.1	44.0	40.8	40.9	40.2
3	5	37.1	32.7	36.5	30.8	33.1	34.3	33.5	31.3	32.0	31.1	37.3	31.2	35.6	33.2	36.0
4	3	36.9	37.0	37.5	39.5	36.8	36.9	36.0	36.1	37.9	38.2	39.3	38.1	36.8	38.9	38.3

2	3	43.3	44.3	43.1	43.2	42.3	41.5	43.5	44.0	44.5	41.5	44.5	42.9	42.5	42.2	41.7
18	2	30.4	29.8	29.7	30.2	30.9	31.0	29.2	29.8	29.7	29.2	30.9	30.2	30.8	29.7	29.5
17	18	36.7	36.1	35.8	36.5	34.4	33.0	34.5	36.1	31.8	34.8	34.2	31.7	36.1	31.6	36.3
12	17	35.0	39.1	35.5	38.2	36.6	37.9	37.5	38.6	38.0	38.1	35.4	38.8	37.0	39.2	38.0
16	12	32.4	32.8	32.6	34.4	32.5	33.7	33.1	32.9	34.5	31.5	33.9	32.1	32.8	33.8	33.0
15	16	27.1	29.1	27.8	28.3	30.4	30.5	27.1	29.1	27.6	30.7	27.4	30.5	27.6	27.3	27.2
14	15	52.1	50.2	49.7	51.4	52.2	51.4	49.6	51.4	52.1	52.7	49.2	50.7	50.9	50.8	50.3
14	12	24.5	25.5	26.0	25.3	23.9	23.1	28.9	26.0	27.5	25.6	28.8	27.1	26.1	24.4	27.7
13	14	55.6	57.9	60.0	56.8	52.6	54.6	54.9	57.1	60.1	57.8	55.1	60.9	61.4	58.2	54.6
19	12	19.7	18.5	19.1	18.5	20.2	20.2	19.1	19.3	20.1	20.0	21.5	21.4	21.5	20.0	19.5
0	19	52.5	48.4	45.8	45.5	50.4	47.5	48.9	52.4	46.2	47.1	45.5	45.0	45.6	46.6	47.1
7	0	29.7	29.6	30.8	29.7	29.4	30.2	31.1	31.7	30.0	30.5	29.0	31.1	29.3	29.8	31.6
19	7	47.4	50.4	49.2	48.6	47.7	51.6	52.4	48.0	48.1	52.2	49.2	45.2	52.0	50.8	51.7
8	7	28.2	25.5	26.1	29.0	28.4	25.8	30.5	25.4	26.9	27.7	29.7	29.0	29.3	30.0	29.2
10	19	52.6	58.5	55.7	56.7	57.5	54.0	57.5	53.7	53.2	56.2	54.3	58.3	56.1	54.7	57.5
13	10	43.0	44.4	47.9	47.5	46.6	46.6	44.8	46.3	46.7	46.6	46.9	44.1	48.4	47.5	44.1
12	13	50.1	47.2	48.9	47.2	51.1	47.3	51.1	47.7	49.8	48.3	49.6	47.5	50.9	51.6	50.5
10	12	50.5	58.9	59.0	60.0	54.5	60.1	55.7	53.0	59.7	52.0	58.8	54.9	51.9	59.0	56.1
11	10	61.2	55.1	56.5	60.0	56.6	64.0	56.6	64.2	59.1	61.9	61.0	59.7	61.6	62.1	59.5
8	10	57.1	58.1	61.4	57.0	56.1	58.1	59.1	58.3	59.2	61.6	58.8	59.5	61.1	60.1	59.8
9	8	29.6	30.8	31.6	31.1	32.3	31.8	27.8	28.4	32.1	31.2	29.2	27.9	30.1	28.0	30.9
17	19	44.4	45.5	46.9	45.5	46.6	42.5	40.6	46.2	44.8	39.0	39.2	46.7	41.4	41.8	41.1
18	19	22.2	21.7	24.4	22.7	24.0	24.1	23.1	21.9	22.5	24.2	22.9	21.6	22.6	22.8	21.9
18	0	51.0	49.7	53.7	50.6	50.9	50.0	50.8	49.8	51.1	54.1	53.4	53.5	54.6	55.7	53.9
2	0	46.1	45.3	43.1	43.0	47.5	48.7	47.5	43.6	47.4	49.0	45.0	44.5	44.7	48.7	48.3
15	12	40.4	40.3	40.9	40.9	39.4	41.9	38.7	43.3	39.3	41.6	41.6	42.6	38.5	38.5	40.6
17	16	25.6	22.4	23.2	23.9	22.6	25.9	24.6	23.9	23.2	25.4	25.6	23.5	22.4	22.7	25.9
19	1	38.9	41.7	40.9	37.4	39.5	40.4	42.0	41.1	39.0	38.0	43.1	43.3	40.0	39.3	40.5
1	7	34.3	34.5	37.4	38.3	38.2	35.8	35.5	38.2	36.9	38.3	34.7	34.2	33.9	35.1	37.2
1	18	47.8	47.9	46.6	47.4	49.1	49.1	47.0	47.5	48.9	44.8	45.3	47.0	45.4	48.0	47.4
1	2	43.1	44.7	41.9	41.1	40.6	42.4	43.4	44.9	45.1	43.1	42.5	41.0	41.2	43.8	44.5
1	19	52.5	48.4	45.8	45.5	50.4	47.5	48.9	52.4	46.2	47.1	45.5	45.0	45.6	46.6	47.1
7	1	29.7	29.6	30.8	29.7	29.4	30.2	31.1	31.7	30.0	30.5	29.0	31.1	29.3	29.8	31.6
18	1	51.0	49.7	53.7	50.6	50.9	50.0	50.8	49.8	51.1	54.1	53.4	53.5	54.6	55.7	53.9
2	1	46.1	45.3	43.1	43.0	47.5	48.7	47.5	43.6	47.4	49.0	45.0	44.5	44.7	48.7	48.3

	Seed	16	17	18	19	20	21	22	23	24	25	26	27	28	29	30
O	D															
20	6	27.0	25.3	26.1	27.2	25.7	26.8	27.0	26.9	25.4	26.6	27.3	26.2	25.1	25.7	25.5
6	5	60.5	56.4	56.0	58.6	61.4	62.8	61.7	59.0	59.6	62.8	59.1	63.1	63.8	60.5	59.4
5	3	26.6	25.1	26.8	24.8	25.7	25.6	26.1	25.7	24.7	26.7	26.0	24.9	26.5	25.2	25.3
3	4	29.7	31.3	33.2	29.5	30.5	35.0	35.1	33.8	30.4	32.2	32.5	30.6	33.6	34.7	31.7
3	2	56.0	55.9	58.4	57.3	56.4	58.7	59.1	57.0	57.8	56.8	58.4	57.4	58.4	56.0	58.0
2	18	62.4	60.2	55.1	63.5	56.2	64.1	61.4	54.2	61.7	62.8	54.3	62.8	57.8	54.1	53.6
18	17	47.1	49.3	48.8	50.2	49.5	51.0	49.2	46.8	47.1	50.4	51.0	47.0	47.4	51.5	47.3
17	12	29.0	29.7	30.8	29.6	34.2	33.7	35.0	34.9	31.2	34.6	31.8	31.4	32.8	32.0	32.4
12	16	31.8	31.9	29.0	35.1	33.7	29.5	30.1	32.3	28.2	30.1	29.4	35.2	34.4	28.4	35.2
16	15	43.9	43.9	37.7	40.5	42.0	38.4	37.7	37.3	42.6	41.0	43.5	40.5	36.6	37.4	40.3
15	14	42.0	48.2	46.9	42.1	46.6	44.9	45.7	44.5	42.8	45.5	46.6	47.8	43.6	43.0	45.5
12	14	19.7	20.3	20.1	19.5	20.7	20.7	20.1	19.5	20.3	19.6	19.6	20.7	20.3	19.4	19.2
14	13	18.9	20.4	18.5	18.6	18.7	20.7	19.1	18.5	21.3	18.6	19.7	18.7	20.7	18.8	19.8
12	19	44.8	44.7	47.9	48.2	46.1	47.0	45.4	49.0	49.2	48.6	47.8	49.2	46.7	46.7	47.3
19	0	41.7	39.1	40.8	37.1	43.1	39.1	42.4	36.0	40.8	40.9	35.0	34.8	34.7	34.3	36.4
0	7	35.5	38.2	38.2	36.8	33.8	38.4	35.8	35.3	38.2	35.4	36.9	36.6	34.2	36.7	38.3
7	19	30.6	30.7	30.7	30.0	32.2	32.0	30.4	30.8	31.2	30.5	31.3	30.4	29.6	30.1	31.5
7	8	24.0	23.9	24.1	24.0	24.1	25.3	25.8	26.6	25.3	25.6	25.1	24.5	25.1	25.7	26.5
19	10	55.6	55.5	54.1	56.0	53.4	55.4	54.9	56.3	57.3	53.6	58.0	55.7	53.5	54.0	58.7
10	13	28.1	25.7	26.2	26.1	29.2	26.2	27.5	25.9	27.2	27.8	25.7	29.1	25.4	25.8	28.9
13	12	41.6	44.3	42.9	41.0	42.6	44.3	45.9	47.0	38.6	41.6	46.4	45.6	46.5	42.6	45.4
12	10	26.1	27.9	27.2	25.5	27.0	25.4	27.7	25.7	26.6	28.0	25.8	27.5	26.7	28.8	28.8
10	11	54.7	54.2	55.6	52.4	52.5	53.6	52.8	55.6	53.6	55.3	54.9	54.6	54.9	53.5	53.9
10	8	54.0	52.1	53.3	53.7	53.5	51.6	53.7	51.8	53.6	53.5	54.2	51.8	52.7	51.9	52.3
8	9	41.4	37.5	37.8	36.0	42.2	39.1	38.0	38.1	35.4	40.1	39.9	42.8	36.3	42.4	36.1
19	17	45.7	50.6	46.8	43.7	43.4	50.6	43.2	44.7	44.7	43.5	43.3	51.7	50.7	49.6	52.5
19	18	52.8	52.4	54.8	52.6	54.2	52.4	54.1	52.3	53.5	53.0	55.9	54.5	54.2	54.4	55.8
0	18	47.3	46.7	45.2	47.2	48.7	45.4	47.2	49.3	48.5	48.0	44.8	47.9	48.9	49.1	47.3
0	2	44.8	44.8	41.3	44.9	40.9	43.8	41.3	43.3	44.6	41.5	44.7	43.7	40.5	41.7	41.4
12	15	33.6	31.1	31.0	32.8	33.0	31.4	31.2	32.3	31.8	31.7	30.3	30.5	33.1	32.2	30.6
16	17	20.2	19.7	20.1	19.7	19.6	20.2	19.5	20.0	20.7	19.4	20.4	20.4	19.5	19.9	20.4
6	20	23.5	21.2	21.0	21.3	21.7	20.5	21.0	22.8	22.6	20.5	20.7	20.5	21.6	21.9	23.1
5	6	43.5	42.8	41.7	41.6	41.1	42.3	40.9	41.9	41.7	40.2	41.5	42.7	43.2	40.8	40.7
3	5	36.0	30.8	36.8	35.1	31.9	34.4	34.1	37.3	32.5	31.5	34.6	31.1	36.2	32.1	32.7
4	3	39.3	38.7	36.9	36.1	40.0	37.4	36.1	37.4	37.5	39.5	39.8	36.1	37.2	38.4	39.4
2	3	42.3	41.8	42.6	43.6	41.9	43.6	42.4	42.6	42.3	44.4	42.7	42.4	42.4	43.6	43.0
18	2	29.9	30.4	29.9	29.6	30.7	29.7	29.5	29.6	30.5	30.5	30.0	29.7	30.4	30.5	30.2
17	18	35.7	32.4	32.0	32.6	35.7	34.6	32.8	35.2	36.7	35.9	36.2	36.4	36.4	36.9	33.1
12	17	37.6	37.7	36.0	36.1	38.3	35.8	39.0	36.7	39.1	36.7	38.1	37.8	38.4	39.0	38.4
16	12	34.4	31.6	33.5	34.3	32.5	32.1	31.6	32.2	33.5	31.7	34.5	34.6	33.2	32.4	33.7
15	16	29.5	27.7	28.4	28.2	28.0	29.0	29.9	29.0	30.1	29.5	29.0	29.4	28.3	30.7	30.1
14	15	49.8	51.4	52.3	50.9	51.5	52.8	49.6	49.7	52.3	50.3	49.3	50.7	50.4	51.6	51.7
14	12	24.1	23.2	27.1	25.4	24.9	23.7	27.2	24.4	25.2	27.3	26.0	27.1	24.5	27.0	23.1
13	14	55.3	57.2	58.1	58.5	59.0	56.7	57.9	53.4	54.3	60.9	54.1	57.3	55.0	60.6	55.6
19	12	19.9	20.8	20.7	18.7	19.5	21.0	19.4	20.6	19.4	20.8	20.4	20.9	21.4	19.4	19.2
0	19	46.8	50.0	46.5	52.9	53.4	46.0	44.3	45.5	49.5	53.9	50.0	45.8	48.7	50.9	51.9
7	0	28.9	30.0	29.5	31.1	31.9	29.7	28.4	31.1	28.5	29.4	28.8	28.2	30.8	28.9	28.1
19	7	47.1	47.7	52.3	47.9	47.2	49.1	45.8	51.4	45.5	48.5	47.9	45.9	45.2	52.7	51.9
8	7	26.1	30.6	29.9	30.8	25.5	25.8	25.4	29.7	30.4	25.3	30.2	26.1	30.1	30.4	27.2
10	19	53.9	58.7	56.0	57.9	56.8	55.7	54.6	56.1	54.7	56.9	53.7	53.1	53.8	52.6	55.1
13	10	47.6	45.1	46.3	43.1	43.9	46.4	44.6	44.3	44.2	44.4	46.4	44.7	43.2	47.8	44.7
12	13	47.0	47.7	49.1	47.7	46.5	46.5	50.2	46.8	50.8	48.5	49.4	50.8	46.6	48.7	49.0
10	12	52.4	51.1	53.2	60.1	52.5	50.5	52.6	55.9	56.3	60.1	49.3	53.8	56.7	54.9	52.9
11	10	54.7	60.3	57.9	56.3	62.7	57.8	60.5	58.6	61.7	54.7	54.3	59.5	57.7	54.8	56.6
8	10	60.5	60.9	60.2	60.1	61.4	56.0	59.9	58.6	60.8	61.1	59.4	57.4	59.2	56.7	61.9
9	8	31.2	28.0	31.3	32.1	30.5	30.3	28.2	31.5	28.1	28.4	31.5	28.9	29.6	30.2	31.9
17	19	39.1	46.5	40.7	41.5	43.1	45.2	39.7	46.2	39.9	45.6	45.5	41.0	44.5	40.1	40.0
18	19	22.6	21.6	21.7	23.7	23.6	23.7	24.4	23.1	21.7	21.8	23.1	24.1	24.4	22.5	21.9
18	0	55.8	51.2	50.0	50.9	54.5	51.0	54.0	52.9	51.9	50.5	52.0	49.7	50.2	56.3	53.1
2	0	45.1	47.6	46.9	43.6	43.9	43.8	44.6	45.5	48.9	48.3	46.6	43.4	48.0	43.3	47.0
15	12	41.9	39.5	41.3	42.7	41.2	43.2	39.4	38.5	38.7	41.4	38.6	43.3	39.0	41.3	41.7

17	16	23.8	25.0	25.7	24.3	23.0	22.5	22.7	25.3	23.6	24.2	23.2	23.7	22.3	22.6	25.0
19	1	41.7	39.1	40.8	37.1	43.1	39.1	42.4	36.0	40.8	40.9	35.0	34.8	34.7	34.3	36.4
1	7	35.5	38.2	38.2	36.8	33.8	38.4	35.8	35.3	38.2	35.4	36.9	36.6	34.2	36.7	38.3
1	18	47.3	46.7	45.2	47.2	48.7	45.4	47.2	49.3	48.5	48.0	44.8	47.9	48.9	49.1	47.3
1	2	44.8	44.8	41.3	44.9	40.9	43.8	41.3	43.3	44.6	41.5	44.7	43.7	40.5	41.7	41.4
1	19	46.8	50.0	46.5	52.9	53.4	46.0	44.3	45.5	49.5	53.9	50.0	45.8	48.7	50.9	51.9
7	1	28.9	30.0	29.5	31.1	31.9	29.7	28.4	31.1	28.5	29.4	28.8	28.2	30.8	28.9	28.1
18	1	55.8	51.2	50.0	50.9	54.5	51.0	54.0	52.9	51.9	50.5	52.0	49.7	50.2	56.3	53.1
2	1	45.1	47.6	46.9	43.6	43.9	43.8	44.6	45.5	48.9	48.3	46.6	43.4	48.0	43.3	47.0

5.3.1.3 Restricted Zones

Restricted Zones are again considered, and the same patterns developed in Stage 2 are used again. RZs are illustrated in Figure 58, below.

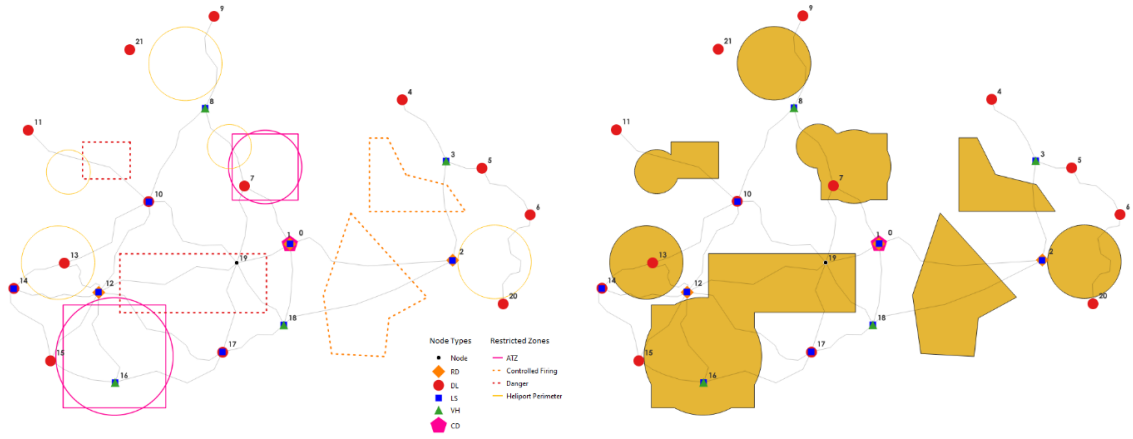

Figure 58: Introduced Restricted Zones and final dissolved shapes.

5.3.1.4 Weather Forecast

Additional information on a probabilistic weather forecast is generated. We assume a weather forecast map to the likes of Figure 54, where areas are characterized based on the probability of falling below or above a certain weather metric. However, since we are specifically interested in adverse conditions for UAV flights, the map only contains information on the exceedance of said metric. We generate a random probabilistic forecast map and convert said information into a DEM-like feature in GIS; "*Pw*" values are translated into altitude or "cost". The forecast is presented in Figure 59, below.

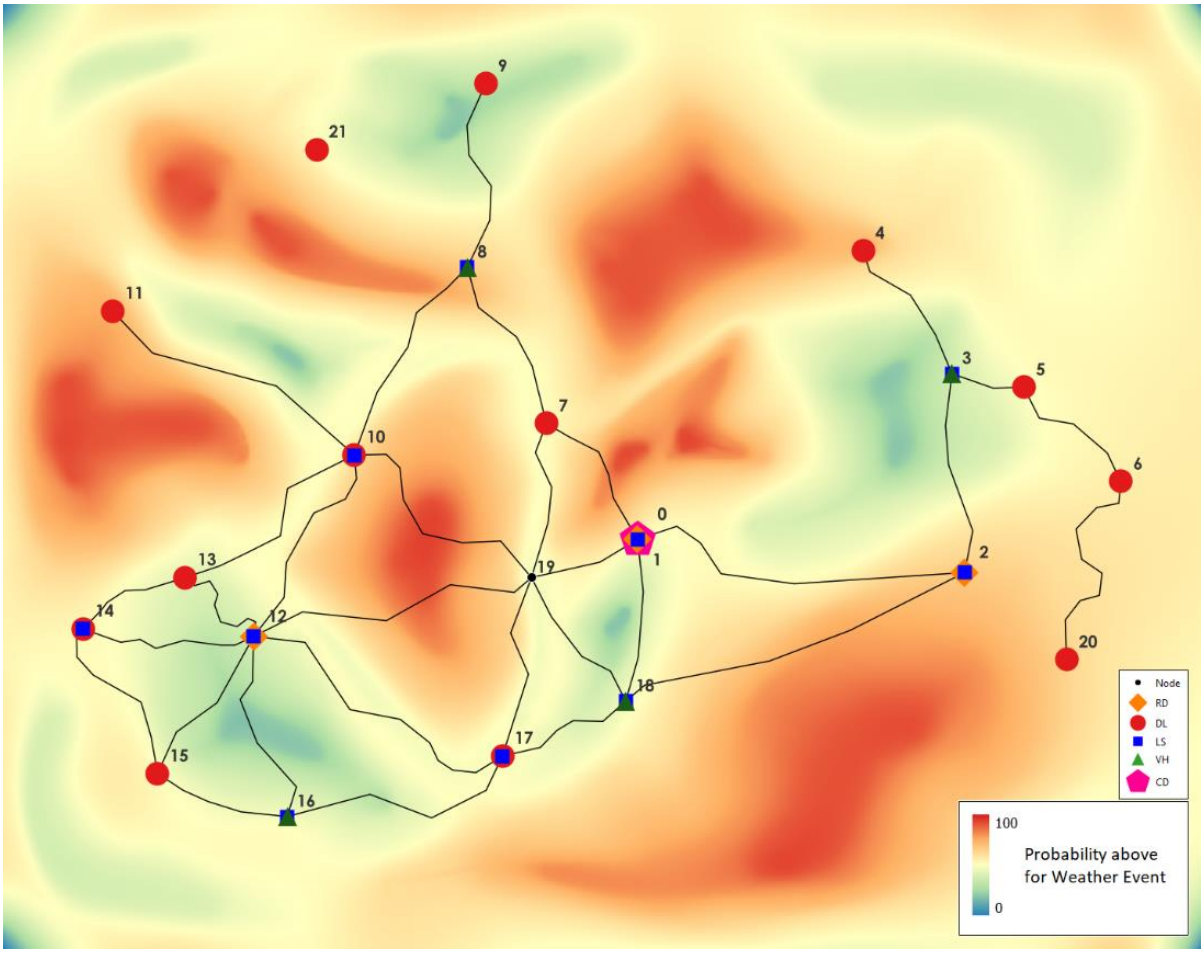

Figure 59: Introduced Probabilistic Weather Forecast.

Performing spatial analysis in GIS, we have further isolated the areas above certain probability thresholds, namely 60%, 70%, 80% and 90%. This is shown in Figure 60.

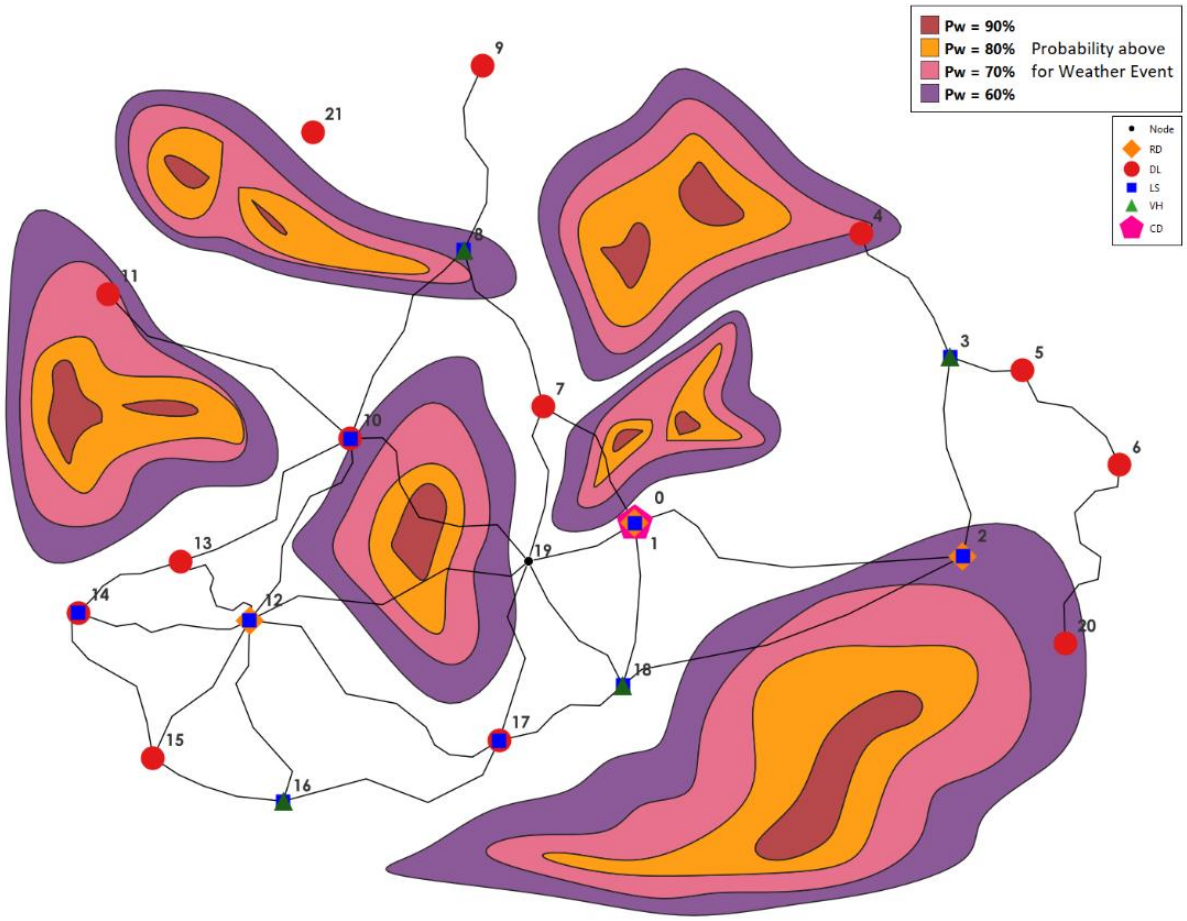

Figure 60: Spatial analysis of Weather Forecast at given thresholds.

5.4 Experiments

We apply our methodology considering the 4 Probability thresholds of 60, 70, 80 and 90% and the 30 seeds of CVN conditions generated. Initial feasible DL-LS UAV connections are found, based on the theoretical maximum UAV range, with straight paths. For each *Pw* scenario, we recalculate the optimal UAV paths for the above LS-DL pairs only, using obstacle avoidance optimal line tools provided in the GIS software packages. RZs and AWZs are considered as obstacles for UAV routing. The following Figures (Figure 61 to Figure 64) show the respective UAV paths.

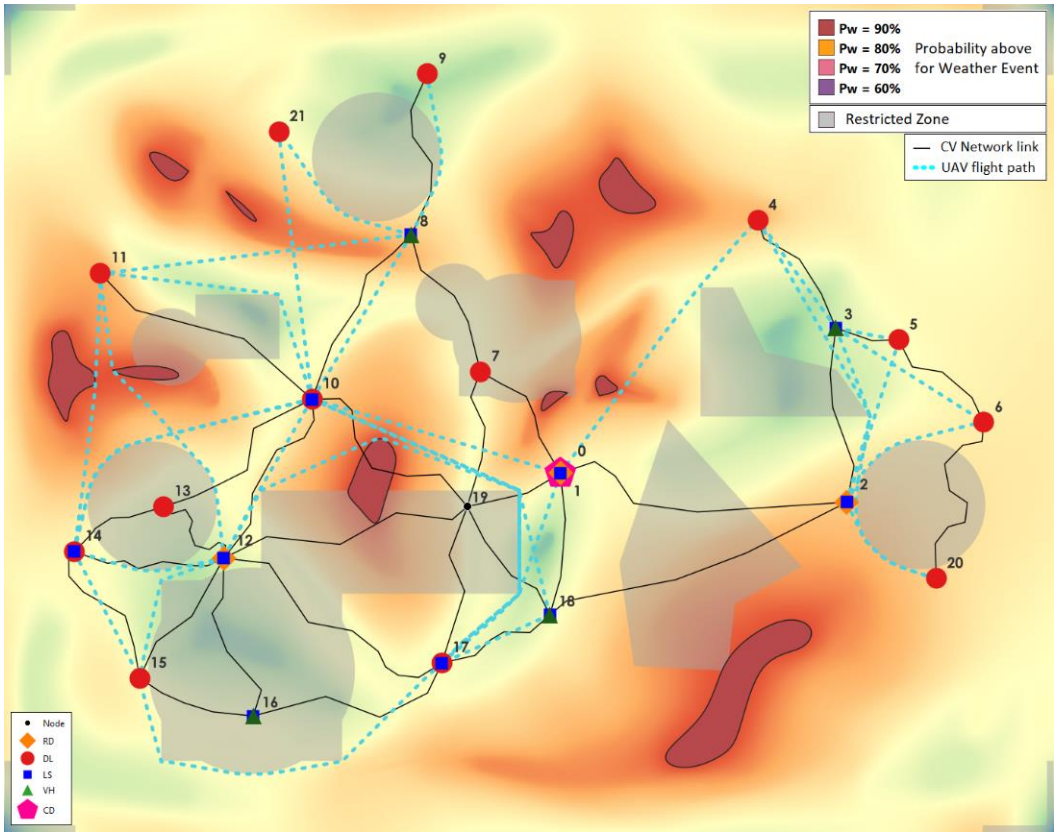

Figure 61: Optimal UAV flight paths for feasible DL - LS pairs at Pw = 90%

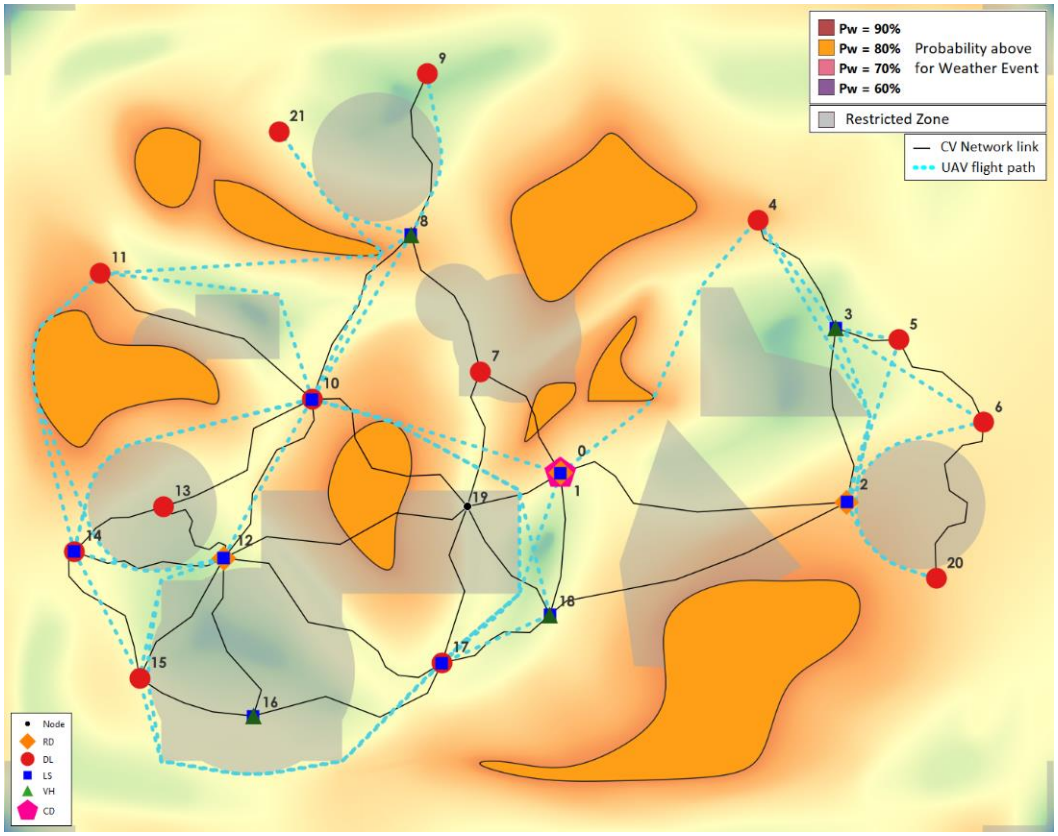

Figure 62: Optimal UAV flight paths for feasible DL - LS pairs at Pw = 80%

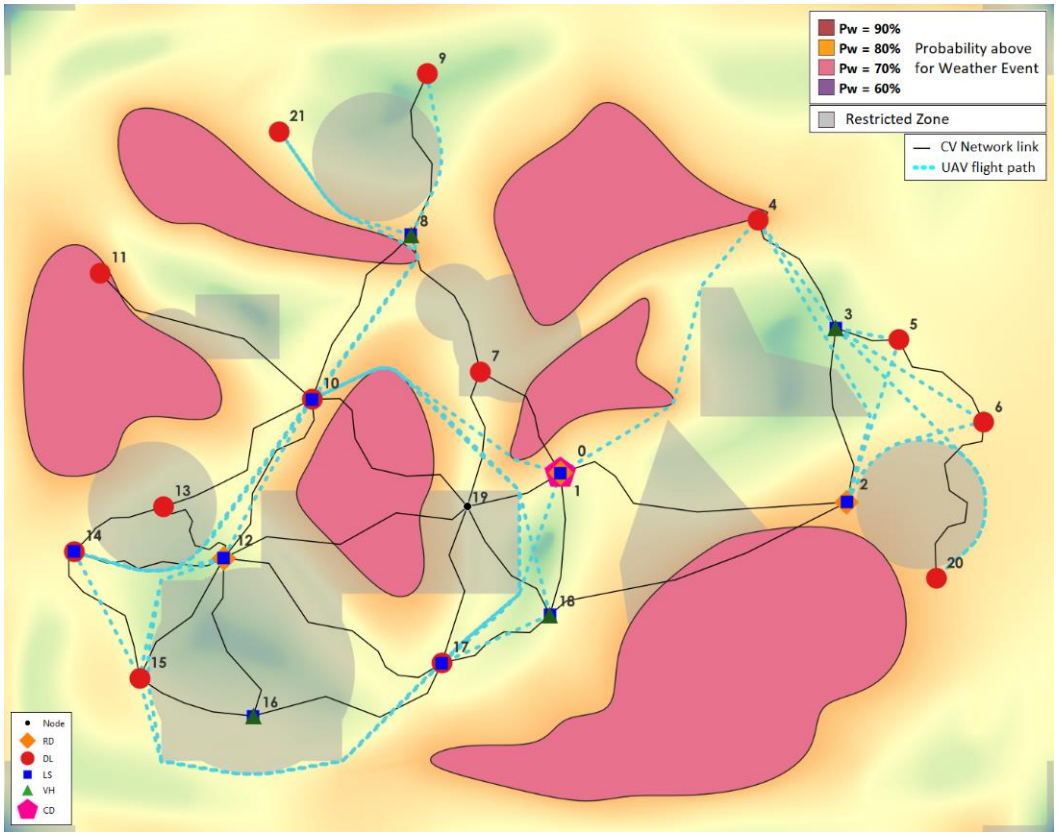

Figure 63: Optimal UAV flight paths for feasible DL - LS pairs at Pw = 70%

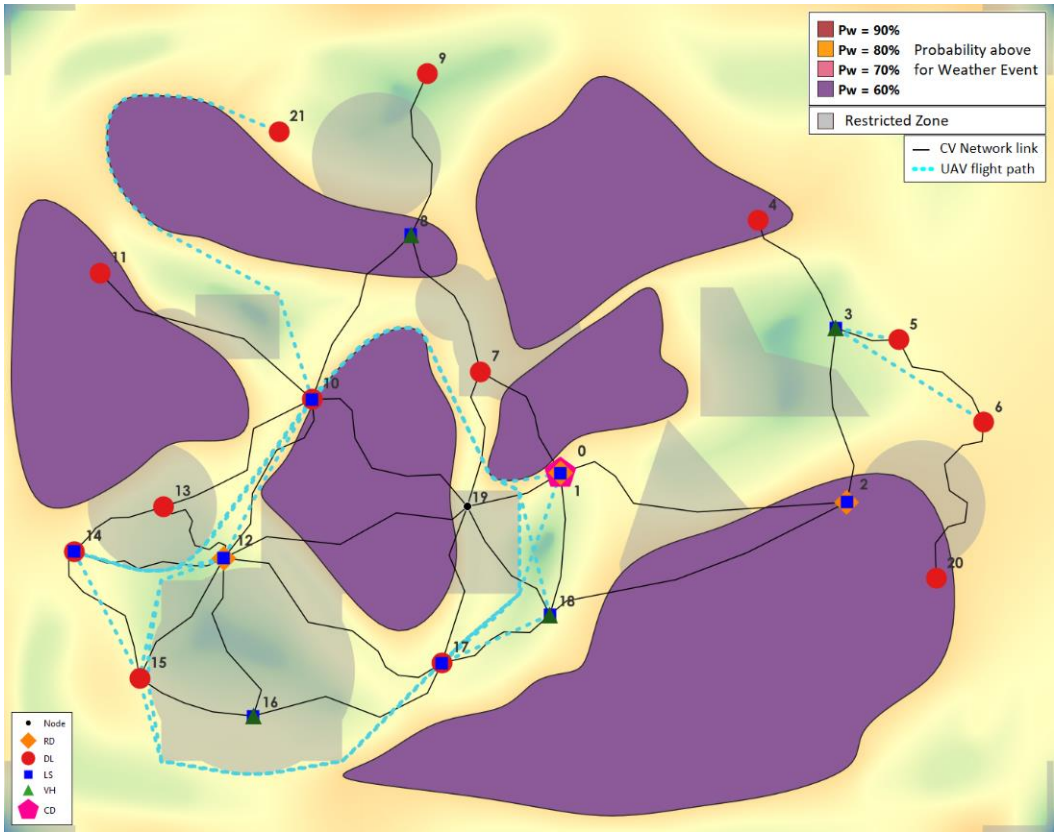

Figure 64: Optimal UAV flight paths for feasible DL - LS pairs at Pw = 60%

Total flight times, $tft_{ij,W}$ are updated based on the new flight paths and feasible UAV connectivity for each one is reevaluated based on UAV range.

Table 29: Updated UAV edge costs (tft_{ij}, sec), considering RZs and AWZs, Pw = 90%

tft_{ij}	0	1	2	3	4	5	6	7	8	9	10	11	12	13	14	15	16	17	18	19	20	21
0	0	0	inf	inf	1785	inf	inf	inf	inf	inf	1452	inf	inf	inf	inf	inf	inf	1305	inf	inf	inf	inf
1	0	0	inf	inf	1785	inf	inf	inf	inf	inf	1452	inf	inf	inf	inf	inf	inf	1305	inf	inf	inf	inf
2	inf	inf	0	inf	1752	979	965	inf	inf	inf	inf	inf	inf	inf	inf	inf	inf	inf	inf	inf	731	inf
3	inf	inf	inf	0	777	406	1002	inf	inf	inf	inf	inf	inf	inf	inf	inf	inf	inf	inf	inf	1692	inf
4	1785	1785	1752	777	0	inf	inf	inf	inf	inf	inf	inf	inf	inf	inf	inf	inf	inf	inf	inf	inf	inf
5	inf	inf	979	406	inf	0	inf	inf	inf	inf	inf	inf	inf	inf	inf	inf	inf	inf	inf	inf	inf	inf
6	inf	inf	965	1002	inf	inf	0	inf	inf	inf	inf	inf	inf	inf	inf	inf	inf	inf	inf	inf	inf	inf
7	inf	inf	inf	inf	inf	inf	inf	0	inf	inf	inf	inf	inf	inf	inf	inf	inf	inf	inf	inf	inf	inf
8	inf	inf	inf	inf	inf	inf	inf	inf	0	969	1094	1743	inf	inf	inf	inf	inf	inf	inf	inf	inf	1006
9	inf	inf	inf	inf	inf	inf	inf	inf	969	0	inf	inf	inf	inf	inf	inf	inf	inf	inf	inf	inf	inf
10	1452	1452	inf	inf	inf	inf	inf	inf	1094	inf	0	1620	1038	inf	1751	inf	inf	2389	1966	inf	inf	1509
11	inf	inf	inf	inf	inf	inf	inf	inf	1743	inf	1620	0	1811	inf	1566	inf	inf	inf	inf	inf	inf	inf
12	inf	inf	inf	inf	inf	inf	inf	inf	inf	inf	1038	1811	0	inf	885	957	inf	3087	inf	inf	inf	inf
13	inf	inf	inf	inf	inf	inf	inf	inf	inf	inf	inf	inf	inf	0	inf	inf	inf	inf	inf	inf	inf	inf
14	inf	inf	inf	inf	inf	inf	inf	inf	inf	inf	1751	1566	885	inf	0	826	inf	inf	inf	inf	inf	inf
15	inf	inf	inf	inf	inf	inf	inf	inf	inf	inf	inf	inf	957	inf	826	0	inf	2257	inf	inf	inf	inf
16	inf	inf	inf	inf	inf	inf	inf	inf	inf	inf	inf	inf	inf	inf	inf	inf	0	inf	inf	inf	inf	inf
17	1305	1305	inf	inf	inf	inf	inf	inf	inf	inf	2390	inf	3087	inf	inf	2257	inf	0	698	inf	inf	inf
18	inf	inf	inf	inf	inf	inf	inf	inf	inf	inf	1966	inf	inf	inf	inf	inf	inf	698	0	inf	inf	inf
19	inf	inf	inf	inf	inf	inf	inf	inf	inf	inf	inf	inf	inf	inf	inf	inf	inf	inf	inf	0	inf	inf
20	inf	inf	731	1692	inf	inf	inf	inf	inf	inf	inf	inf	inf	inf	inf	inf	inf	inf	inf	inf	0	inf
21	inf	inf	inf	inf	inf	inf	inf	inf	1006	inf	1509	inf	inf	inf	inf	inf	inf	inf	inf	inf	inf	0

Table 30: Adjacency matrix for UAV (x^{UAV}_{ij}), considering RZs and AWZs, Pw = 90%

x^{UAV}_{ij}	0	1	2	3	4	5	6	7	8	9	10	11	12	13	14	15	16	17	18	19	20	21
0	-	-	-	-	1	-	-	-	-	-	1	-	-	-	-	-	-	1	-	-	-	-
1	-	-	-	-	1	-	-	-	-	-	1	-	-	-	-	-	-	1	-	-	-	-
2	-	-	-	-	1	1	1	-	-	-	-	-	-	-	-	-	-	-	-	-	1	-
3	-	-	-	-	1	1	1	-	-	-	-	-	-	-	-	-	-	-	-	-	1	-
4	1	1	1	1	-	-	-	-	-	-	-	-	-	-	-	-	-	-	-	-	-	-
5	-	-	1	1	-	-	-	-	-	-	-	-	-	-	-	-	-	-	-	-	-	-
6	-	-	1	1	-	-	-	-	-	-	-	-	-	-	-	-	-	-	-	-	-	-
7	-	-	-	-	-	-	-	-	-	-	-	-	-	-	-	-	-	-	-	-	-	-
8	-	-	-	-	-	-	-	-	-	1	1	1	-	-	-	-	-	-	-	-	-	1
9	-	-	-	-	-	-	-	-	1	-	-	-	-	-	-	-	-	-	-	-	-	-
10	1	1	-	-	-	-	-	-	1	-	-	1	1	-	1	-	-	-	-	-	-	1
11	-	-	-	-	-	-	-	-	1	-	1	-	-	-	1	-	-	-	-	-	-	-
12	-	-	-	-	-	-	-	-	-	-	1	-	-	-	1	1	-	-	-	-	-	-
13	-	-	-	-	-	-	-	-	-	-	-	-	-	-	-	-	-	-	-	-	-	-
14	-	-	-	-	-	-	-	-	-	-	1	1	1	-	-	1	-	-	-	-	-	-

Table 31: Updated UAV edge costs (tft_{ij}, sec), considering RZs and AWZs, Pw = 80%

tft_{ij}	0	1	2	3	4	5	6	7	8	9	10	11	12	13	14	15	16	17	18	19	20	21
0	0	0	inf	inf	1824	inf	inf	inf	inf	inf	1453	inf	inf	inf	inf	inf	inf	1305	inf	inf	inf	inf
1	0	0	inf	inf	1824	inf	inf	inf	inf	inf	1453	inf	inf	inf	inf	inf	inf	1305	inf	inf	inf	inf
2	inf	inf	0	inf	1752	979	965	inf	inf	inf	inf	inf	inf	inf	inf	inf	inf	inf	inf	inf	731	inf
3	inf	inf	inf	0	777	406	1002	inf	inf	inf	inf	inf	inf	inf	inf	inf	inf	inf	inf	inf	1692	inf
4	1824	1824	1752	777	0	inf	inf	inf	inf	inf	inf	inf	inf	inf	inf	inf	inf	inf	inf	inf	inf	inf
5	inf	inf	979	406	inf	0	inf	inf	inf	inf	inf	inf	inf	inf	inf	inf	inf	inf	inf	inf	inf	inf
6	inf	inf	965	1002	inf	inf	0	inf	inf	inf	inf	inf	inf	inf	inf	inf	inf	inf	inf	inf	inf	inf
7	inf	inf	inf	inf	inf	inf	inf	0	inf	inf	inf	inf	inf	inf	inf	inf	inf	inf	inf	inf	inf	inf
8	inf	inf	inf	inf	inf	inf	inf	inf	0	969	1094	1765	inf	inf	inf	inf	inf	inf	inf	inf	inf	1006
9	inf	inf	inf	inf	inf	inf	inf	inf	969	0	inf	inf	inf	inf	inf	inf	inf	inf	inf	inf	inf	inf
10	1453	1453	inf	inf	inf	inf	inf	inf	1094	inf	0	1620	1038	inf	1751	inf	inf	2396	1973	inf	inf	1786
11	inf	inf	inf	inf	inf	inf	inf	inf	1765	inf	1620	0	2460	inf	1735	inf	inf	inf	inf	inf	inf	inf
12	inf	inf	inf	inf	inf	inf	inf	inf	inf	inf	1038	2460	0	inf	885	957	inf	3135	inf	inf	inf	inf
13	inf	inf	inf	inf	inf	inf	inf	inf	inf	inf	inf	inf	inf	0	inf	inf	inf	inf	inf	inf	inf	inf

14	inf	inf	inf	inf	inf	inf	inf	inf	inf	inf	1751	1735	885	inf	0	826	inf	inf	inf	inf	inf	inf
15	inf	inf	inf	inf	inf	inf	inf	inf	inf	inf	inf	inf	957	inf	826	0	inf	2257	inf	inf	inf	inf
16	inf	inf	inf	inf	inf	inf	inf	inf	inf	inf	inf	inf	inf	inf	inf	inf	0	inf	inf	inf	inf	inf
17	1305	1305	inf	inf	inf	inf	inf	inf	inf	inf	2398	inf	3135	inf	inf	2257	inf	0	698	inf	inf	inf
18	inf	inf	inf	inf	inf	inf	inf	inf	inf	inf	1973	inf	inf	inf	inf	inf	inf	698	0	inf	inf	inf
19	inf	inf	inf	inf	inf	inf	inf	inf	inf	inf	inf	inf	inf	inf	inf	inf	inf	inf	inf	0	inf	inf
20	inf	inf	731	1692	inf	inf	inf	inf	inf	inf	inf	inf	inf	inf	inf	inf	inf	inf	inf	inf	0	inf
21	inf	inf	inf	inf	inf	inf	inf	inf	1006	inf	1786	inf	inf	inf	inf	inf	inf	inf	inf	inf	inf	0

Table 32: Adjacency matrix for UAV (x^{UAV}_{ij}), considering RZs and AWZs, Pw = 80%

x^{UAV}_{ij}	**0**	**1**	**2**	**3**	**4**	**5**	**6**	**7**	**8**	**9**	**10**	**11**	**12**	**13**	**14**	**15**	**16**	**17**	**18**	**19**	**20**	**21**
0	-	-	-	-	-	-	-	-	-	-	1	-	-	-	-	-	-	1	-	-	-	-
1	-	-	-	-	-	-	-	-	-	-	1	-	-	-	-	-	-	1	-	-	-	-
2	-	-	-	-	1	1	1	-	-	-	-	-	-	-	-	-	-	-	-	-	1	-
3	-	-	-	-	1	1	1	-	-	-	-	-	-	-	-	-	-	-	-	-	1	-
4	-	-	1	1	-	-	-	-	-	-	-	-	-	-	-	-	-	-	-	-	-	-
5	-	-	1	1	-	-	-	-	-	-	-	-	-	-	-	-	-	-	-	-	-	-
6	-	-	1	1	-	-	-	-	-	-	-	-	-	-	-	-	-	-	-	-	-	-
7	-	-	-	-	-	-	-	-	-	-	-	-	-	-	-	-	-	-	-	-	-	-
8	-	-	-	-	-	-	-	-	-	1	1	1	-	-	-	-	-	-	-	-	-	1
9	-	-	-	-	-	-	-	-	1	-	-	-	-	-	-	-	-	-	-	-	-	-
10	1	1	-	-	-	-	-	-	1	-	-	1	1	-	1	-	-	-	-	-	-	1
11	-	-	-	-	-	-	-	-	1	-	1	-	-	-	1	-	-	-	-	-	-	-
12	-	-	-	-	-	-	-	-	-	-	1	-	-	-	1	1	-	-	-	-	-	-
13	-	-	-	-	-	-	-	-	-	-	-	-	-	-	-	-	-	-	-	-	-	-
14	-	-	-	-	-	-	-	-	-	-	1	1	1	-	-	1	-	-	-	-	-	-

Table 33: Updated UAV edge costs (tft_{ij}, sec), considering RZs and AWZs, Pw = 70%

tft_{ij}	**0**	**1**	**2**	**3**	**4**	**5**	**6**	**7**	**8**	**9**	**10**	**11**	**12**	**13**	**14**	**15**	**16**	**17**	**18**	**19**	**20**	**21**
0	0	0	inf	inf	1888	inf	inf	inf	inf	inf	1604	inf	inf	inf	inf	inf	inf	1305	inf	inf	inf	inf
1	0	0	inf	inf	1888	inf	inf	inf	inf	inf	1604	inf	inf	inf	inf	inf	inf	1305	inf	inf	inf	inf
2	inf	inf	0	inf	1752	979	965	inf	inf	inf	inf	inf	inf	inf	inf	inf	inf	inf	inf	inf	1662	inf
3	inf	inf	inf	0	777	406	1002	inf	inf	inf	inf	inf	inf	inf	inf	inf	inf	inf	inf	inf	1826	inf
4	1888	1888	1752	777	0	inf	inf	inf	inf	inf	inf	inf	inf	inf	inf	inf	inf	inf	inf	inf	inf	inf
5	inf	inf	979	406	inf	0	inf	inf	inf	inf	inf	inf	inf	inf	inf	inf	inf	inf	inf	inf	inf	inf
6	inf	inf	965	1002	inf	inf	0	inf	inf	inf	inf	inf	inf	inf	inf	inf	inf	inf	inf	inf	inf	inf
7	inf	inf	inf	inf	inf	inf	inf	0	inf	inf	inf	inf	inf	inf	inf	inf	inf	inf	inf	inf	inf	inf
8	inf	inf	inf	inf	inf	inf	inf	inf	0	969	1141	inf	inf	inf	inf	inf	inf	inf	inf	inf	inf	1006
9	inf	inf	inf	inf	inf	inf	inf	inf	969	0	inf	inf	inf	inf	inf	inf	inf	inf	inf	inf	inf	inf
10	1604	1604	inf	inf	inf	inf	inf	inf	1141	inf	0	inf	1038	inf	1792	inf	inf	2586	2162	inf	inf	2046
11	inf	inf	inf	inf	inf	inf	inf	inf	inf	inf	inf	0	inf	inf	inf	inf	inf	inf	inf	inf	inf	inf
12	inf	inf	inf	inf	inf	inf	inf	inf	inf	inf	1038	inf	0	inf	885	957	inf	3135	inf	inf	inf	inf
13	inf	inf	inf	inf	inf	inf	inf	inf	inf	inf	inf	inf	inf	0	inf	inf	inf	inf	inf	inf	inf	inf
14	inf	inf	inf	inf	inf	inf	inf	inf	inf	inf	1791	inf	885	inf	0	826	inf	inf	inf	inf	inf	inf
15	inf	inf	inf	inf	inf	inf	inf	inf	inf	inf	inf	inf	957	inf	826	0	inf	2257	inf	inf	inf	inf
16	inf	inf	inf	inf	inf	inf	inf	inf	inf	inf	inf	inf	inf	inf	inf	inf	0	inf	inf	inf	inf	inf
17	1305	1305	inf	inf	inf	inf	inf	inf	inf	inf	2587	inf	3135	inf	inf	2257	inf	0	698	inf	inf	inf
18	inf	inf	inf	inf	inf	inf	inf	inf	inf	inf	2162	inf	inf	inf	inf	inf	inf	698	0	inf	inf	inf
19	inf	inf	inf	inf	inf	inf	inf	inf	inf	inf	inf	inf	inf	inf	inf	inf	inf	inf	inf	0	inf	inf
20	inf	inf	1662	1826	inf	inf	inf	inf	inf	inf	inf	inf	inf	inf	inf	inf	inf	inf	inf	inf	0	inf
21	inf	inf	inf	inf	inf	inf	inf	inf	1006	inf	2046	inf	inf	inf	inf	inf	inf	inf	inf	inf	inf	0

Table 34: Adjacency matrix for UAV (x^{UAV}_{ij}), considering RZs and AWZs, Pw = 70%

x^{UAV}_{ij}	**0**	**1**	**2**	**3**	**4**	**5**	**6**	**7**	**8**	**9**	**10**	**11**	**12**	**13**	**14**	**15**	**16**	**17**	**18**	**19**	**20**	**21**
0	-	-	-	-	-	-	-	-	-	-	1	-	-	-	-	-	-	1	-	-	-	-
1	-	-	-	-	-	-	-	-	-	-	1	-	-	-	-	-	-	1	-	-	-	-
2	-	-	-	-	1	1	1	-	-	-	-	-	-	-	-	-	-	-	-	-	1	-
3	-	-	-	-	1	1	1	-	-	-	-	-	-	-	-	-	-	-	-	-	-	-
4	-	-	1	1	-	-	-	-	-	-	-	-	-	-	-	-	-	-	-	-	-	-
5	-	-	1	1	-	-	-	-	-	-	-	-	-	-	-	-	-	-	-	-	-	-

6	-	-	1	1	-	-	-	-	-	-	-	-	-	-	-	-	-	-	-	-	-	-
7	-	-	-	-	-	-	-	-	-	-	-	-	-	-	-	-	-	-	-	-	-	-
8	-	-	-	-	-	-	-	-	-	1	1	-	-	-	-	-	-	-	-	-	-	1
9	-	-	-	-	-	-	-	-	1	-	-	-	-	-	-	-	-	-	-	-	-	-
10	1	1	-	-	-	-	-	-	1	-	-	-	1	-	1	-	-	-	-	-	-	-
11	-	-	-	-	-	-	-	-	-	-	-	-	-	-	-	-	-	-	-	-	-	-
12	-	-	-	-	-	-	-	-	-	-	1	-	-	-	1	1	-	-	-	-	-	-
13	-	-	-	-	-	-	-	-	-	-	-	-	-	-	-	-	-	-	-	-	-	-
14	-	-	-	-	-	-	-	-	-	-	1	-	1	-	-	1	-	-	-	-	-	-

Table 35: Updated UAV edge costs (tft_{ij}, sec), considering RZs and AWZs, Pw = 60%

tft_{ij}	0	1	2	3	4	5	6	7	8	9	10	11	12	13	14	15	16	17	18	19	20	21
0	0	0	inf	inf	inf	inf	inf	inf	inf	inf	2046	inf	inf	inf	inf	inf	inf	1305	inf	inf	inf	inf
1	0	0	inf	inf	inf	inf	inf	inf	inf	inf	2046	inf	inf	inf	inf	inf	inf	1305	inf	inf	inf	inf
2	inf	inf	0	inf	inf	inf	inf	inf	inf	inf	inf	inf	inf	inf	inf	inf	inf	inf	inf	inf	inf	inf
3	inf	inf	inf	0	inf	406	1002	inf	inf	inf	inf	inf	inf	inf	inf	inf	inf	inf	inf	inf	inf	inf
4	inf	inf	inf	inf	0	inf	inf	inf	inf	inf	inf	inf	inf	inf	inf	inf	inf	inf	inf	inf	inf	inf
5	inf	inf	inf	406	inf	0	inf	inf	inf	inf	inf	inf	inf	inf	inf	inf	inf	inf	inf	inf	inf	inf
6	inf	inf	inf	1002	inf	inf	0	inf	inf	inf	inf	inf	inf	inf	inf	inf	inf	inf	inf	inf	inf	inf
7	inf	inf	inf	inf	inf	inf	inf	0	inf	inf	inf	inf	inf	inf	inf	inf	inf	inf	inf	inf	inf	inf
8	inf	inf	inf	inf	inf	inf	inf	inf	0	inf	inf	inf	inf	inf	inf	inf	inf	inf	inf	inf	inf	inf
9	inf	inf	inf	inf	inf	inf	inf	inf	inf	0	inf	inf	inf	inf	inf	inf	inf	inf	inf	inf	inf	inf
10	2046	2046	inf	inf	inf	inf	inf	inf	inf	inf	0	inf	1038	inf	1792	inf	inf	2947	2524	inf	inf	3088
11	inf	inf	inf	inf	inf	inf	inf	inf	inf	inf	inf	0	inf	inf	inf	inf	inf	inf	inf	inf	inf	inf
12	inf	inf	inf	inf	inf	inf	inf	inf	inf	inf	1038	inf	0	inf	885	957	inf	3135	inf	inf	inf	inf
13	inf	inf	inf	inf	inf	inf	inf	inf	inf	inf	inf	inf	inf	0	inf	inf	inf	inf	inf	inf	inf	inf
14	inf	inf	inf	inf	inf	inf	inf	inf	inf	inf	1791	inf	885	inf	0	826	inf	inf	inf	inf	inf	inf
15	inf	inf	inf	inf	inf	inf	inf	inf	inf	inf	inf	inf	957	inf	826	0	inf	2257	inf	inf	inf	inf
16	inf	inf	inf	inf	inf	inf	inf	inf	inf	inf	inf	inf	inf	inf	inf	inf	0	inf	inf	inf	inf	inf
17	1305	1305	inf	inf	inf	inf	inf	inf	inf	inf	2947	inf	3135	inf	inf	2257	inf	0	698	inf	inf	inf
18	inf	inf	inf	inf	inf	inf	inf	inf	inf	inf	2524	inf	inf	inf	inf	inf	inf	698	0	inf	inf	inf
19	inf	inf	inf	inf	inf	inf	inf	inf	inf	inf	inf	inf	inf	inf	inf	inf	inf	inf	inf	0	inf	inf
20	inf	inf	inf	inf	inf	inf	inf	inf	inf	inf	inf	inf	inf	inf	inf	inf	inf	inf	inf	inf	0	inf
21	inf	inf	inf	inf	inf	inf	inf	inf	inf	inf	3088	inf	inf	inf	inf	inf	inf	inf	inf	inf	inf	0

Table 36: Adjacency matrix for UAV (x^{UAV}_{ij}), considering RZs and AWZs, Pw = 60%

x^{UAV}_{ij}	0	1	2	3	4	5	6	7	8	9	10	11	12	13	14	15	16	17	18	19	20	21
0	-	-	-	-	-	-	-	-	-	-	-	-	-	-	-	-	-	1	-	-	-	-
1	-	-	-	-	-	-	-	-	-	-	-	-	-	-	-	-	-	1	-	-	-	-
2	-	-	-	-	-	-	-	-	-	-	-	-	-	-	-	-	-	-	-	-	-	-
3	-	-	-	-	-	1	1	-	-	-	-	-	-	-	-	-	-	-	-	-	-	-
4	-	-	-	-	-	-	-	-	-	-	-	-	-	-	-	-	-	-	-	-	-	-
5	-	-	-	1	-	-	-	-	-	-	-	-	-	-	-	-	-	-	-	-	-	-
6	-	-	-	1	-	-	-	-	-	-	-	-	-	-	-	-	-	-	-	-	-	-
7	-	-	-	-	-	-	-	-	-	-	-	-	-	-	-	-	-	-	-	-	-	-
8	-	-	-	-	-	-	-	-	-	-	-	-	-	-	-	-	-	-	-	-	-	-
9	-	-	-	-	-	-	-	-	-	-	-	-	-	-	-	-	-	-	-	-	-	-
10	-	-	-	-	-	-	-	-	-	-	-	-	1	-	1	-	-	-	-	-	-	-
11	-	-	-	-	-	-	-	-	-	-	-	-	-	-	-	-	-	-	-	-	-	-
12	-	-	-	-	-	-	-	-	-	-	1	-	-	-	1	1	-	-	-	-	-	-
13	-	-	-	-	-	-	-	-	-	-	-	-	-	-	-	-	-	-	-	-	-	-
14	-	-	-	-	-	-	-	-	-	-	1	-	1	-	-	1	-	-	-	-	-	-

The Service Nodes Pool (SN_k) for each DL is produced. It is worth noting that when lower confidence in forecast is selected, DLs have more limited assignment options, since some paths can no longer be executed. This can happen because either the DL or the LS falls

within a no-fly area, or because the updated flight path's total flight time exceeds the UAV range. Notably, under Pw = 60%, item 13 (located on Node 21), cannot be delivered either by CV or UAV, so this call will have to be cancelled. Table 37 shows the potential service nodes for each DL, resulting from the above analysis.

Table 37: Service Nodes Pool for Items, per Weather Forecast Scenario

Item (k)	Node (d_k)	Service Nodes Pool [SN_k]			
		Pw = 90%	Pw = 80%	Pw = 70%	Pw = 60%
1	4	['4', '0', '1', '2', '3']	['4', '2', '3']	['4', '2', '3']	['4']
2	5	['5', '2', '3']	['5', '2', '3']	['5', '2', '3']	['5', '3']
3	6	['6', '2', '3']	['6', '2', '3']	['6', '2', '3']	['6', '3']
4	7	['7']	['7']	['7']	['7']
5	9	['9', '8']	['9', '8']	['9', '8']	['9']
6	10	['10', '0', '1', '8', '12', '14']	['10', '0', '1', '8', '12', '14']	['10', '0', '1', '8', '12', '14']	['10', '12', '14']
7	11	['11', '8', '10', '14']	['11', '8', '10', '14']	['11']	['11']
8	13	['13']	['13']	['13']	['13']
9	14	['14', '10', '12']	['14', '10', '12']	['14', '10', '12']	['14', '10', '12']
10	15	['15', '12', '14']	['15', '12', '14']	['15', '12', '14']	['15', '12', '14']
11	17	['17', '0', '1', '18']	['17', '0', '1', '18']	['17', '0', '1', '18']	['17', '0', '1', '18']
12	20	['20', '2', '3']	['20', '2', '3']	['20', '2']	['20']
13	21	['8', '10']	['8', '10']	['8']	*[(no service)]*

For every Scenario, SC_{TW}, the respective seed's CV link travel times, $ct_{ij,T}$, are used for all relative calculations. Sub-paths (nodes $\widehat{S_{ij}}$, edges $\widehat{S_{(i,j)}}$), between nodes are calculated using the A* algorithm (Hart, Nilsson, & Raphael, 1968). By implementing the AROnGA, a benchmark solution for each scenario is obtained. The optimization algorithm is run multiple times for each scenario, to avoid missing an even better solution, because of potential local minima entrapments. The solution features a minimum total operations time, TOT_{TW}^{min}.

Table 38: Benchmark solution TOT for each Scenario

Seed	TOT_{TW}^{min} (sec)			
No	Pw = 90%	Pw = 80%	Pw = 70%	Pw = 60%
1	17254.37	17357.06	19313.74	30026.49
2	17037.6	17080.29	19140.06	31269.8
3	17304.48	17107.17	17898.02	32118.2
4	17183.86	17424.87	18850.66	34445.35
5	17091.02	17267.28	18094.89	31162.95
6	17051.6	17154.29	19041.81	32444.25
7	16967.73	17010.42	17817.36	32888.2
8	16929.83	17032.52	18068.75	31419.5
9	17050.81	17265.72	18392.34	30918.41
10	17111.56	17154.25	17941.08	32869.8
11	17117.87	18572.03	18078.14	31771.98
12	17396.54	17458.39	18713.29	31408.95
13	17331.62	17912.38	18089.26	32704.41

14	16813.96	16856.65	17575.38	32269.08
15	16836.18	16998.86	17675.42	32363.35
16	17297.96	17661.77	18808.39	32273.38
17	16982.43	17223.15	17891.34	33134.36
18	17134.69	17237.38	18024.82	31774.46
19	16910.51	17256.32	18232.15	31178.88
20	17592.35	17635.04	18374.9	33814.77
21	17178.89	17281.58	18013.08	31477.1
22	17192.75	17454.72	19359.49	34143.58
23	17118.12	17111.2	18009.42	32080.94
24	16839.37	16942.06	18012.9	32377.86
25	17226.31	17089	18752.7	31549.68
26	16986.16	17200.96	17928.83	32702.52
27	17473.45	17516.14	18069.77	30442.2
28	17271.92	17330.34	18093.73	32777.06
29	17288.01	18362.71	18763.22	33741.98
30	17064.99	17107.68	17979.79	31751.01

The above benchmarks are used for obtaining a Global Solution for each Weather Forecast confidence threshold. During the GSO process, every candidate solution, *Z*, is evaluated using each Scenario's $tft_{ij,W}$, $ct_{ij,T}$ and generated shortest paths, against the respective TOT_{TW}^{min}. The mean of the differences is used as a minimization target for the AROnGA. For each Weather Forecast probability threshold, a dedicated solution is produced, assigning items to a service node and a mode, naming the mandatory nodes with action and the sequence of visit through these nodes. Again, the optimization algorithm is run multiple times to avoid missing a better solution. Only the best solution is kept. Table 39 shows the results of the GSO for each Weather Forecast scenario.

Table 39: Global Solutions for each Scenario

Item (k)	Node (d_k)	Service Nodes Pool [SN_k]	Service Node (lk)	Mode	Service Nodes Pool [SN_k]	Service Node (lk)	Mode
		Pw = 90%			**Pw = 80%**		
1	4	['4', '0', '1', '2', '3']	2	UAV	['4', '2', '3']	2	UAV
2	5	['5', '2', '3']	2	UAV	['5', '2', '3']	2	UAV
3	6	['6', '2', '3']	2	UAV	['6', '2', '3']	2	UAV
4	7	['7']	7	CV	['7']	7	CV
5	9	['9', '8']	8	UAV	['9', '8']	8	UAV
6	10	['10', '0', '1', '8', '12', '14']	8	UAV	['10', '0', '1', '8', '12', '14']	0	UAV
7	11	['11', '8', '10', '14']	8	UAV	['11', '8', '10', '14']	8	UAV
8	13	['13']	13	CV	['13']	13	CV
9	14	['14', '10', '12']	12	UAV	['14', '10', '12']	12	UAV
10	15	['15', '12', '14']	12	UAV	['15', '12', '14']	12	UAV
11	17	['17', '0', '1', '18']	0	UAV	['17', '0', '1', '18']	0	UAV
12	20	['20', '2', '3']	2	UAV	['20', '2', '3']	2	UAV
13	21	['8', '10']	8	UAV	['8', '10']	8	UAV
	T_M^v	['0', '2', '7', '8', '12', '13']			['0', '2', '7', '8', '12', '13']		
	$\tilde{S}_v^M$	['0', '2', '7', '8', '12', '13', '1']			['0', '2', '12', '13', '8', '7', '1']		

$\widehat{S^{M}_{(e)}}$	[('0', '2'), ('2', '7'), ('7', '8'), ('8', '12'), ('12', '13'), ('13', '1')]	[('0', '2'), ('2', '12'), ('12', '13'), ('13', '8'), ('8', '7'), ('7', '1')]
Mean dTOT	**332.7 sec / 5.5 min**	**168.2 sec / 2.8 min**
Mean TOT$_{TW^{min}}$	17134.6 sec / 285.6 min	17335.4 sec / 288.9 min
Min/Max TOT$_{TW^{min}}$	280.2 / 293.2 min	280.9 / 309.5 min

Item (k)	**Node (d_k)**	**Service Nodes Pool [SN_k]**	**Service Node (l_k)**	**Mode**	**Service Nodes Pool [SN_k]**	**Service Node (l_k)**	**Mode**
		Pw = 70%			**Pw = 60%**		
1	4	['4', '2', '3']	2	UAV	['4']	4	CV
2	5	['5', '2', '3']	2	UAV	['5', '3']	5	CV
3	6	['6', '2', '3']	2	UAV	['6', '3']	6	CV
4	7	['7']	7	CV	['7']	7	CV
5	9	['9', '8']	8	UAV	['9']	9	CV
6	10	['10', '0', '1', '8', '12', '14']	0	UAV	['10', '12', '14']	12	UAV
7	11	['11']	11	UAV	['11']	11	CV
8	13	['13']	13	CV	['13']	13	CV
9	14	['14', '10', '12']	12	UAV	['14', '10', '12']	12	UAV
10	15	['15', '12', '14']	12	UAV	['15', '12', '14']	12	UAV
11	17	['17', '0', '1', '18']	0	UAV	['17', '0', '1', '18']	0	UAV
12	20	['20', '2']	2	UAV	['20']	20	CV
13	21	['8']	8	UAV	[(no service)]	n/a	n/a
	T^{v}_{M}	['0', '2', '7', '8', '11', '12', '13']			['0', '4', '5', '6', '7', '9', '11', '12', '13', '20']		
	$\widehat{S^{M}_{v}}$	['0', '2', '7', '8', '11', '13', '12', '1']			['0', '6', '20', '5', '4', '7', '11', '9', '12', '13', '1']		
	$\widehat{S^{M}_{(e)}}$	[('0', '2'), ('2', '7'), ('7', '8'), ('8', '11'), ('11', '13'), ('13', '12'), ('12', '1')]			[('0', '6'), ('6', '20'), ('20', '5'), ('5', '4'), ('4', '7'), ('7', '11'), ('11', '9'), ('9', '12'), ('12', '13'), ('13', '1')]		
	Mean dTOT	**264.1 sec / 4.4 min**			**754.4 sec / 12.6 min**		
	Mean TOT$_{TW^{min}}$	18300.2 sec / 305.0 min			32176.7 sec / 536.3 min		
	Min/MaxTOT$_{TW^{min}}$	292.9 / 322.7 min			500.4 / 574.1 min		

The following figures illustrate the relative solutions, by highlighting the mandatory nodes, their order of visit, as well as the UAV connections used for item delivery.

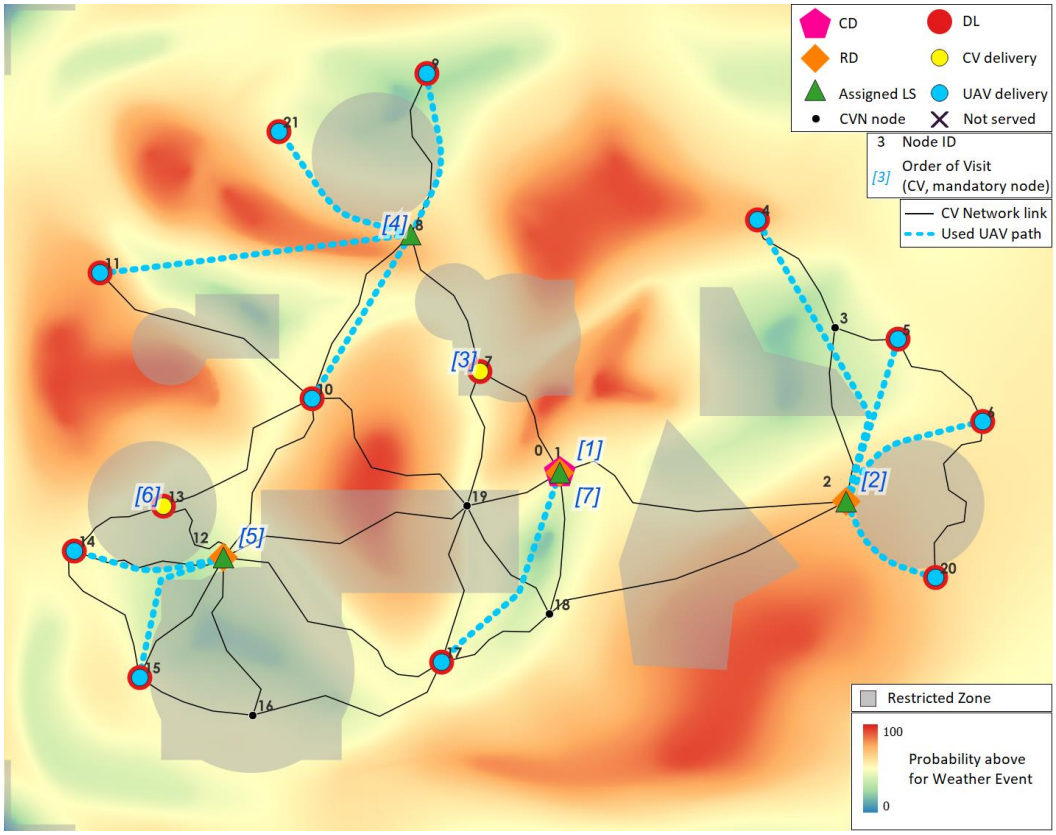

Figure 65: Illustration of estimated global solution at Pw = 90%

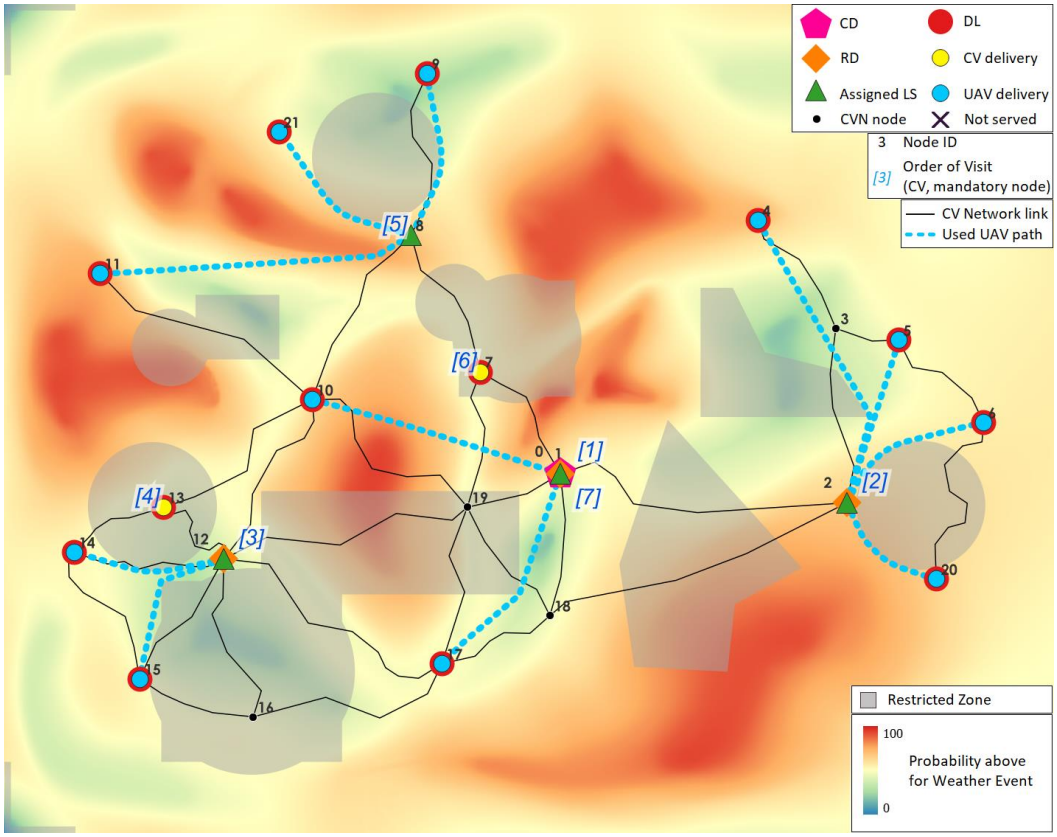

Figure 66: Illustration of estimated global solution at Pw = 80%

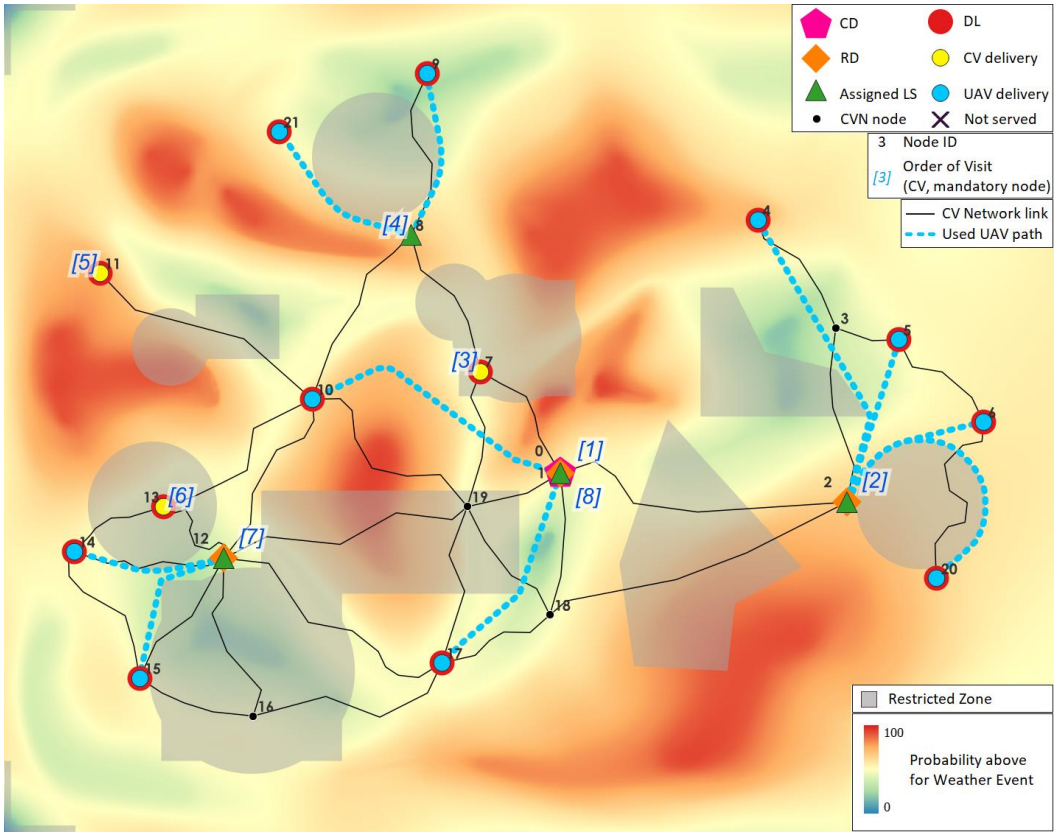

Figure 67: Illustration of estimated global solution at Pw = 70%

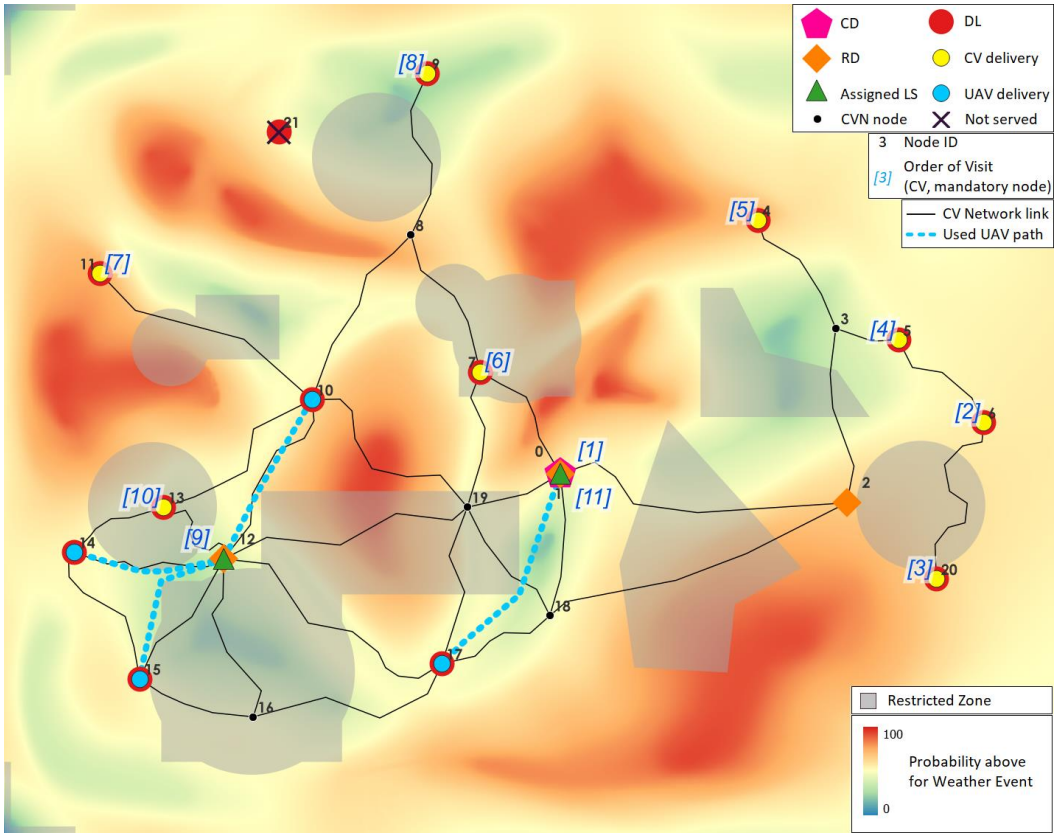

Figure 68: Illustration of estimated global solution at Pw = 60%

Let's give a practical meaning to the results above. For example, for the case of Pw = 90%, the average TOT_{TW}^{min} expected would be 285.6 min (minimum: 280.2 min, maximum: 293.2 min). If the assignment and basic routing suggestion is followed, no matter the conditions on the road, the performance of planned operations will be, on average, 5.5 min slower than the theoretical best for the conditions met, that is 1.94% off the average value among generated seeds. This is essentially the average time the planner should be prepared to "sacrifice" for a more reliable and satisfactory result in operations performance. For the case of Pw = 80%, only some extra 2.8 min (or 0.97% of the average expected TOT_{TW}^{min} = 288.9 min) are sacrificed to achieve robust performance, no matter the conditions arising. It is also evident that, as confidence in Weather Forecast goes lower, more items are assigned to CV, because of less UAV connections and longer flight times. Sometimes a counterintuitive solution may appear, however we should have in mind that this is intended to tackle any conditions met on the network and not just a specific case.

5.5 Discussion

The methodology can yield optimal solutions for given conditions concerning the CVN and the airspace and then provide a robust solution which performs well under a variety of circumstances. It offers the option of selecting the level of risk a planner is willing to take (in terms of CVN conditions and the Weather) and proposes how the items should be delivered and what route the CV should follow to avoid excess delays. It does not provide a total route for the CV but highlights the mandatory nodes and the order of visit, for prior planning. The actual path must be selected on-the-road, after leaving each of the mandatory nodes. If the conditions are given, the methodology proposes an exact path for the CV as well. Additionally, it is reasonable to expect that a larger and more complex network would offer more alternatives in assignment and routing and the global solution would fare -on average- worse from the theoretical best for each generated scenario. Another factor contributing to the increase of TOTs is the size and shape complexity of RZs and AWZs, which lead to potentially longer UAV flight paths and less LS options for each DL. Further research can elaborate more on the above matters, allowing for more precise planning beforehand.

6 Conclusions

This research aspired to design a powerful platform for combined conventional vehicle and unmanned aerial vehicle parcel deliveries, assisting with strategic decision making and operations optimization. The framework was conceived in a theoretical basis and then mathematically modelled for further analysis. A tailored solution optimization methodology through a nested-GA was developed, which can be used both under known and uncertain conditions. In the process, the framework and solution methodology were blended with modern GIS software and its associated tools, seamlessly working with background analysis and optimization algorithms executed in a more basic programming environment.

Common practical challenges in such operations, like unfavorable network geometries, off-grid delivery locations, airspace restrictions, adverse weather and uncertainties on the road are addressed through the core structure and various adaptation provisions of the framework and the solution methodology. Ignoring airspace constraints, like no-fly zones and the weather, is a major simplification of how combined CV-UAV schemes can practically work. The basis of our platform can be used with a variety of transport modes serving as conventional vehicles, such as trucks, trains, or sea vessels, while parcel deliveries can be substituted with any other form of service, such as humanitarian assistance, inspection etc. The entire model and solution methodology are practical tools for decision-making and strategic planning, but we specifically offer some novelties. For example, our variable Launch Site types for LARO, the tailored Assignment and Routing Optimization nested GA, the consideration of airspace restrictions of any shape and size, the inclusion of GIS tools in the process, the modularity of our platform, and most importantly, the inclusion of all the above in a single, comprehensive, and holistic approach could be highlighted. In terms of the transport system setup, further research could be directed toward including more CVs instead of one, considering altitude and terrain specifics and the stochastic nature of travel times both for the CV and UAVs.

Using and modifying the original core framework to include restricted airspace, weather routing and finally achieve stochastic planning under uncertainty has been a very interesting research path, proving the openness and the extended possibilities of our approach, but also the flawed simplification often assumed in similar modelling efforts.

Practical implementation is made easy through a simplified input and output workflow, which is separated from the more complicated internal calculations process. Nevertheless, a strong mathematical background in both the formulation and the solution methodology ensures the integrity of our platform. At the same time, it allows for custom interventions in infrastructure and vehicle parameters and the execution of preference-based strategies which may use only part of the optimization tools developed. Experimental use of the framework under various scenarios may also help with identifying the best strategies in infrastructure development, i.e., best locations for remote or central depots, virtual hubs etc.

During this research, several challenges were met, whether expected or coming up as a surprise. Trying to come up with a simplified concept which, at the same time, can cover a lot of different cases implies deep understanding of the problem and several original concepts had to be modified after their weaknesses were exposed through experiments. However, this process is integral for verifying our approach's correctness and testing it to its limits never was a matter of doubt. As already stated in the description of the original workflow, individual methods can be used to further optimize the process. For instance, the AROnGA which was specifically developed to yield optimal solutions under known or stochastic conditions needs proper calibration and extensive runs to provide good suggestions. Any suitable optimization method which can produce assignment and routing solutions (using can the previously obtained Service Nodes Pool) could replace our tailored algorithm and maybe perform even better. Additionally, in the real world of parcel delivery, multiple trucks are used and each one serves a cluster of items to be delivered. A modification of our methodology, adding an extra step for multiple truck assignment and routing, could be a very interesting evolution. Moreover, regarding UAV path planning, a three-dimensional approach should be followed if terrain elevation features extreme changes, extending above the anticipated UAV operating altitude.

Airspace and on-ground restrictions are notoriously tight within core urban areas and the use of UAVs can be limited. Thus, in terms of practical implementation, we suggest that our model is more suitable for suburban and inter-city deliveries, i.e., serving various satellite towns around a city or using the main highway network and its rest areas and parking lots

for UAV deployment. Another interesting case would be using the railway network; the train serves as a CV, moving along its fixed route and some stations are equipped to become RDs.

Albeit these or other limitations, it has been our core philosophy to pave an unobstructed way for future evolution, in terms of what vehicles cooperate and how, the inclusion of additional parameters affecting conventional vehicles or UAVs etc. It is our hope that this work can be used to the greater benefit and above all serve the original motivation: moving towards more efficient and sustainable transport, providing better services, life quality and social equity for all.

Bibliography

Agatz, N., Bouman, P., & Schmidt, M. (2018). Optimization Approaches for the Traveling Salesman Problem with Drone. *Transportation Science, 52*.

Applegate, D., Bixby, R., Chvátal, V., & Cook, W. (1995). *Finding cuts in the TSP (a preliminary report).* Center for Discrete Mathematics & Theoretical Computer Science.

Applegate, D., Bixby, R., Chvátal, V., & Cook, W. (2008). The Traveling Salesman Problem. In *Combinatorial Optimization: Theory and Algorithms* (4 ed., Vol. 21, pp. 527-562). Berlin/Heidelberg, Germany: Springer.

Bellman, R. (1962). Dynamic Programming Treatment of the Travelling Salesman Problem. *Journal of the ACM, 9*(1), 61-63.

Bertsimas, D. J., & Simchi-Levi, D. (1996). A New Generation of Vehicle Routing Research: Robust Algorithms, Addressing Uncertainty. *Operations Research, 44*(2), 286-304. doi:10.1287/opre.44.2.286

Bickel, P., & Doksum, K. (2015). *Mathematical Statistics Basic Ideas and Selected Topics, Volume I* (2nd ed., Vol. I). Chapman & Hall.

Boysen, N., Briskorn, D., Fedtke, S., & Schwerdfeger, S. (2018). Drone delivery from trucks: Drone scheduling for given truck routes. *Networks, 72*(4), 506-527. doi:https://doi.org/10.1002/net.21847

Chang, Y. S., & Lee, H. J. (2018). Optimal delivery routing with wider drone-delivery areas along a shorter truck-route. *Expert Systems With Applications, 104*, 307-317.

Choset, H., Lynch, K. M., Hutchinson, S., Kantor, G., Burgard, W., Kavraki, L. E., & Thrun, S. (2005). *Principles of Robot Motion Theory, Algorithms, and Implementations.* (R. C. Arkin, Ed.) The MIT Press / Bradford Books.

Dantzig, G. B., Fulkerson, R., & Johnson, S. (1954). Solution of a large-scale Traveling Salesman Problem. *Operations Research, 2*, 393-410.

Davies, C. (2020, February 17). The carbon cost of home delivery and how to avoid it. *Horizon: The EU Research & Innovation Magazine*. Retrieved March 14, 2023, from Horizon, The

EU Research & Innovation Magazine: https://ec.europa.eu/research-and-innovation/en/horizon-magazine/carbon-cost-home-delivery-and-how-avoid-it

Dijkstra, E. W. (1959). A note on two problems in connexion with graphs. *Numerische mathematik, 1*, 269-271.

DJI. (2023). *DJI Matrice 300 RTK Specs*. Retrieved August 2023, from DJI Enterprise: https://enterprise.dji.com/matrice-300/specs

Doswell, C., & Brooks, H. (2023, March 21). Retrieved from NOAA National Severe Storms Laboratory: https://www.nssl.noaa.gov/users/brooks/public_html/prob/Probability.html

Doswell, C., Duncomb, R., & Brooks, H. (1996). Verification of VORTEX94 Forecasts. *15th Conference on Weather Analysis and Forecasting* (pp. 387-390). Norfolk, VA: American Meteorological Society.

Douglas, D. H. (1994). Least-cost Path in GIS Using an Accumulated Cost Surface and Slopelines. *Cartographica: The International Journal for Geographic Information and Geovisualization, 31*(3), 37-51. doi:10.3138/D327-0323-2JUT-016M

EASA. (2022). *Easy Access Rules for Unmanned Aircraft Systems.* European Union Aviation Safety Agency. European Union. Retrieved from https://www.easa.europa.eu/en/regulations/uas-unmanned-aircraft-systems

Erbao, C., & Mingyong, L. (2009). A hybrid differential evolution algorithm to vehicle routing problem with fuzzy demands. *Journal of Computational and Applied Mathematics, 231*(1), 302-310. doi:10.1016/j.cam.2009.02.015

ESRI. (2023). *Connect locations with optimal paths.* Retrieved June 2023, from ArcGIS Pro: https://pro.arcgis.com/en/pro-app/latest/tool-reference/spatial-analyst/connect-locations-with-optimal-paths.htm

ESRI. (2023). *Flow Direction.* Retrieved June 2023, from ArcGIS Destktop: https://desktop.arcgis.com/en/arcmap/latest/tools/spatial-analyst-toolbox/flow-direction.htm

ESRI. (2023). *How Flow Direction Works.* Retrieved June 2023, from ArcGIS Desktop: https://desktop.arcgis.com/en/arcmap/latest/tools/spatial-analyst-toolbox/how-flow-direction-works.htm

European Commission. (2017, 11 8). *Emission performance standards for new passenger cars and for new light commercial vehicles.* Brussels: European Commission. Retrieved 2023, from European Commission: https://oeil.secure.europarl.europa.eu/oeil/popups/ficheprocedure.do?reference=2017/0293(COD)&l=en

FAA. (2016). Chapter 15 - Airspace. In F. A. Administration, *Pilots Handbook of Aeronautical Knowledge.* Federal Aviation Administration.

FAA. (2022). In P. 2.-E.-E. Classification, *Aeronautical Information Publication (AIP).* Federal Aviation Administration.

Ferrandez, S. M., Harbison, T., Weber, T., Sturges, R., & Rich, R. (2016). Optimization of a Truck-drone in Tandem Delivery Network Using K-means and Genetic Algorithm Sergio. *Journal of Industrial Engineering and Management, 9*(2), 374-388.

Flying Basket. (2023). *FB3 - The most compact drone in the world able to carry 100 kg*. Retrieved August 2023, from Flying Basket: https://flyingbasket.com/fb3

Garey, M. R., & Johnson, D. S. (1979). *Computers and Intractability: A Guide to NP-Completeness.* New York: WH Freeman.

Gendreau, M., Laporte, G., & Séguin, R. (1996). Stochastic vehicle routing. *European Journal of Operational Research, 88*(1), 3-12. doi:10.1016/0377-2217(95)00050-X

Glover, F. (1986). Future paths for integer programming and links to artificial intelligence. *Computers & Operations Research, 13*(5), 533-549.

Glover, F. (1989). Tabu Search - Part I. *ORSA Journal on Computing, 1*(3), 190-206.

Glover, F. (1990). Tabu Search - Part II. *ORSA Journal on Computin, 2*(1), 4-32.

González-Rodríguez, P. L., Canca, D., Andrade-Pineda, J. L., Calle, M., & Leon-Blanco, J. M. (2020). Truck-drone team logistics: A heuristic approach to multi-drop route planning.

Transportation Research Part C: Emerging Technologies, 114, 657–680. doi:https://doi.org/10.1016/j.trc.2020.02.030

Hart, P. E., Nilsson, N. J., & Raphael, B. (1968). A Formal Basis for the Heuristic Determination of Minimum Cost Paths. *IEEE Transactions on Systems Science and Cybernetics, 4*, 100-107.

HCAA. (2023). *Drone Aware - GR (DAGR)*. (Hellenic CAA) Retrieved from https://dagr.hasp.gov.gr/

Held, M., & Karp, R. M. (1962, March). *Journal of the Society for Industrial and Applied Mathematics, 10*, 196-210.

Holland, J. H. (1975). *Adaptation in Natural and Artificial Systems.* (A. Arbor, Ed.) University of Michigan Press (2nd Edition, MIT Press, 1992).

ICAO. (2005). *Annex 2 to the Convention on Civil Aviation - Rules of the Air* (10 ed.). International Civil Aviation Organization.

ICAO. (2018). *Annex 11 to the Convention on International Civil Aviation - Air Traffic Services.* International Civil Aviation Organization.

ICAO. (2022). *Annex 14 to the Convention on International Civil Aviation - Aerodromes - Aerodromes Design and Operations* (9 ed., Vol. I). International Civil Aviation Organization.

Iliopoulou, C., Kepaptsoglou, K., & Karlaftis, M. G. (2015). Route planning for a sea plane service: The case of the Greek Islands. *Computers&OperationsResearch, 59*, 66-77.

Iliopoulou, C., Kepaptsoglou, K., & Schinas, O. (2018). Energy supply security for the Aegean islands: A routing model with risk and environmental considerations. *Energy Policy, 113*, 608-620.

ITF. (2021). *Ready for Take Off? Integrating Drones into the Transport System.* Paris: OECD Publishing.

Jenson, S. K., & Domingue, J. O. (1988). Extracting Topographic Structure from Digital Elevation Data for Geographic Information System Analysis. *Photogrammetric Engineering and Remote Sensing, 54*(11), 1593-1600.

Jeonga, H., Song, B., & Lee, S. (2019). Truck-drone hybrid delivery routing: Payload-energy dependency and No Fly zones. *International Journal of Production Economics, 214*, 220-233. doi:https://doi.org/10.1016/j.ijpe.2019.01.010

Kamon, I., Rimon, E., & Rivlin, E. (1998). TangentBug: A Range-Sensor-Based Navigation Algorithm. *The International Journal of Robotics Research, 17*(9), 934-953. doi:https://doi.org/10.1177/027836499801700903

Kamon, I., Rivlin, E., & Rimon, E. (1996). A new range-sensor based globally convergent navigation algorithm for mo-bile robots. *IEEE International Conference on Robotics and Automation*, (pp. 429-435). doi:https://doi.org/10.1109/ROBOT.1996.503814

Kepaptsoglou, K., Fountas, G., & Karlaftis, M. G. (2015). Weather impact on containership routing in closed seas: A chance-constraint optimization approach. *Transportation Research Part C: Emerging Technologies, 55*, 139-155. doi:10.1016/j.trc.2015.01.027

Khatib, O. (1985). Real-time obstacle avoidance for manipulators and mobile robots. *IEEE Interna-tional Conference on Robotics and Automation*, (pp. 500-505). doi:https://doi.org/10.1109/ROBOT.1985.1087247

Kirkpatrick, S., Gelatt, C. D., & Vecchi, M. P. (1983). Optimization by Simulated Annealing. *Science, 220*(4598), 671-680.

Koenig, S., Likhachev, M., & Furcy, D. (2004). Lifelong Planning A∗. *Artificial Intelligence, 155*(1-2), 93-136.

Korf, R. E. (1985). Depth-first iterative-deepening: An optimal admissible tree search. *Artifical Intelligence, 27*(1), 97-109.

Lenstra, J. K., & Kan, A. H. (1981). Complexity of vehicle routing and scheduling problems. *Networks, 11*(2), 221-227.

Leon-Blanco, J., Gonzalez-R, P., Andrade-Pineda, J., Canca, D., & Calle, M. (2022). A multi-agent approach to the truck multi-drone routing problem. *Expert Systems With Applications, 195*, 116604. doi:https://doi.org/10.1016/j.eswa.2022.116604

Li, H., & Wang, F. (2022). Branch-price-and-cut for the truck–drone routing problem with time windows. *Naval Research Logistics, 70*(2), 184-204. doi:https://doi.org/10.1002/nav.22087

Li, H., Chen, J., Wang, F., & Zhao, Y. (2022). Truck and drone routing problem with synchronization on arcs. *Naval Research Logistics, 69*(6), 884-901. doi:https://doi.org/10.1002/nav.22053

Little, J. D., Murty, K. G., Sweeney, D. W., & Karel, C. (1963). An algorithm for the traveling salesman problem. *Operations Research, 11*, 972-989.

Lumelsky, V., & Stepanov, A. A. (1987). Path-planning strategies for a point mobile automaton moving amidst un-known obstacles of arbitrary shape. *Algorithmica, 2*(1-4), 403-430. doi:https://doi.org/10.1007/BF01840369

MacQueen, J. B. (1967). Some methods for classification and analysis of multivariate observations. In L. Le Cam, & J. Neyman (Ed.), *Proceedings of the 5th Berkeley Symposium on Mathematical Statistics and Probability. 1*, pp. 281-297. University of California Press.

Macrina, G., Pugliese, L., Guerriero, F., & Laporte, G. (2020). Drone-aided routing: A literature review. *Transportation Research Part C: Emerging Technologies, 120*. doi:10.1016/j.trc.2020.102762

Marinelli, M., Caggiani, L., Ottomanelli, M., & Dell'Orco, M. (2017). En route truck–drone parcel delivery for optimal vehicle routing strategies. *IET Intelligent Transport Systems, 12*(4).

Matternet. (2023). *Matternet*. Retrieved September 2023, from https://mttr.net/.

Matternet. (2023). *Matternet - M2*. Retrieved August 2023, from Matternet: https://www.engineeringforchange.org/solutions/product/matternet-m2/

McKinsey & Company. (2021, May). *"Up in the air: How do consumers view advanced air mobility?"*. (B. Kloss, & R. Riedel, Eds.) Retrieved June 1, 2021, from

https://www.mckinsey.com/industries/aerospace-and-defense/our-insights/up-in-the-air-how-do-consumers-view-advanced-air-mobility

Momeni, M., Mirzapour Al-e-Hashem, S., & Heidari, A. (2023). A new truck-drone routing problem for parcel delivery by considering energy consumption and altitude. *Annals of Operations Research*. doi:https://doi.org/10.1007/s10479-023-05381-8

Moshref-Javadi, M., Hemmati, A., & Winkenbach, M. (2020). A truck and drones model for last-mile delivery: A mathematical model and heuristic approach. *Applied Mathematical Modelling, 80*, 290-318.

Moshref-Javadi, M., Lee, S., & Winkenbach, M. (2020). Design and evaluation of a multi-trip delivery model with truck and drones. *Transportation Research Part E, 136*.

Murphy, A. (1991). Forecast verification: Its Complexity and Dimensionality. *Monthly Weather Review, 119*(7), 1590-1601. doi:https://doi.org/10.1175/1520-0493(1991)119<1590:FVICAD>2.0.CO;2

Murphy, A., & Winkler, R. (1984, September). Probability Forecasting in Meterology. *Journal of the American Statistical Association, 79*(387), 489-500. doi:https://doi.org/10.2307/2288395

Murphy, A., & Winkler, R. (1987). A General Framework for Forecast Verification. *Monthly Weather Review, 115*(7), 1330-1339. doi:https://doi.org/10.1175/1520-0493(1987)115<1330:AGFFFV>2.0.CO;2

Murray, C. C., & Chu, A. G. (2015). The flying sidekick traveling salesman problem: Optimization of drone-assisted parcel delivery. *Transportation Research Part C, 54*, 86-109.

Murray, C. C., & Raj, R. (2020). The multiple flying sidekicks traveling salesman problem: Parcel delivery with multiple drones. *Transportation Research Part C, 110*, 368-398.

Qin, C., Zhu, A. X., Pei, T., Li, B., Zhou, C., & Yang, L. (2007). n adaptive approach to selecting a flow partition exponent for a multiple flow direction algorithm. *International Journal of Geographical Information Science, 21*(4), 443-458. doi:10.1080/13658810601073240

Rardin, R. L. (2015). *Optimization in Operations Research* (2nd ed.). Pearson Higher Education, Inc.

Rashid, A. T., Ali, A. A., Frasca, M., & Fortuna, L. (2017). Path planning and obstacle avoidance based on shortest distance algorithm. *Path planning and obstacle avoidance based on shortest dis-tance algorithm. Second Al-Sadiq International Conference on Multidisciplinary in IT and Communication Science and Applications.*

Roland Berger Gmbh. (2020, February 19). *"Cargo Drones: The Future of Parcel Delivery (USD 5.5 billion market)"*. (S. Baur, & M. Hader, Eds.) Retrieved September 10, 2022, from https://www.rolandberger.com/en/Point-of-View/Cargo-drones-The-future-of-parcel-delivery.html

Ross, S. (2010). *A first course in probability* (8th ed.). Upper Saddle River, N.J.: Pearson Prentice Hall.

Salama, M. R., & Srinivas, S. (2022). Collaborative truck multi-drone routing and scheduling problem: Package delivery with flexible launch and recovery sites. *Transportation Research Part E, 164*.

Salama, M., & Srinivas, S. (2022). Collaborative truck multi-drone routing and scheduling problem: Package delivery with flexible launch and recovery sites. *Transportation Research Part E, 164*, 102788. doi:https://doi.org/10.1016/j.tre.2022.102788

Tarboton, D. G. (1997). A new method for the determination of flow directions and upslope areas in grid digital elevation models. *Water Resources Research, 33*(2), 309-319. doi:10.1029/96WR03137

Witkamp, B., van Gijlswijk, R., Bolech, M., Coosemans, T., & Hooftman, N. (2017). *The transition to a Zero Emission Vehicles fleet for cars in the EU by 2050: Pathways and impacts: An evaluation of forecasts and backcasting the COP21 commitments.* Vrije Universiteit Brussel. Brussels: European Alternative Fuels Observatory. Retrieved March 14, 2023, from https://researchportal.vub.be/en/publications/the-transition-to-a-zero-emission-vehicles-fleet-for-cars-in-the-

World Climate Service. (2021, 09 08). *WCS Blog - Analysis from the World Climate Service*. Retrieved 03 21, 2023, from World Climate Service: https://www.worldclimateservice.com/2021/09/08/probability-forecast/

Wu, L., & Hifi, M. (2020). Discrete scenario-based optimization for the robust vehicle routing problem: The case of time windows under delay uncertainty. *Computers & Industrial Engineering, 145*, 106491. doi:10.1016/j.cie.2020.106491

Zhan, W., Wang, W., Chen, N., & Wang, C. (2014). Efficient UAV Path Planning with Multiconstraints in a 3D Large Battlefield Environment. *Mathematical Problems in Engineering*, 1-12. doi:10.1155/2014/597092

Zhang, M., Su, C., Liu, Y., Hu, M., & Zhu, Y. (2016). Unmanned aerial vehicle route planning in the presence of a threat environment based on a virtual globe platform. *ISPRS International Journal of Geo-Information, 5*(10). doi:10.3390/ijgi5100184

Zhou, H., Qin, H., Cheng, C., & Rousseau, L.-M. (2023). An exact algorithm for the two-echelon vehicle routing problem. *Transportation Research Part B, 168*, 124-150. doi:https://doi.org/10.1016/j.trb.2023.01.002